

Copyright

by

Anthony Michael Smith

2011

**The Dissertation Committee for Anthony Michael Smith Certifies that this is the
approved version of the following dissertation:**

**Microbiological Activity and Organic Pollutant Fate and Transport in
Sediments and Sediment Caps**

Committee:

Danny Reible, Supervisor

Mary Jo Kirsits, Co-Supervisor

Philip Bennett

Robert Gilbert

Howard Liljestrand

**Microbiological Activity and Organic Pollutant Fate and Transport in
Sediments and Sediment Caps**

by

Anthony Michael Smith, B.S.; M.S.E.

Dissertation

Presented to the Faculty of the Graduate School of

The University of Texas at Austin

in Partial Fulfillment

of the Requirements

for the Degree of

Doctor of Philosophy

The University of Texas at Austin

August 2011

Dedication

To Innocent Charles, once an aspiring chemist and now a guide on Mt. Kilimanjaro.

I certainly am fortunate to have had this opportunity.

Acknowledgements

This experience is largely the fault of Dean Streetman, whose address at a banquet described PhD research as “the only time in your life that you will be able to invest yourself completely in one problem”. For some reason, that sounded appealing.

So many great experiences, so many people to thank. I owe gratitude

- . . . to the members of my committee -- to Danny Reible and Mary Jo Kirisits, my advisors, for their guidance, encouragement, and patience; to Phil Bennett for introducing me to the fascinating world of geomicrobiology and for permitting me to use several instruments in his lab; to Bob Gilbert for an outstanding course and several great trips to post-Katrina New Orleans; and to Howard Liljestrand for keeping an open door and sharing his incredible breadth of knowledge;
- . . . to all who have passed through the Reible and Kirisits research groups, even Shawn, who tried to derail my degree pursuit by hanging a dart board in the office; to Xiaoxia Lu for being the “go to” person at all times, to Sungwoo Bae for advice about all things nucleic acid; and to YS Hong for all sorts of help and great discussion about Korean cuisine;
- . . . to the group of climbers that helped me preserve dwindling sanity: Bryant, Leo, Lisa, Eric, Cindy, Dave, Neil, Wil, and Ellison;
- . . . to all that have given me help in the lab, including Erika Kase, Charles Perng, Stacy Louie, Charlene Vela, Justincredible Davis, and Will Wolfe;
- . . . to many great generations of office-mates: Shawn, Wil, Casey, Brian, Jasmine, Gabe, and Dave; Nate and Mara, and “the family”, Katie, Brent and Fei;

. . . to Rebecca, Marcy, Susan, and Sharon for keeping the administrative machine rolling
no matter what I happened to stick in the spokes;
. . . to Charlie and Chia-Chen for keeping the mechanical and analytical machines rolling
(figuratively, of course);
. . . to my family, whose well of support and encouragement is infinite;
. . . and to Cindy, for being the other biggest part of my life for the last five years.
Thank you all, you were an integral part of this accomplishment.

Microbiological Activity and Organic Pollutant Fate and Transport in Sediments and Sediment Caps

Anthony Michael Smith, Ph.D.

The University of Texas at Austin, 2011

Supervisors: Danny Reible and Mary Jo Kirisits

Contaminated surficial sediments represent a potential point of entry into the food web for environmental pollutants that are toxic to fish, wildlife, and humans. One approach for managing polluted sediments is in situ capping, the placement of clean fill material, such as sand, atop the polluted sediments. A cap stabilizes the underlying sediment and physically separates pollutants from benthic organisms that inhabit the sediment/water interface. Additionally, a sediment cap can be amended with sorbents to sequester hydrophobic organic chemicals. While the physical processes affecting contaminant transport in sediment caps are readily modeled, fate and transport processes mediated by sediment bacteria are location-specific and thus highly uncertain.

Laboratory bench-scale tests were employed to aid in the design of a sediment cap in Onondaga Lake. Recognizing the importance of bacterial activity beneath the benthic zone for affecting the risks of contaminant exposure, anaerobic processes were emphasized. A combination of batch and column tests were used to determine whether (1) bacteria in sediments were capable of biotransforming methylated and chlorinated benzenes, (2) the ability to biotransform the contaminants of interest would be translated from the sediments to a sand cap, (3) the rate of biogenic gas production in sediments would threaten the integrity of a sand cap, and (4) the contribution of gas-phase

contaminant transport to the overall transport of contaminants from the sediments was significant.

The apparent anaerobic biotransformation of toluene in a sand cap was supported by detection of a genetic biomarker for anaerobic toluene degradation, the development of substantial biomass in the sand column, apparent anaerobic biotransformation of toluene in sediment slurries, and the concomitant reduction of iron in the sand column. The dissimilarity in bacterial community composition between sediment and sand cap samples suggests that contaminant biotransformation capability cannot be predicted from community analysis. For sediments that failed to demonstrate biotransformation potential, amending a sand column with organophilic clay proved effective at retarding transport of the contaminants of interest.

This work advances methods for characterizing bacterial processes in sediments and demonstrates the potential for anaerobic biotransformation of organic contaminants in sand caps.

Table of Contents

List of Tables	xv
List of Figures	xvii
List of Acronyms.....	xx
List of Symbols	xxi
Chapter 1. Introduction.....	1
1.1 Overview	1
1.2 Research Objectives and Dissertation Outline	2
Chapter 2. Background.....	4
2.1 Contaminated Sediments.....	4
2.2 Remediation Options for Contaminated Sediments	5
2.2.1 Sediment Management Objectives.....	5
2.2.2 Cap Colonization by Microorganisms and Bacterial Metabolic Activity	6
2.2.3 Bacterial activity in sediments beneath a cap	8
2.3 Requirements for Contaminant Biotransformation.....	10
2.3.1 Microorganisms Capable of Catalyzing Pollutant Biotransformation	10
2.3.2 Bioavailable Nutrients, Energy Sources, and Electron Acceptors	11
2.3.3 Moisture, pH, and Temperature	12
2.3.4 The Absence of Toxicity	13
2.3.5 The Removal of Metabolites.....	13
2.4 Modeling Contaminant Fate and Transport	14
2.4.1 Modeling Contaminant Biotransformation.....	14
2.4.2. The Governing Equation for Solute Transport in Porous Media	14
2.5 Contaminants of Study.....	15

4.2.4 Biomass Density Determination	71
4.2.5 Statistical Analysis	72
4.3 Results and Discussion.....	73
4.3.1 Upflow Columns – Fluxes of Contaminants and Geochemical Indicators of Anaerobic Metabolism.....	73
4.3.2 Detection of bssA in Sediment and Sand from Column 70049..	78
4.3.3 Bacterial Community Diversity and Community Similarity in Column 60105.....	79
4.3.4 Biomass Quantification in Column 60105	85
4.4 Conclusions	86
Chapter 5. Thermodynamic and Kinetic Considerations for Contaminant Biotransformation in Sand-Capped Sediment Column Experiments	89
5.1 Introduction	89
5.2 Methods.....	90
5.2.1 General Column Operation.....	90
5.2.2 Model description and identification of relevant transport parameters	91
5.2.3 Breakthrough of hydraulic tracer and parameter fitting	92
5.2.3.1 Hydraulic Tracer Test	92
5.2.3.2 Hydraulic Parameter Estimation.....	94
5.2.4 Contaminant Transport and Biotransformation	94
5.2.4.1 Development of relevant equations	94
5.2.4.2 Procedure for simulating solute effluent profiles	97
5.2.5 Measurement of Biogeochemical Indicators of Metabolism	97
5.3 Results and Discussion.....	98
5.3.1 Hydraulic Transport Parameters	98
5.3.2 Contaminant Biotransformation.....	100
5.3.3 Geochemical Indicators of Anaerobic Metabolism.....	104
5.3.4 Hydrogen, Reaction Thermodynamics, and Biochemical Kinetics	107

5.3.4.1 The Thermodynamic Feasibility of Toluene Fermentation	107
5.3.4.2 Microbial Dehalogenation and Competition with Methanogens	111
5.4 Summary and Conclusions	113
Chapter 6. Organophilic Clay Slows the Migration of Volatile Organic Pollutants Through Sand-Based Sediment Caps	115
6.1 Introduction	115
6.2 Materials and Methods	116
6.2.1 Batch isotherms	116
6.2.2 Upflow columns	119
6.2.3 Hydraulic parameter estimation and breakthrough simulation	122
6.3 Results and Discussion	123
6.3.1 Isotherms	123
6.3.2 Column Breakthrough Curves	127
6.3.3 Comparison of Sorption in Batch Isotherms and Column Tests	132
6.4 Conclusions	134
Chapter 7: Conclusions and Recommendations for Future Work	137
7.1 Conclusions	137
7.1.1 Bench Scale Tests Aided in the Design of a Sediment Cap for Onondaga Lake	137
7.1.2 Contaminant Biotransformation is Possible in Sand-Based Sediment Caps	137
7.1.3 Bacterial Community Structure Differs Significantly Between Sediment and Sand and Thus Can Not Be Used to Predict Potential Metabolic Activity in Sand Caps Based on Activity Observed in Sediments	141
7.1.4 Organoclays Can Be Effective Cap Amendments for Select Single- and Double-ring Aromatics	142
7.2 Recommendations for Future Work	142
7.2.1 Bacteria and Archaea Clone Libraries	142

7.2.2 Estimate the Biologically-Reducible Fraction of Ferric Iron in Sand	143
7.2.3 Identification of Contaminant-Degrading Bacteria by Molecular Methods	143
7.2.4 Biodegradation of Contaminants Sorbed to Cap Amendments	144
7.2.5 Examine Inhibition of Biotransformation by Sediment Contaminants	145
Appendix A. Supplemental Material for Chapter 3	146
A1. Headspace Gas Chromatography with Flame Ionization Detection	146
A2. Liquid Scintillation Counting	148
A3. Calculations for Estimating Volumes of Biogenic Gas Production	149
A4. ¹⁴ C-Toluene Biodegradation Slurries	151
A5. Biogenic Gas Production	152
A6. Gas-Phase Contaminant Transport	153
A7. Sand Grain Size Distribution	154
Appendix B. Supplemental Material for Chapter 4	155
B1. Dissolved Methane Analysis by Gas Chromatography with Flame Ionization Detector (GC-FID)	155
B2. Sulfide Analysis by the Methylene Blue Method	156
B3. Ferrous Iron by the Phenanthroline Method	157
B4. Microbially-reducible Ferric Iron	158
B4.1 Quantitation of Fe(II)	158
B4.2 Quantitation of Fe(III) and Fe(II)	158
B5. Chloride, Phosphate, and Sulfate Analysis by Ion Chromatography	159
B6. Microbial Biomass by Phospholipid Quantification	160
B7. Sequences of PCR primers	162
B8. Surface Area Analysis	163
Appendix C. Supplemental Material for Chapter 5	164
C1. Fit of transport equation without reaction	164
C2. Dissolved Hydrogen	165

Appendix D. Supplemental Material for Chapter 6	168
D1. Calibration Curves for Hydraulic Tracers fluorescein and Bromide ...	168
References.....	169
Vita	186

List of Tables

Table 2.1: Oxidized and reduced species common in anaerobic bacterial metabolism in sediments	8
Table 2.2: Relevant properties of the contaminants of interest in sediments from Onondaga Lake.	17
Table 2.3: Median and maximum anaerobic degradation rates compiled from literature for BTEX and naphthalene by Aronson and Howard (1997) and for BTEX by Suarez and Rifai (1999).	22
Table 2.4: Anaerobic degradation rates for chlorobenzenes under methanogenic conditions	24
Table 3.1: Composition of APW used for sediment slurries to test COI biotransformation and gas production.	41
Table 3.2: Extent of biotransformation of COI under anaerobic conditions	43
Table 3.3: The mean and standard deviation of counts per minute (CPM) per mL for the pH 14 fraction (i.e., non-purgeable intermediates and CO ₂) of aqueous slurry samples after 70 days	50
Table 4.1: Sand cap column influent and steady-state effluent concentrations for columns 60105 and 70049	74
Table 4.2: Physical properties of sand and sediments and bacterial cell densities normalized by mass or surface area	85
Table 5.1: Fit pore water velocity (v), fit dispersion (D), calculated dispersivity (α), calculated influent bromide concentration (C ₀), and the coefficient of determination (R ²) for tracer breakthrough curves	99
Table 5.2: Response of reaction rate constant, k, to dispersion coefficient (D) and retardation factor (R) for column 70049	104
Table 6.1: Relevant properties and stock concentrations for sorption isotherms.	119
Table 6.2: Upflow column hydraulic parameters and sediment depth at the top of the core	120

Table 6.3: Residual analyte concentrations in sparged pore water and best-fit parameters for Freundlich and linear isotherms	123
Table 6.4: Summary of retardation factors (R) and coefficients of determination (R^2) in upflow columns with sediments from two locations with either a 15-cm thick cap of only sand or a cap with a 1-cm thick layer of organoclay topped by 14 cm of sand.....	128
Table A1: Settings and operating conditions for gas chromatography analysis of aqueous samples by headspace sample injection with flame ionization detection	146
Table A2: Representative GC-FID calibration for a 2-mL aqueous sample in a 9-mL headspace vial.....	147
Table A3: Settings for Beckman Liquid Scintillation Counter.....	148
Table A4: Data from ^{14}C -toluene biodegradation slurries.....	151
Table A5: Cumulative gas production volumes in anaerobic sediment slurries normalized to sediment mass.....	152
Table A6: Contaminant fluxes observed in gas-phase transport column tests	153
Table A7: Size distribution of sand provided by the N.Y. State Department of Transportation (NYSDOT).....	154
Table B1: Reagents for the analysis of ferrous iron by the phenanthroline method.	157
Table C1: Summary of fit of transport equation without reaction to column effluent data	164

List of Figures

Figure 2.1: Example sediment cap configurations (U.S. EPA, 2005).....	6
Figure 2.2: Proposed degradation pathway of monoaromatics by the benzoyl-CoA pathway.	20
Figure 3.1: Conceptualization of gas-phase contaminant transport through a sediment cap	27
Figure 3.2: Map of the southeastern shore of Onondaga Lake with SMU delineation.	30
Figure 3.3: Laboratory column set-up for simulating flow through sand-capped sediment.....	34
Figure 3.4: Apparatus for measuring gas-phase contaminant flux.....	37
Figure 3.5: Contaminant loadings on sediments representative of each SMU.	38
Figure 3.6: Dissolved concentrations of biogeochemical indicators of anaerobic metabolism.....	40
Figure 3.7: Identical slurries with sediment from location 70049 incubated at 22°C and 12°C	44
Figure 3.8: Breakthrough curves for toluene and monochlorobenzene in a sand column connected in series to a column containing sediment from location 70049.....	49
Figure 3.9: Maximum values for (a) the cumulative volume of gas produced (μL of gas per gram of sediment) and (b) the rate of gas production (μL of gas per gram of sediment per day) in each SMU at three incubation temperatures.....	52
Figure 3.10: Gas-phase flux of 1,4-dichlorobenzene from a column packed with sediment from location 10118	55
Figure 3.11: Gas-phase contaminant fluxes observed in column tests and predicted from aqueous-phase concentrations and equilibrium partitioning to the gas phase.....	56

Figure 3.12: Theoretical flow diagram showing cap design considerations based on laboratory tests of contaminant biotransformation	60
Figure 3.13: Theoretical flow diagram showing cap design considerations based on laboratory tests of gas production and contaminant transport	61
Figure 4.1: Laboratory column set-up for simulating sand-capped sediment	67
Figure 4.2: Toluene influent and effluent observations in column 70049	77
Figure 4.3: Ferrous iron concentrations in sand cap column influent and effluent samples from column 70049.....	77
Figure 4.4: Amplification of the <i>bssA</i> gene	79
Figure 4.5: T-RFLP electropherograms from sediment DNA.	81
Figure 4.6: T-RFLP electropherograms for sections of the sand column	82
Figure 4.7: Bacterial community similarity indices.	84
Figure 5.1: Material balance on bromide for the sand cap column.....	93
Figure 5.2: Tracer influent profile, effluent observations, and best-fit effluent profile.	98
Figure 5.3: Toluene concentration profiles in columns with sediments from four distinct locations	101
Figure 5.4: Effluent-to-influent ratio against contaminant half-life at steady-state for two different values of dispersion.....	103
Figure 5.5: Ferrous iron concentrations in sand cap influent and effluent	105
Figure 5.6: Dissolved methane concentrations normalized to maximum concentration in effluent from cap and sediment samples	106
Figure 5.7: Dissolved hydrogen concentrations in cores from column 60105	111
Figure 6.1: Schematic for organoclay-amended sand cap columns and sand only (“baseline”) cap columns.....	121

Figure 6.2: Freundlich isotherms for ethylbenzene, naphthalene, toluene, total xylenes, monochlorobenzene, and the three dichlorobenzene	124
Figure 6.3: Solute adsorption to PM-199 organoclay as a function of (a) solubility and (b) dipole moment.....	126
Figure 6.4: Breakthrough curves for baseline column 1A and organoclay-amended columns 1B	130
Figure 6.5: Breakthrough curves for baseline column 2A and organoclay-amended columns 2B	131
Figure 6.6: Comparison of adsorption in column and batch tests.....	134
Figure B1: A representative calibration curve for dissolved methane by GC-FID. .	155
Figure B2: A representative calibration curve for sulfide analysis.....	156
Figure B3: A representative calibration curve for ferrous iron.....	157
Figure B4: Calibration curves for chloride, phosphate, and sulfate.....	159
Figure B5: A representative calibration curve for molybdophosphate.	161
Figure C1: Calibration curve for hydrogen on the reducing gas analyzer.....	167
Figure D1: Standard curves for the hydraulic tracers fluorescein and bromide. .	168

List of Acronyms

APW	--	artificial porewater
BSA	--	bovine serum albumin
<i>bssA</i>	--	benzylsuccinate synthase, subunit α
BTEX	--	benzene, toluene, ethylbenzene, and xylene
COIs	--	contaminants of interest
DOC	--	dissolved organic carbon
DNA	--	deoxyribonucleic acid
dNTP	--	deoxynucleoside triphosphate
EDTA	--	ethylene diamine tetraacetic acid
FISH	--	fluorescent in situ hybridization
GC-FID	--	gas chromatography with flame ionization detector
ILWD	--	in-lake waste deposit
MCAWW	--	Methods for the Chemical Analysis of Water and Wastes
NAPL	--	non-aqueous phase liquid
N.Y. DEC	--	New York State Department of Environmental Conservation
OLSW	--	Onondaga Lake surface water
OTU	--	operational taxonomic unit
PAH	--	polycyclic aromatic hydrocarbon
PCB	--	polychlorinated biphenyl
PCR	--	polymerase chain reaction
rRNA	--	ribosomal ribonucleic acid
SIP	--	stable isotope probing
SMU	--	sediment management unit
SUVA	--	specific ultra-violet absorbance
TEA	--	terminal electron acceptor
TEAP	--	terminal electron-accepting process
T-RFLP	--	terminal-restriction fragment length polymorphism
U.S. EPA	--	United States Environmental Protection Agency

List of Symbols

$1/n$	=	Freundlich exponent [--]
BC	=	Bray-Curtis similarity index
C	=	substrate concentration [$M_{\text{substrate}} L^{-3}$]
C_e	=	aqueous-phase concentration at equilibrium [$M L^{-3}$]
C_g	=	gas-phase concentration [$M L^{-3}$]
C_w	=	concentration in water [$M L^{-3}$]
D	=	dispersion coefficient [$L^2 T^{-1}$]
D_{eff}	=	effective (tortuosity-corrected) diffusion coefficient [$L^2 T^{-1}$]
D_w	=	molecular diffusivity in water [$L^2 T^{-1}$]
$E_{1/D}$	=	Simpson's evenness index
E_{var}	=	the Smith-Wilson evenness index
f_{OC}	=	organic carbon fraction [--]
H	=	Henry's Law constant
J	=	Jaccard's index of similarity
k	=	first-order rate constant [T^{-1}]
K_d	=	linear partitioning coefficient [$M_i M_{\text{sorbent}}^{-1} / M_i L_{\text{aq}}^{-3}$]
K_f	=	Freundlich coefficient [$M_i^{1-1/n} L^{3/n} M_{\text{sorbent}}^{-1}$]
K_{ow}	=	octanol-water partitioning coefficient [$M_i L^{-3}_{\text{octanol}} / M_i$]
K_s	=	half-saturation coefficient [$M_{\text{substrate}} L^{-3}$]
L_{column}	=	column length [L]
M_i	=	mass of species i [M]
M_{sorbent}	=	mass of sorbent [M]
P	=	Peclet number (Lv/D) [--]
P_v	=	pure-phase vapor pressure [$M L^{-1} T^{-2}$]
q	=	ratio of mass of sorbate to mass of sorbent
\hat{q}	=	maximum substrate utilization rate [$M_{\text{substrate}} M_{\text{cells}}^{-1} T^{-1}$]
Q	=	volumetric flow rate [$L^3 T^{-1}$]
R	=	retardation factor [--]
t	=	time [T]
T	=	dimensionless time (Vt/L_{column}) [--]
v	=	interstitial (porewater) velocity [$L T^{-1}$]
X	=	biomass concentration [$M_{\text{cells}} L^{-3}$].
z	=	depth [L]
Z	=	dimensionless position (z/L) [--]
α	=	hydrodynamic dispersivity [L]
ε	=	medium porosity [--]
μ	=	Damkohler number (kL/v) [--]
ρ_b	=	solid bulk density [$M_{\text{solids}} L_{\text{Total}}^{-3}$]
Ψ	=	solution to the transport equation

Chapter 1. Introduction

1.1 OVERVIEW

Contaminated sediments pose potential health risks to aquatic organisms as well as to higher trophic-level consumers. Roughly one-hundred watersheds in the United States contain “areas of probable concern” stemming from the contamination of surface water sediments and the perceived risk of exposure (U.S. EPA, 2005). Minimizing the risks of exposure by organisms to sediment-borne contaminants requires effective, long-term, sediments-management solutions.

The remediation of polluted surface water sediments poses many technical challenges. Common methods for remediation include dredging, monitored natural attenuation, and in situ capping. Dredging is typically accepted by stakeholders because contaminant mass is physically removed from the site, but consideration must be given to particle suspension, dredging residuals, and costs and logistics associated with transportation, treatment, and disposal of the dredged material. Monitored natural attenuation relies on a combination of transport processes and contaminant sinks to attenuate contaminant flux, with contaminant removal occurring over long periods of time. In situ capping is the placement of clean sand, soil, or sediment atop impaired sediments. The contaminant mass is left in place, but capping effectively separates benthic organisms from underlying sediment contaminants, thus reducing the potential for contaminant exposure by benthos.

In situ capping is an increasingly popular alternative for the management of contaminated sediments. In addition to serving as a physical barrier between biota and sediment pollutants, recent research suggests that the cap can be colonized by bacteria from the sediment that are capable of transforming contaminants passing through the cap. The overarching purpose of this research is to assess the potential and limitations of biotransformation of select contaminants in

sediment caps and to evaluate methods for characterizing biological activity, specifically contaminant biotransformation and biogenic gas production, in sediments and sediment caps. Improved understanding of biological processes in sediments and caps could reduce uncertainty in contaminant fate and transport modeling and aid in the design of sediment caps.

1.2 RESEARCH OBJECTIVES AND DISSERTATION OUTLINE

The characterization of microbiological processes in sediment caps was pursued via four research objectives. Chapter 2 reviews the relevant literature, and Chapters 3-6 address the following objectives:

- (1) Assess the potential for contaminant biotransformation and gas-phase pollutant transport resulting from biogenic gas production in sediments and sand caps and evaluate laboratory methods for aiding in sediment cap design (Chapter 3),
- (2) Demonstrate that a sand cap can become a zone of contaminant biotransformation at low temperature and at redox potentials representative of a cap at depth, and assess whether comparing bacterial community structure in sediments and in a sand cap is useful for predicting potential metabolic activity in a sand cap based on observed activity in sediments (Chapter 4),
- (3) Describe the operation of anaerobic sand-capped sediment columns and examine thermodynamic and kinetic explanations for results with regard to contaminant biotransformation (Chapter 5),
- (4) Evaluate the performance of an organophilic clay capping amendment (for enhanced adsorption of dissolved hydrocarbons) for consideration at locations lacking demonstrable biotransformation capability (Chapter 6).

Conclusions, implications, and recommendations for future work are presented in Chapter 7.

Chapter 2. Background

2.1 CONTAMINATED SEDIMENTS

Approximately 10% of sediments in surface water bodies in the United States are considered “sufficiently contaminated with toxic pollutants to pose potential risks to fish and to humans and wildlife that eat fish” (U.S. EPA, 1998). The list of contaminants includes nutrients such as nitrogen and phosphorus that contribute to eutrophication as well as organic chemicals and metals that have toxicological effects on fish, wildlife, and humans. Some chemicals, including hydrocarbons, may be ingested by benthic organisms (inhabitants of surface sediments), stored in lipids, and transferred to predators further up the food web (Schwarzenbach et al., 2003). The limited ability of aquatic organisms to metabolize or purge certain sediment contaminants from their bodies can pose health risks to higher-order consumers such as humans.

Benthic organisms represent likely points of pollutant introduction into the food web because of their direct and potentially prolonged contact with contaminated sediments (Apitz et al., 2004). Routes of exposure include absorption and ingestion of aqueous phase contaminants as well as ingestion of sediment-bound chemicals that desorb from the sediment and partition to the organism (Schwarzenbach et al., 2003). Fate and transport mechanisms controlling benthic organism exposure to pollutants include contaminant sorption and desorption between the sediments and the aqueous phase, transport within the aqueous phase by advection and diffusion, bioturbation (the mixing of sediments by benthic organisms), sediment particle suspension, and biotic and abiotic contaminant transformation (Apitz et al., 2004). Identification and quantitative description of chemical fate and transport processes, such as biotransformation, are necessary for evaluating sediment management strategies intended to reduce contaminant exposure risks (U.S. EPA, 2005).

2.2 REMEDIATION OPTIONS FOR CONTAMINATED SEDIMENTS

2.2.1 Sediment Management Objectives

The goal of polluted-sediment management is often to minimize contaminant uptake by biota to prevent human exposure (Perele, 2010). In-situ capping is a remediation strategy involving the placement of clean fill material, such as sand or gravel, atop contaminated sediments to isolate the chemicals of concern from the benthic community (Figure 1.1). Sediment caps, typically about one meter in thickness, function to stabilize contaminated sediments and prevent sediment suspension, inhibit contaminant remobilization by bioturbation, and isolate contaminants from the overlying water column (U.S. EPA, 2005). Additionally, recent studies suggest that a sediment cap can become a zone of contaminant biotransformation following colonization by bacteria from the sediment (Hyun et al., 2006; Himmelheber et al., 2009).

Capping has proven effective at reducing contaminant fluxes from sediments into the benthic zone (Schaaning et al., 2006). Application of a sediment cap increases the distance that a chemical must migrate to reach the overlying water, and transport of the chemical is retarded according to its tendency to sorb to the cap material (Thoma et al., 1993). For a traditional sand cap subject to diffusion-controlled transport, fluxes of hydrophobic chemicals including polycyclic aromatic hydrocarbons (PAHs) and polychlorinated biphenyls (PCBs) to the overlying water are generally sufficiently reduced to meet risk reduction goals (Eek et al., 2008). However, certain site conditions require that engineered or natural recovery measures be enhanced to meet management objectives. For example, sediment contaminated with highly soluble and low-sorbing chemicals, such as monoaromatic compounds, may require cap amendments for enhanced sequestration, substantial mass removal by biotransformation, or both.

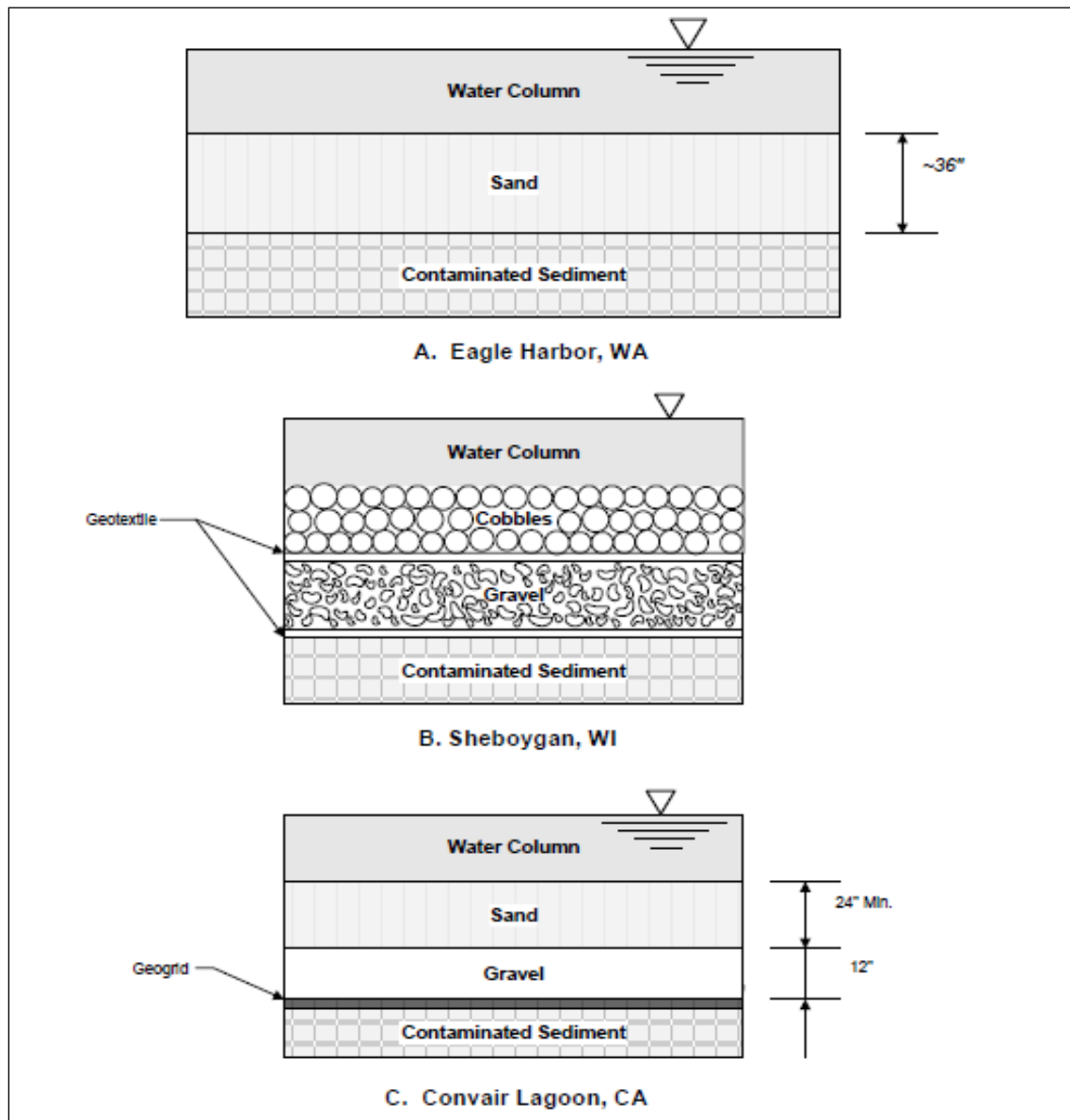


Figure 1.1: Example sediment cap configurations (U.S. EPA, 2005).

2.2.2 Cap Colonization by Microorganisms and Bacterial Metabolic Activity

Following placement of a sediment cap, it can become colonized by microorganisms from the sediment (Himmelheber et al., 2008), contributing to a vertical translation of thermodynamically-stratified redox zones (namely oxic, denitrifying, iron-reducing, sulfidogenic, and methanogenic). The distance over which this stratification exists is

approximately 10 cm in freshwater sediments (Nealson, 1997; Himmelheber et al., 2008), and roughly the top half of this zone is subject to substantial bioturbation (Matisoff et al., 1985). Most of the cap and all of the underlying sediment are reduced, and methanogenesis is the predominant terminal electron accepting process (TEAP) (Capone and Kiene, 1988; Schink, 1988; Fava and Agathos, 2006). Bioturbation and the presence of oxygen are two factors that affect bacterial metabolic activity in sediments and sediment caps.

While the top several centimeters of sediments or a sediment cap are subject to bioturbation, the aerobic zone is often less than one cm thick and lies completely within the bioturbation zone. The activity of benthic organisms has been shown to encourage bacterial growth (Smith, 2006) and to stimulate bacterial degradation of PAHs under aerobic conditions (Chung and King, 1999) as compared to sediments that were not subjected to bioturbation. Considering that rates of hydrocarbon oxidation are typically greater for aerobic than anaerobic environments, the potential for contaminant biodegradation in zones of sediments or sediment caps that are aerobic and subject to bioturbation is considerable. However, the aerobic layer is comparatively thin, and because the zone of bioturbation extends beyond the aerobic layer into the anaerobic region, aerobic contaminant biodegradation alone is insufficient for minimizing exposure by benthos to pollutants. For example, the point of compliance for contaminant concentrations in porewater in a sediment cap in Onondaga Lake is 30 cm beneath the interface between the cap and overlying surface water (N.Y. DEC and U.S. EPA, 2005), well below the aerobic zone.

The comparative thicknesses of anaerobic and aerobic regions of sediments mean that anaerobic processes can contribute substantially to hydrocarbon metabolism (Hunkeler et al., 1998). In freshwater sediment caps, hydrocarbon oxidation is likely coupled with the reduction

of nitrate, manganese oxides, ferric oxides, and carbon dioxide, while sulfate reduction contributes minimally given the low sulfate concentrations typically encountered in freshwater systems. Following exhaustion of thermodynamically favored terminal electron acceptors (TEAs) in the sand cap, methanogenesis will become the dominant TEAP; substrates will be fermented to hydrogen, carbon dioxide, and low molecular weight fatty acids with subsequent methane production (Hoehler et al., 1998).

TEAPs have been shown to influence pollutant biodegradation rates in anaerobic sediments (Phelps and Young, 1999), and their biogeochemical signatures can provide an additional line of evidence for contaminant mineralization (Maurer and Rittmann, 2004). Dominant TEAPs can be identified by depletion of the oxidized species (e.g., disappearance of sulfate along a flow path) or production of the reduced species (e.g., formation of sulfide) (Table 2.1), though abiotic reactions such as the reduction of manganese- and iron-oxides by sulfides or the reduction of manganese-oxides by ferrous iron (van Cappellan and Wang, 1996) can confound biological TEAP identification (Maurer and Rittmann, 2004).

Table 2.1: Oxidized and reduced species common in anaerobic bacterial metabolism in sediments in order of thermodynamic yield (Stumm and Morgan, 1996).

Process	Oxidized Species	Reduced Species
Manganese reduction	$\text{MnO}_{2(s)}$	Mn^{2+}
Iron reduction	$\text{FeOOH}_{(s)}$	Fe^{2+}
Sulfate reduction	SO_4^{2-}	S^{2-}
Methanogenesis	CO_2	CH_4

2.2.3 Bacterial activity in sediments beneath a cap

Placement of a sediment cap alters redox conditions and carbon availability with implications for biogenic gas production and bacterial contaminant transformation. Sediments

are further reduced following placement of a cap and methanogenesis or acetogenesis are the dominant TEAPs in the underlying sediments. Anaerobic metabolism resulting in production of carbon dioxide and methane may lead to the formation of a separate gas phase. In addition to aqueous advective and diffusive transport, contaminants can be transported with gas bubbles by absorbing into a bubble (by volatility) or attaching to the surface of a bubble (by hydrophobicity) (Yuan et al., 2007; 2009). Once the pressure of biogenic gas bubbles surpasses a threshold, the gas is released rapidly in a process called “ebullition”. The release of gas transports absorbed and attached contaminants to the overlying water and may create preferential flow paths, allowing aqueous advective and diffusive transport of contaminants to proceed with reduced retardation.

Methane is produced only by a subclass of bacteria called Archaea, which includes hydrogenotrophs that consume carbon dioxide and hydrogen to form methane, and acetoclastic methanogens that ferment acetate to carbon dioxide and methane. The substrates required for methanogenesis are produced by heterotrophs that decompose large organic molecules to low molecular weight fatty acids that can be fermented; these fermentation products (e.g., hydrogen, carbon dioxide, and acetate) are substrates for methanogens (Lovley and Klug, 1982). The labile organic matter required by heterotrophs decreases with sediment depth, and the placement of a cap restricts the deposition of new labile organic matter to the sediment. This suggests that the rate of biogenic gas production will decrease over time in capped sediments and that the duration of gas production depends upon the composition of the cap and the mobility of labile hydrocarbons (Wang et al., 2009).

Reduction of the porewater oxidation-reduction potential in capped sediments has positive and negative implications for bacterial metabolic activity. Reactions such as reductive dehalogenation (i.e., substitution of a halogen atom by a hydrogen atom) require reduced

conditions (Dolfing and Harrison, 1992), which can result from capping. However, dehalogenation also requires a steady supply of electron donor, which, as mentioned above, can become depleted in capped sediments. Dechlorination of perchloroethylene and trichloroethylene in sediments capped with sand required electron donor supplementation (Himmelheber et al., 2007), demonstrating the potential for biostimulation of the dechlorinating bacterial community in capped sediments.

2.3 REQUIREMENTS FOR CONTAMINANT BIOTRANSFORMATION

Several requirements must be satisfied for the biotransformation of organic pollutants to proceed. These include the presence of (1) microorganisms that produce degradative enzymes, (2) energy sources, (3) electron acceptors, (4) nutrients, and (5) moisture; appropriate (6) pH and (7) temperature; (8) the absence of toxicity; and (9) the removal of metabolites (Cookson, 1995; Alvarez and Illman, 2006). Previous research suggests that these requirements can be satisfied in sand-based sediment caps (Hyun et al., 2006; Himmelheber, 2008).

2.3.1 Microorganisms Capable of Catalyzing Pollutant Biotransformation

For microorganisms capable of pollutant biodegradation to be present in a sediment cap, they must either be indigenous to the sediment (with subsequent migration to the cap) or seeded in the cap material by bioaugmentation. Biodegradation in a sand cap was demonstrated in column tests with the PAHs naphthalene, fluorene, phenanthrene, and anthracene (Hyun et al., 2006). The capped sediment had been exposed to coal tar, and degradation was found to be a function of the degree of aeration of the artificial groundwater. Microbial analysis of the cap was not performed, but column results suggested the presence of sediment-borne bacteria capable of aerobic PAH degradation in the sand cap. Himmelheber et al. (2009) operated sand-capped sediment columns with a steep redox gradient and observed bacterial densities in sand smaller

than, but comparable to, those in sediments. Seemingly, the development of a bacterial community that includes contaminant-degraders at bacterial densities sufficient for contaminant biodegradation can develop in sand-based sediment caps.

2.3.2 Bioavailable Nutrients, Energy Sources, and Electron Acceptors

In addition to the presence of appropriate microorganisms, pollutant biotransformation requires nutrients, energy sources, and electron acceptors. Sediments are generally rich in nutrients including nitrogen, phosphorus, and sulfur, but are often carbon-limited (Alexander, 1999). Whether hydrocarbon contaminants serve as sources of carbon and energy or as terminal electron acceptors, contaminant bioavailability might be limited because of mass transfer processes such as sorption to sediment particles or partitioning into a non-aqueous phase liquid (Alvarez and Illman, 2006). Though it is generally accepted that only dissolved contaminants are bioavailable, that notion has been challenged by recent reports of biotransformation of chlorobenzenes sorbed to sediment particles (Lee et al., 2009) and organophilic clays (Witthuhn et al., 2006), as well as biotransformation of 2,4-dinitrophenol sorbed to organophilic clays (Witthuhn et al., 2005).

Bioavailable contaminant concentrations must be sufficiently high to induce the expression of genes involved in degradation (Alexander, 1999), but not so high that they or their metabolic intermediates impart toxicity to the bacteria. For example, aerobic biodegradation of toluene was initiated at concentrations near 50 $\mu\text{g/L}$ (Robertson and Button, 1987), while catechol, an intermediate of aerobic benzene degradation, was found to be inhibitory to *Pseudomonas putida* strain F1 at a concentration of 10 mg/L (Muñoz et al., 2007). While contaminant biotransformation in sediments can be inhibited by toxicity due to high contaminant

concentrations, biotransformation reactions may proceed at the lower contaminant concentrations characteristic of a sand cap.

Electron acceptor bioavailability does not require dissolution into the aqueous phase. For instance, the reduction of sediment-bound manganese- and iron-oxides can occur in subsurface anaerobic respiration (Lovley, 1993) by direct contact between cell and mineral, electron shuttles such as dissolved organic matter, or nanowires (Weber et al., 2006). Although the oxidation of many common pollutants is thermodynamically feasible even in highly reduced environments, the addition of a thermodynamically-favored electron acceptor may stimulate biological activity (Barker, 2004). In a laboratory sand cap colonized by sediment bacteria, dissimilatory iron-reduction was the dominant TEAP (Himmelheber et al., 2008), suggesting that sand that is rich in iron-oxide content could supply an electron donor to bacteria in the cap.

2.3.3 Moisture, pH, and Temperature

In subaqueous sediments, satisfaction of the requirement for moisture is assured. Porewater pH, however, is potentially more variable, especially over distances that separate microenvironments. Pollutant biotransformation has been shown to slow as porewater pH deviates from neutrality (Atlas, 1981). Fahy et al. (2008) isolated bacteria from a BTEX-contaminated aquifer with groundwater pH ranging from 7.6 – 12.3. While each of the 14 isolates was able to degrade benzene at pH 6 - 8, only two degraded benzene at pH > 9.0. The inclusion of minerals in a sediment cap for adjusting and buffering abnormally high pH porewater in contaminated sediments is being investigated (Vlassopoulos et al., 2011) and might be a means to promote pollutant biotransformation.

Porewater temperature theoretically affects the rates of contaminant biodegradation but is not likely to completely inhibit biodegradation at temperatures typical of surface water sediments

(i.e., 5°C - 15°C). Biodegradation of PCBs at 4°C (Williams and May, 1997), of diesel hydrocarbons at 5°C (Whyte et al., 1998), and of PAHs at 8°C (Aislabie et al., 1998) has been reported. A decrease in temperature of 10°C typically decreases reaction rates by half (Cookson, 1995); thus biodegradation studies conducted near 20°C tend to over-predict rates of reaction in the field. However, biodegradation can be rapid at low temperatures, as evidenced by the observation of comparable rates of mineralization of toluene in sediments from a near-arctic aquifer and a temperate aquifer at 5°C and 20°C, respectively (Bradley and Chapelle, 1995).

2.3.4 The Absence of Toxicity

Impaired sediments are frequently affected by more than a single pollutant, and the contaminant mixture can impart toxicity to microbiota and inhibit biotransformation (Fava and Agathos, 2006). Toxicity in a sand cap is likely less than that in sediments because contaminant concentrations will be reduced in a cap relative to sediments (Lampert, 2010) and chemicals will not all migrate at the same rate, thus potentially diminishing the inhibitory effect created by the mixture of pollutants. Reduced toxicity in a sand cap is one factor that might contribute to biotransformation in the cap despite an apparent lack of biotransformation in the underlying sediments.

2.3.5 The Removal of Metabolites

While select microorganisms are capable of completely degrading contaminants to innocuous end-products in pure culture, most are not. Intermediates in metabolic degradation pathways might be toxic to bacteria upon accumulation and thus require removal by other bacteria. Additionally, fermentative pathways result in the production of hydrogen and acetate that must be removed to prevent degradation reactions from becoming thermodynamically infeasible. The diversity of metabolic niches typical of sediments facilitates removal of

metabolites, both to prevent the development of toxicity and to maintain thermodynamic feasibility for degradation reactions (Nealson, 1997).

2.4 MODELING CONTAMINANT FATE AND TRANSPORT

2.4.1 Modeling Contaminant Biotransformation

Biological catabolism of a substrate is typically described by the Monod equation (Rittmann and McCarty, 2001):

$$\frac{dC}{dt} = -\frac{\hat{q}C}{K_s + C} X \quad \text{Equation 2.1}$$

where C = substrate concentration [$M_{\text{substrate}} L^{-3}$]
 \hat{q} = the maximum substrate utilization rate [$M_{\text{substrate}} M_{\text{cells}}^{-1} T^{-1}$]
 K_s = half-saturation coefficient [$M_{\text{substrate}} L^{-3}$], and
 X = biomass concentration [$M_{\text{cells}} L^{-3}$].

In natural systems, it is common that $C \ll K_s$, so Equation 2.1 simplifies to a first-order expression

$$\frac{dC}{dt} = -kC \quad \text{Equation 2.2}$$

where k is the first-order reaction rate constant [T^{-1}]. A first-order kinetic expression is assumed to apply in all biodegradation tests described henceforth.

2.4.2. The Governing Equation for Solute Transport in Porous Media

Solute transport in porous media subject to advection, dispersion, linear sorption, and first-order reaction is described by

$$R \frac{\partial C}{\partial t} = D \frac{\partial^2 C}{\partial z^2} - v \frac{\partial C}{\partial z} - kC \quad \text{Equation 2.3}$$

where R is the retardation factor [--], the ratio of the total mass (i.e. sorbed and mobile) of species i in a control volume to the mass of species i in the mobile phase; D is the dispersion

coefficient [L^2/T]; z is position [L]; v is porewater velocity [L/T]; and the other variables are as defined previously. The retardation factor is the ratio of the total material in a control volume to the material in the aqueous phase of that volume, computed by

$$R = 1 + \frac{\rho_b K_d}{\varepsilon} \quad \text{Equation 2.4}$$

where ρ_b is the solid bulk density [$M_{\text{solids}} / L^3_{\text{Total}}$], ε is the medium porosity [--], and K_d is the linear partitioning coefficient [$M_i/M_{\text{sorbent}} / M_i/L^3_{\text{aq}}$], where M_i is the mass of species i , M_{sorbent} is the mass of sorbent, and L^3_{aq} is the aqueous-phase volume. Transformed to non-dimensional variables, Equation 2.3 becomes

$$R \frac{\partial C}{\partial T} = \frac{1}{P} \frac{\partial^2 C}{\partial Z^2} - \frac{\partial C}{\partial Z} - \mu C \quad \text{Equation 2.5}$$

where T is dimensionless time (Vt/L , where L is the column length), P is the Peclet number (Lv/D), Z is the dimensionless position (z/L), and μ is the Damkohler number (kL/v). Specific solutions to the general transport equation depend on initial and boundary conditions and are described on an individual basis.

2.5 CONTAMINANTS OF STUDY

2.5.1 Contaminants in Onondaga Lake Sediments

The studied chemicals are those found in Onondaga Lake sediments and include 1,2-dichlorobenzene, 1,3-dichlorobenzene, 1,4-dichlorobenzene, and monochlorobenzene, the semi-volatile PAH naphthalene, and the common, volatile groundwater contaminants benzene, ethylbenzene, toluene, and xylene (BTEX). Relevant properties are summarized in Table 2.2.

Onondaga Lake is located slightly north of Syracuse, New York. Its surface area and mean depth are roughly 11.9 square kilometers and 10.9 meters, respectively (Effler and Harnett,

1996). A chemical plant operated on the western shore of the lake from 1884 – 1986 disposed of large quantities of wastes in or around the lake including chloride salts, calcium carbonate, and chlorinated hydrocarbons (Effler, 1987; Rowell, 1996). Additionally, a wastewater treatment facility that discharges effluent to the lake began operating in 1960. Before 1980, flow exceeding 170 million gallons per day bypassed the plant and was discharged directly to the lake, elevating nutrient and bacterial loadings (Effler, 1987). Plagued by hypoxic zones, eutrophication, bacterial loadings, and hazardous chemical contamination, Onondaga Lake was placed on EPA's Superfund National Priority List on December 16, 1994 (U.S. EPA, 2011). According to a draft plan, management of the lake bottom will include sediment dredging, capping, and monitored natural attenuation (N.Y. DEC, 2009). As noted in Section 2.2.2, the Record of Decision for Onondaga Lake states that, for sediments that will be capped, the point of compliance for contaminant concentrations in sediment cap porewater is 30 cm below the interface between the cap and the overlying water (N.Y. DEC and U.S. EPA, 2005). Because sediment contaminants will only be exposed to anaerobic conditions in sediments and in the cap beneath the point of compliance, anaerobic processes (i.e., biotransformation and biogenic gas production) will be emphasized in this study.

Table 2.2: Relevant properties of the contaminants of interest in sediments from Onondaga Lake.

Chemical	Molecular Formula	Formula Weight (g/mol)	Density (g/mL)	Henry's Constant (C_g/C_w) ^a	Vapor Pressure, P_v (Pa) ^b	Aqueous Solubility, $C_{\text{solubility}}$ (μM) ^b	$\log K_{ow}$ ^{b,c}	$D_w \times 10^{-5}$ (cm^2/s) ^{d,e}
1,2-Dichlorobenzene	$\text{C}_6\text{H}_4\text{Cl}_2$	147.0	1.30	0.040	199.53	891.3	3.40	0.552
1,3-Dichlorobenzene	$\text{C}_6\text{H}_4\text{Cl}_2$	147.0	1.29	0.067	281.84	831.8	3.47	0.552
1,4-Dichlorobenzene	$\text{C}_6\text{H}_4\text{Cl}_2$	147.0	1.25	0.053	112.20	501.2	3.45	0.552
Benzene	C_6H_6	78.1	0.88	0.150	12589	22390	2.17	0.682
Chlorobenzene	$\text{C}_6\text{H}_5\text{Cl}$	112.6	1.11	0.089	1584.9	4074	2.78	0.608
Ethylbenzene	C_8H_{10}	106.2	0.86	0.183	1230.3	1585	3.20	0.546
Naphthalene	C_{10}H_8	128.2	1.16	0.020	11.220	251.2	3.33	0.500
Toluene	C_7H_8	92.2	0.87	0.160	3715.4	6026	2.69	0.604
m-Xylene	C_8H_{10}	106.2	0.86	0.169	1096.5	1514	3.30	0.546

^a EPA Office of Solid Waste and Emergency Response, at 15°C
(<http://www.epa.gov/athens/learn2model/part-two/onsite/esthenry.html>)

^b Schwarzenbach et al. (2003)

^c K_{ow} is the octanol-water partitioning coefficient ($C_{\text{oct}}/C_{\text{water}}$), an indicator of a chemical's hydrophobicity

^d D_w is the molecular diffusivity in water, the proportionality constant relating the concentration gradient to the flux of a solute

^e At 12°C after Hayduk and Laudie (1974), using 1.22 centipoise for the viscosity of water

2.5.2 Biotransformation of the Contaminants of Study

BTEX biotransformation under anaerobic conditions has been studied extensively (Grbic-Galic and Vogel, 1987; Holliger and Zehnder, 1996). BTEX are highly soluble in water and therefore demonstrate high mobility through porous media. They are not common contaminants in surface-water sediments but might be present in sediment porewater due to upwelling of polluted groundwater or to dumping of BTEX-containing wastes into surface water bodies. Biodegradation of BTEX has been observed under denitrifying, iron-reduction, sulfate-reduction, and methanogenic conditions (Vogel and Grbic-Galic, 1986; Wilson et al., 1986; Grbic-Galic and Vogel, 1987; Edwards and Grbic-Galic, 1994; Lovley et al., 1995; Kazumi et al., 1997; Anderson et al., 1998; Kunapuli et al., 2008).

The initial step in the anaerobic biodegradation of benzene is believed to be activation by addition of one of three possible functional groups: (1) a hydroxyl group to give phenol (Grbic-Galic and Vogel, 1987), (2) a carboxyl group to produce benzoate (Coates et al., 2002), or (3) a methyl group to form toluene (Caldwell and Suflita, 2000), with pathways largely converging to benzoyl-CoA (Harwood et al., 1998). Prevalence of the pathway through toluene is anecdotally supported by the inhibition of benzene degradation by toluene; the reaction does not become thermodynamically favorable until the reaction product (toluene) is largely removed (Da Silva and Alvarez, 2004; Kunapuli et al., 2008). Toluene degradation proceeds through fumarate addition to form benzylsuccinate, a biomarker of anaerobic biodegradation (Beller, 2002; Young and Phelps, 2005). Similarly, methylbenzylsuccinate and ethylbenzylsuccinate are indicators

of anaerobic biodegradation of xylene isomers and ethylbenzene, respectively (Beller, 2002; Alumbaugh et al., 2004; Young and Phelps, 2005). Biomarker detection in groundwater contaminant plumes offers evidence of microbial biodegradation.

Chlorobenzenes are common industrial chemicals used as pesticides, dyes, and intermediates in the manufacture of other chemicals (Meek et al., 1994). In anaerobic environments they may be biotransformed by dehalogenation, as has been observed in several freshwater bodies in Germany, including the Rhine (Beurskens et al., 1995) and Saale (Nowak et al., 1996) Rivers and the Bitterfeld aquifer (Braeckvelt et al., 2007). Specifically, dehalogenation of dichlorobenzenes to monochlorobenzene has been reported (Ramanand et al., 1993; Masunaga et al., 1996 Fung et al., 2009) with subsequent dehalogenation to benzene (Fung et al., 2009) and further transformation as described previously (Figure 2.2).

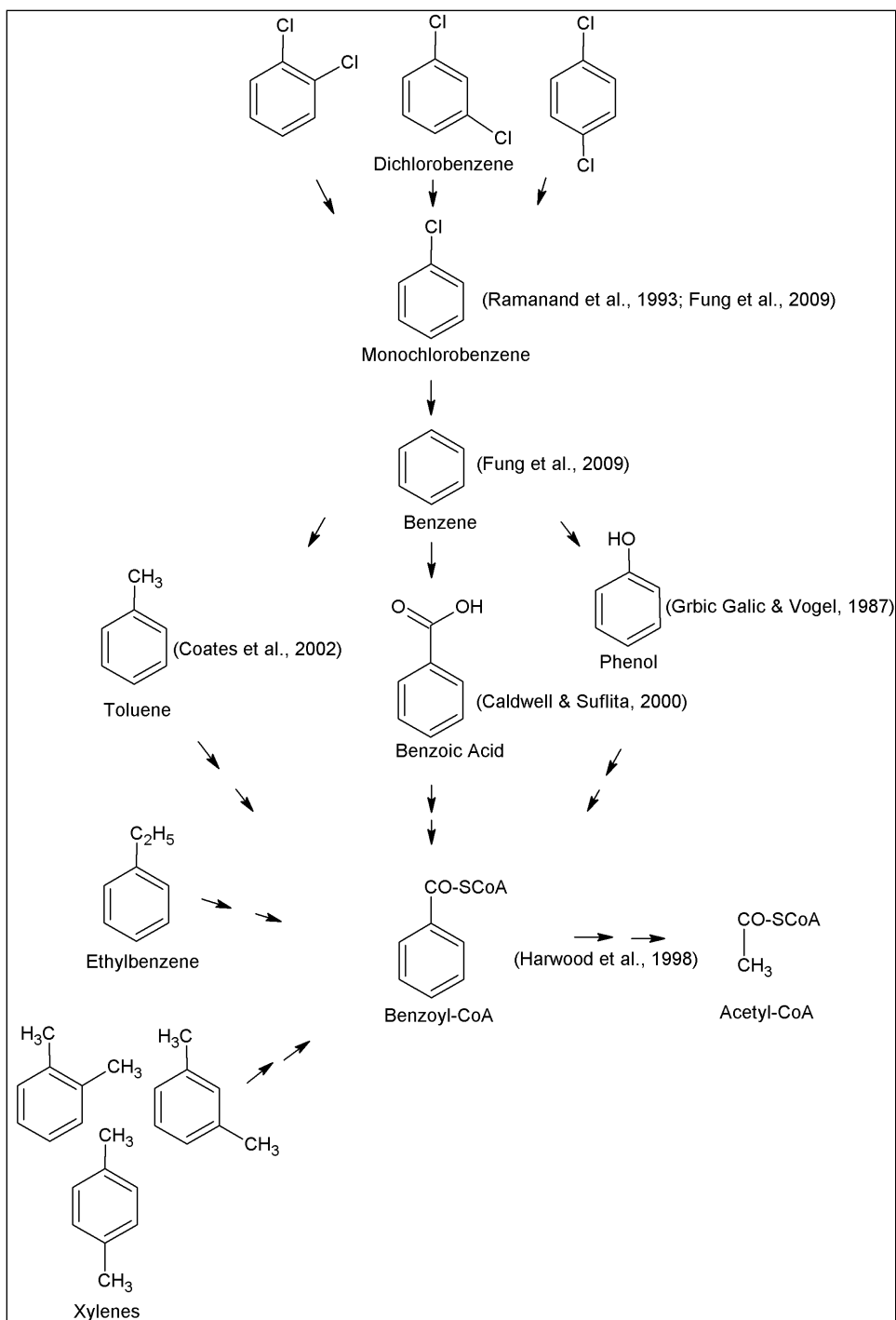


Figure 2.2: Proposed degradation pathway of monoaromatics by the Benzoyl-CoA pathway. Double arrows indicate multiple intermediary reactions.

Naphthalene is a widespread contaminant in surface-water sediments whose degradation is well-characterized (Neilson and Allard, 2008). Metabolic pathways and bacteria capable of utilizing naphthalene as a sole carbon and energy source have been identified (Zhang and Young, 1997). Additionally, stable isotope probing (SIP) has been applied to identify active naphthalene-degrading bacteria in a soil bioreactor (Singleton et al., 2005). Only recently has naphthalene degradation under methanogenic conditions been observed. Chang et al. (2005, 2006) observed decreased biotransformation rates of naphthalene and phenanthrene in enrichment cultures that received 2-bromoethanesulfonic acid, an inhibitor of methanogenesis, as compared with cultures that did not receive a methanogenesis inhibitor. The biotransformation of other PAHs is believed to be thermodynamically feasible under methanogenic conditions (Dolfing et al., 2009). Metabolic biomarkers for naphthalene under anaerobic conditions include a variety of naphthoic acids (Phelps et al., 2002) which are products of carboxylation reactions (Zhang and Young, 1997).

Because oxygen is rapidly consumed in the top few millimeters of sediments or sediment caps, contaminant biotransformation beneath the benthic zone will be exclusively anaerobic. Reviews of rates of anaerobic contaminant biotransformation in laboratory and field studies are summarized in Tables 2.3 and 2.4.

Table 2.3a: Mean and Maximum anaerobic degradation rates (day^{-1}) from n observations compiled from literature by Aronson and Howard (1997).

TEA		Benzene	Toluene	Ethylbenzene	o-Xylene	m-Xylene	p-Xylene	Naphthalene
Fe(II)	n	11	10	8	8	8	8	--
	Mean	0.0035	0.021	0.0011	0.0078	0.0052	0.005	--
	Max	0.024	0.087	0.0032	0.056	0.02	0.02	--
SO ₄	n	9	9	7	5	4	3	--
	Mean	0.016	0.049	0.0098	0.16	0.091	0.079	--
	Max	0.047	0.11	0.029	0.065	0.17	0.17	--
CO ₂	n	16	22	14	11	8	7	--
	Mean	0.005	0.029	0.05	0.021	0.021	0.015	--
	Max	0.052	0.186	0.46	0.21	0.1	0.08	--
Mixed	n	25	17	17	16	16	18	11
	Mean	0.004	0.004	0.002	0.003	0.002	0.002	0.012
	Max	0.087	4.8	0.078	0.057	0.025	0.031	0.043

Table 2.3b: Median and Maximum anaerobic degradation rates (day^{-1}) from n observations compiled from literature by Suarez and Rifai (1999).

TEA		Benzene	Toluene	Ethylbenzene	o-Xylene	m-Xylene	p-Xylene
Fe(II)	n	20	13	7	8	8	8
	Median	0.005	0.01	0.002	0.002	0.002	0.002
	Max	0.034	0.045	0.017	0.016	0.037	0.037
SO ₄	n	16	14	8	6	7	4
	Median	0.003	0.035	0.001	0.011	0.056	0.009
	Max	0.049	0.21	0.007	0.084	0.32	0.022
CO ₂	n	15	24	12	12	12	10
	Median	0	0.021	0.001	0.001	0.001	0.003
	Max	0.077	0.186	0.054	0.214	0.104	0.081

Table 2.4: Estimated anaerobic degradation rates (day^{-1}) for chlorobenzenes under methanogenic conditions. The incubation temperature was 30°C in experiments by Fung et al. (2009) but was not reported by Ramanand et al. (1993).

		Fung et al. (2009)	Ramanand et al. (1993)
1,2-Dichlorobenzene	Min	0.90	0.017
	Max	1.13	0.080
1,3-Dichlorobenzene	Min	0.366	0.068
	Max	0.513	0.257
1,4-Dichlorobenzene	Min	0.204	0.023
	Max	0.758	0.148
Monochlorobenzene	Min	0.076	Not reported
	Max	0.148	Not reported

Chapter 3. Assessment of Bacterial Activity for Sediment Cap Design: A Case Study in Onondaga Lake

3.1 INTRODUCTION

Pollutants in sediments can be transported to other environmental compartments, such as biota, water, and air, and pose a risk of exposure to humans. Such risks can be reduced by impeding pollutant transport from the sediment compartment by capping, or placement of clean granular material (e.g., sand, soil, or gravel) atop the contaminated sediments. In situ sediment caps physically isolate the chemicals of concern from benthic and aquatic communities, prevent particle suspension that can lead to contaminant desorption in the water column, and reduce the fluxes of dissolved contaminants (U.S. EPA, 2005). While reduction of dissolved contaminant flux by physical isolation has been demonstrated in laboratory tests (Wang et al., 1991; Schaaning et al., 2006; Eek et al., 2008) and modeled mathematically (Thoma et al., 1993; Reible et al., 2009), microbiological processes influencing contaminant fate and transport in the cap and the underlying sediment require further investigation (Reible, 2004).

Sediment caps, which typically range in thickness from a few centimeters to one hundred centimeters, are commonly comprised of layers of different media. For example, sand or gravel placed directly atop the sediment isolate the underlying contaminants and may be covered by a layer of coarse material for added stability and resistance to hydraulic shear. Layers of one or more “active” capping materials, such as activated carbon or organophilic clay, might be included to immobilize non-aqueous phase liquids

(NAPLs) or to improve sequestration of dissolved hydrophobic contaminants. Sediment cap design involves specification of cap materials and their respective thicknesses to reduce contaminant fluxes to target levels over a long period of time.

In addition to isolating sediment pollutants, a cap may become a zone of contaminant biotransformation following colonization by bacteria from the sediment (Himmelheber et al., 2009). Hyun et al. (2006) reported degradation of naphthalene and phenanthrene in a layer of sand placed atop coal-tar contaminated sediments in laboratory columns. The potential for reductive dehalogenation of the common groundwater contaminants tetrachloroethylene and trichloroethylene was demonstrated in a sand column inoculated with *Dehalococcoides* spp. packed in a column atop sediment from the Anacostia River (Himmelheber, 2008). These examples illustrate the potential for contaminant biotransformation within sediment caps. Improved predictability of reaction rates within a cap could lead to cost savings in cap materials and placement.

The effects of cap placement on the underlying sediment, particularly processes that can promote contaminant transport, must be considered. Consolidation beneath the cap may result in the upward mobilization of porewater and the transport of NAPL or dissolved phase contaminants (Alshawabkeh et al., 2005; Kim et al., 2009). Placement of a cap also leads to the underlying sediment becoming more reduced and alters the sediment biogeochemistry (Johnson et al., 2010), which can cause an increase in the rate of production of biogenic gases such as methane. A corresponding increase in gas flux across the sediment/cap interface has multiple implications. First, gas ebullition can physically damage caps and create preferential flow paths that may expedite contaminant

transport (Johnson et al., 2002; Reible, 2004; Reible et al., 2006). Second, contaminants may be transported by gas bubbles (Figure 3.1). Volatile contaminant transport either in the gas phase or on the hydrophobic surfaces of gas bubbles has been demonstrated (Yuan et al., 2007), as has mobilization of NAPLs (McLinn and Stolzenburg, 2009). Third, gas bubbles trapped in pores in the cap will reduce the aqueous fraction of porosity in the cap (Amos and Mayer, 2006), resulting in increased chemical velocities of dissolved contaminants and expedited aqueous-phase transport. As with contaminant biotransformation, improved understanding of contaminant transport mechanisms associated with microbiological gas production will lead to improved management of contaminated sediments.

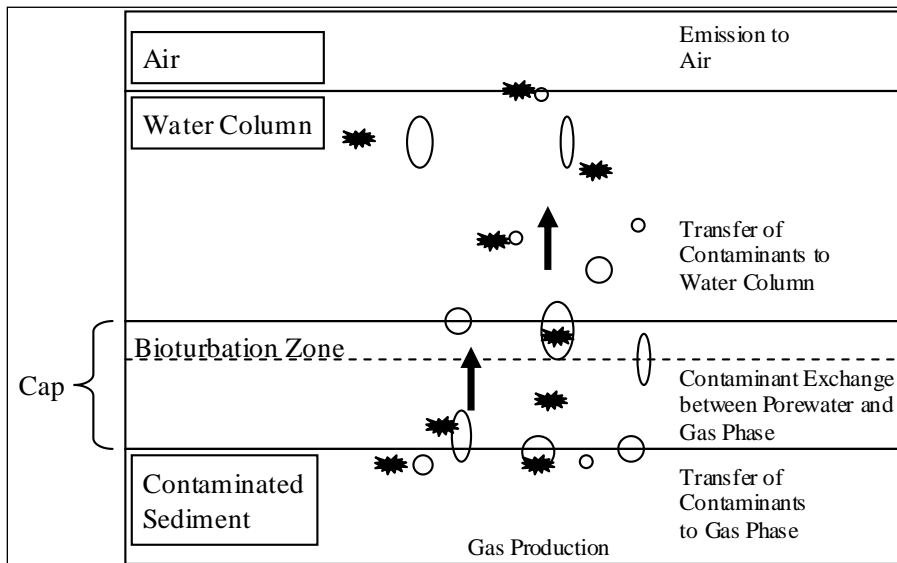


Figure 3.1: Conceptualization of gas-phase contaminant transport through a sediment cap. Modified from Yuan et al. (2007) with permission.

Contaminant biotransformation and biogenic gas production are site-specific processes that effect contaminant transport and thus have implications for sediment cap design. Bench-scale methods for the evaluation of contaminant biotransformation, gas production, and gas-phase contaminant transport in sediment samples from Onondaga Lake to aid in design of a sediment cap are described. These tests are applicable to sediment evaluations or cap designs at other sites.

3.2 MATERIALS AND METHODS

3.2.1 Site Description

Onondaga Lake is located near Syracuse, New York, and has a surface area and mean depth of 11.9 square kilometers and 10.9 meters, respectively (Effler and Harnett, 1996). Allied Chemical Company operated on the western shore from 1884-1986 and manufactured coke, organic chemicals (including benzene, toluene, ethylbenzene, xylenes (BTEX), chlorobenzenes, and naphthalene), soda ash, caustic potash, caustic soda, and more (Lizlovs, 2005). Waste disposal practices contributed to pollution of Onondaga Lake and Nine-Mile Creek. Additionally, a wastewater treatment facility that discharges effluent to the lake began operating in 1960. Before 1980, wastewater flow exceeding 170 million gallons per day bypassed the plant and was discharged directly to the lake, elevating nutrient and bacteria levels (Effler and Harnett, 1996). Plagued by hypoxic zones, eutrophication, high bacteria loadings, high salinity, and hazardous chemical contamination, Onondaga Lake was placed on EPA's Superfund National Priority List on December 16, 1994 (U.S. EPA, 2011). A draft plan for management of

the lake bottom including sediment dredging, capping, and monitored natural attenuation was recently approved by the New York State Department of Environmental Conservation (N.Y. DEC, 2009).

3.2.2 Field Sample Description

Three-inch diameter cores from 12 locations were collected from Sediment Management Units (SMUs) 1, 6, and 7 in Onondaga Lake on November 15, 2006. SMU 1 encompasses the in-lake waste deposit (ILWD), a disposal site for solid Solvay waste which was characterized as “a white, chalky, calcite-related material containing calcium carbonate, calcium silicate, magnesium hydroxide, and smaller amounts of other carbonates, sulfates, salts, and metallic oxides” (Lizlovs, 2005). SMU 7 is adjacent, comprising the southern corner of the lake, with SMU 6 and the mouth of Onondaga Creek to the northeast (Figure 3.2). Note that the first number of the five-digit sampling location refers to the SMU from which the sample was collected (e.g., samples from location 10116 were collected from SMU 1). Cores were shipped on ice to the University of Texas-Austin and stored in the dark at 4°C prior to use. All sediment handling except for centrifugation and aerobic slurry preparation was done in an anaerobic chamber (97% N₂, 3% H₂) (Coy Laboratories, Grass Lake, MI).



Figure 3.2: Map of the southeastern shore of Onondaga Lake with SMU delineation. Sampling locations are indicated with a green asterisk.

3.2.3 Sediment and Porewater Analysis

Porewater pH profiles were measured by microelectrode (Diamond General, Ann Arbor, MI) in one core from each location in 5-cm intervals. Following profiling, sediment was transferred to 500-mL polypropylene centrifuge bottles (Beckman Coulter Inc., Fullerton, CA) and centrifuged in a Beckman J2-21 centrifuge at 10,000 x g (9500 rpm with JA-10 rotor) at 4°C for 30 minutes (U.S. EPA, 2001). Porewater was removed from centrifuged bottles and either transferred directly to VOA vials for volatiles analysis

by SW-846 EPA method 8260B or filtered through 0.2- μ m syringe filters (Pall Life Sciences, East Hills, NY) into vials for analysis of metals (calcium, iron, potassium, magnesium, manganese, sodium, and phosphorus) by method 6010B, anions (chloride, nitrate, nitrite, orthophosphate, and sulfate) by the U.S. EPA's Methods for the Chemical Analysis of Water and Wastes (MCAWW) method 300.0A, dissolved organic carbon by method MCAWW 415.1, or ammonia by method MCAWW 350.1. Contaminant loadings on sediments also were measured by method 8260B. Sediment porewater and contaminant loadings were analyzed by Severn Trent Laboratories, Inc. (now TestAmerica Laboratories, Inc.) in Austin, TX. Sediment organic carbon was measured by CHN analysis at the University of Texas Marine Sciences Institute-Port Aransas.

Artificial porewater (APW) recipes were created for each SMU by averaging dissolved analyte concentrations for locations within that SMU. Centrifuged sediment was transferred to glass jars, sealed under anaerobic conditions, and stored at 4°C.

3.2.4 Sediment Slurries for Contaminant Biotransformation Potential

Centrifuged sediment was split and one fraction was autoclaved at 15 psi and 130°C for 60 minutes on three consecutive days. Microcosms were prepared with either 1% or 5% (w/v) wet sediment in SMU-specific APW for aerobic and anaerobic samples, respectively. Autoclaved sediment was used for abiotic controls. Triplicate slurries were created for each biotic and abiotic combination of sediment core location and incubation temperature. Bottles were capped with Mininert valves (Restek Corp., Bellefonte, PA) and spiked with a cocktail of contaminants of interest (COIs) at a nominal starting mass

of 0.2 mg per bottle. Microcosms were tumbled in the dark at either the median annual groundwater temperature (12°C) or a bounding temperature favorable for biological activity ($22 \pm 2^\circ\text{C}$). In intervals of weeks to months, 2-mL aqueous samples were transferred to 9-mL headspace vials and analyzed by gas chromatography with flame ionization detection (GC-FID) (Appendix A1). Minimum calibration concentrations were 20 µg/L for all analytes.

To explore the possibility of COI biotransformation following pH neutralization in the high-pH ILWD, SMU 1 APW was adjusted to pH 7.0. Biotransformation potential was evaluated with sediment from location 10118 in (1) pH-neutral SMU 1 APW, (2) SMU 7 APW, and (3) pH-neutral SMU 1 APW with 0.5 g of sediment from location 70049. Condition 1 evaluated whether biotransformation activity was inhibited by high porewater pH despite the presence of contaminant-degrading microorganisms in sediment from location 10118. Condition 2 examined the effect of pH neutralization and bioaugmentation with bacteria that demonstrated biotransformation capability. Condition 3 determined whether solute concentrations in SMU 1 APW might have inhibited biotransformation. Both aerobic and anaerobic slurries were created with 1% or 5% solids (w/v) in triplicate with autoclaved controls, as above, and tumbled in the dark at 22°C.

3.2.5 Sand-Capped Sediment Columns for Contaminant Biotransformation

Sediment cores from 8 locations were extruded into 15-cm glass columns (Kimball-Kontes, Vineland, NJ). Sand selected for its organic carbon content ($>0.1\%$)

and satisfying New York State Department of Transportation grain size specifications for concrete sand (Appendix A) was sieved through a 2-mm sieve (U.S. standard mesh size 10) and packed into glass columns (15-cm length, 4.8-cm inner diameter) (Kimble-Kontes, Vineland, NJ) with surface water from SMU 1. Each sediment column was connected in series with a single sand column by PEEK tubing (VICI Valco, Brockville, Ontario, Canada) (Figure 3.3). Stainless steel three-way valves were installed for sample collection (1) between the sediment and sand columns and (2) at the downstream end of the sand cap column. Columns were connected to a peristaltic pump at a flow rate corresponding to a Darcy velocity of 0.25 cm/day, which is about 10-100 times higher than seepage velocities predicted on-site. Flow was recirculated from the sand cap column to the sediment column except during sample collection, during which time sample volumes were replaced by withdrawal from a reservoir of deaerated surface water. Sand cap influent and effluent were collected in 2-mL amber vials that were pre-filled with 0.5 mL of purge-and-trap grade methanol. Samples were stored without headspace and sample volumes were determined gravimetrically. Samples were analyzed by Method 8260B by DHL Analytical (Round Rock, TX).

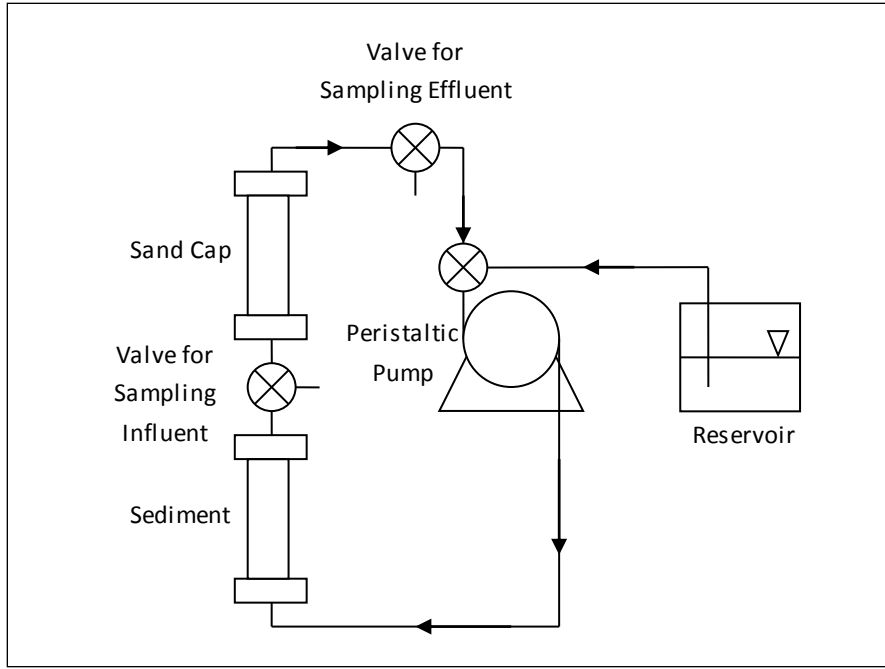


Figure 3.3: Laboratory column set-up for simulating flow through sand-capped sediment.

Sand column influent and effluent concentrations over time were used to estimate the rate of contaminant biotransformation and the extent of solute retardation in the sand matrix with the program CXTFIT, which solves the one-dimensional advection/dispersion equation with reaction (Equation 3.1) (Toride et al., 1999). In non-dimensional variables:

$$R \frac{\partial C}{\partial T} = \frac{1}{P} \frac{\partial^2 C}{\partial Z^2} - \frac{\partial C}{\partial Z} - \mu C \quad \text{Equation 3.1}$$

where R is the retardation factor, C is the aqueous phase pollutant concentration, T is dimensionless time, P is the Peclet number (porewater velocity \times column length / dispersion), Z is dimensionless position, and μ is the Damköhler number (column length $\times k$ / porewater velocity, where k is the first-order degradation rate constant).

Optimization of the retardation factor, dispersion coefficient, and first-order biodegradation rate constant was performed with CXTFIT, which uses the Levenberg-Marquardt algorithm for minimizing the sum of squared errors between the predicted and observed effluent concentrations over time.

3.2.6 ^{14}C -Toluene Microcosms

Approximately 2 g of sand or sediment were transferred from columns to autoclaved 40-mL amber vials. Vials were filled with deaerated autoclaved surface water that was either unamended or amended with 1X trace metal solution SL6 (Quayle and Pfennig, 1975), 40 mg/L of $(\text{NH}_4)_3\text{PO}_4$, and 200 mg/L of NH_4Cl . The redox indicator resazurin was added at a concentration of 1 mg/L to the unamended and amended waters and reduced with 0.5 mg/L dithiothreitol. Vials were spiked with uniformly ring-labeled ^{14}C -toluene (Sigma-Aldrich, St. Louis, MO) to concentrations of 1.0 μM . “Live” microcosms were operated in triplicate while singlet controls were either killed with 100 mg/L HgCl_2 (Grbic-Galic and Vogel, 1987) or operated without sand or sediment. Vials were capped with Mininert valves (Restek, Bellefonte, PA) and incubated in the dark at 12°C on an orbital shaker at 60 revolutions per minute.

Periodic sampling was conducted inside the anaerobic chamber. One mL of water was added to 20-mL scintillation vials containing one of the following: 10 mL of scintillation fluid (ScintSafe 50%, Fisher Scientific, Inc.), 2 mL of 1 N HCl, or 2 mL of 1 N NaOH. The vial containing scintillation fluid was capped and mixed immediately, while the samples containing HCl and NaOH were sparged with nitrogen gas for five

minutes at a flow rate of 100 mL/min prior to addition of 10 mL of scintillation fluid. Radioactivity was measured on a Beckman LS-5000TD scintillation counter (Beckman Coulter, Brea, CA) with settings according to Putz (2004) (Appendix A). Total radioactivity was measured in the unsparged sample and carbonate was quantified as the difference between the basic and acidic samples of non-purgeable radioactivity.

3.2.7 Gas Production

Wet sediment (10 – 20 g) was added to 30-mL glass tubes that were filled two-thirds to three-quarters full with deaerated APW in an anaerobic glove box. The tube was sealed with a butyl rubber stopper and aluminum crimp cap. Tubes were incubated in duplicate at 7°C, 12°C, and 22°C. Gas production in the sediment was measured weekly by shaking tubes to release entrapped gas from the sediment and puncturing the septum with a needle attached to a U-tube manometer containing a solution of 1.4 N Na₂SO₄ in 1.0 N H₂SO₄ (Method 2720 B) (Eaton et al., 2005) to measure the difference between headspace and atmospheric pressures (Appendix A).

3.2.8 Gas-Phase Contaminant Transport

Gas-phase contaminant flux was estimated by passing nitrogen gas through a sediment column and collecting the effluent in a hexane trap (Figure 3.4). Sediments were extruded from cores into 15-cm long, 4.8-cm inner-diameter chromatography columns (Kimble-Kontes, Vineland, NJ). Nitrogen gas flowed through the column at a rate of 1.2 µL/min, corresponding to the maximum gas production rate observed, and was regulated with a low-flow mass controller (Alicat Scientific, Tucson, AZ). The effluent gas was bubbled in a trap containing 10-mL of hexane that was periodically analyzed by

direct injection gas chromatography with a flame ionization detector to estimate contaminant fluxes from the sediment. Benzene was not analyzed by this method because the sample peak was masked by the hexane solvent peak on the GC. The volume of hexane in the trap was measured at each sampling to account for volatile hexane loss and subsequently refilled to 10 mL. Volatile losses of analytes from the hexane trap were estimated to be insignificant given their small mole fractions in hexane and comparatively small pure phase vapor pressures.

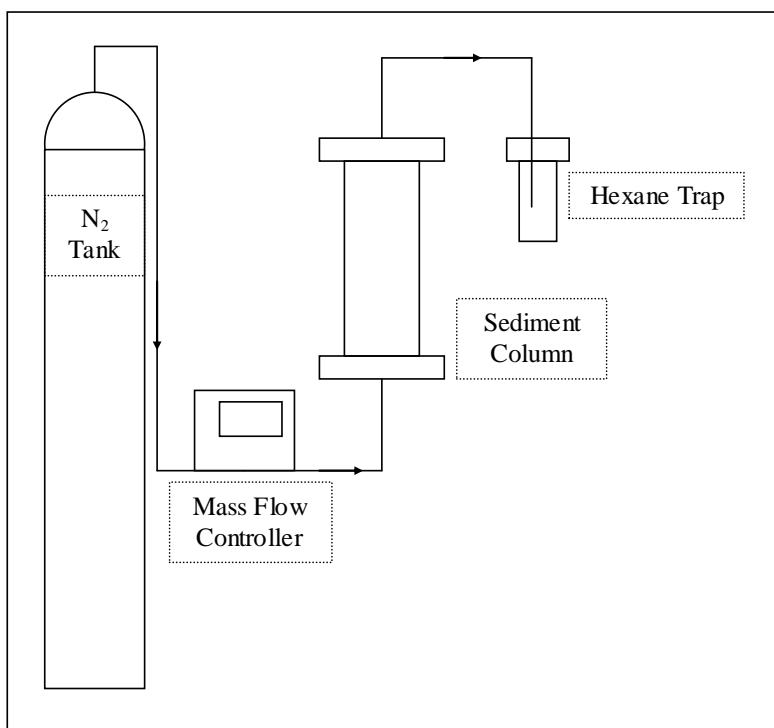


Figure 3.4: Apparatus for measuring gas-phase contaminant flux.

3.3 RESULTS AND DISCUSSION

3.3.1 Sediment and Porewater analysis

SMU 1 sediments consisted of Solvay waste material and were fine-grained and light gray in color with an organic carbon fraction (f_{OC}) of 0.4 – 2.0%. SMU 6 sediments were coarse and sandy with f_{OC} of 0.8 – 5.1%, while sediments from SMU 7 locations were fine-grained and highly cohesive with f_{OC} 1.9 – 5.9%. Contaminant loadings on sediments varied by location but generally were greatest in SMU 1 followed by SMU 7 then SMU 6 (Figure 3.5). Chlorobenzenes and xylenes were among the highest in all SMUs, and naphthalene also was high in SMU 1.

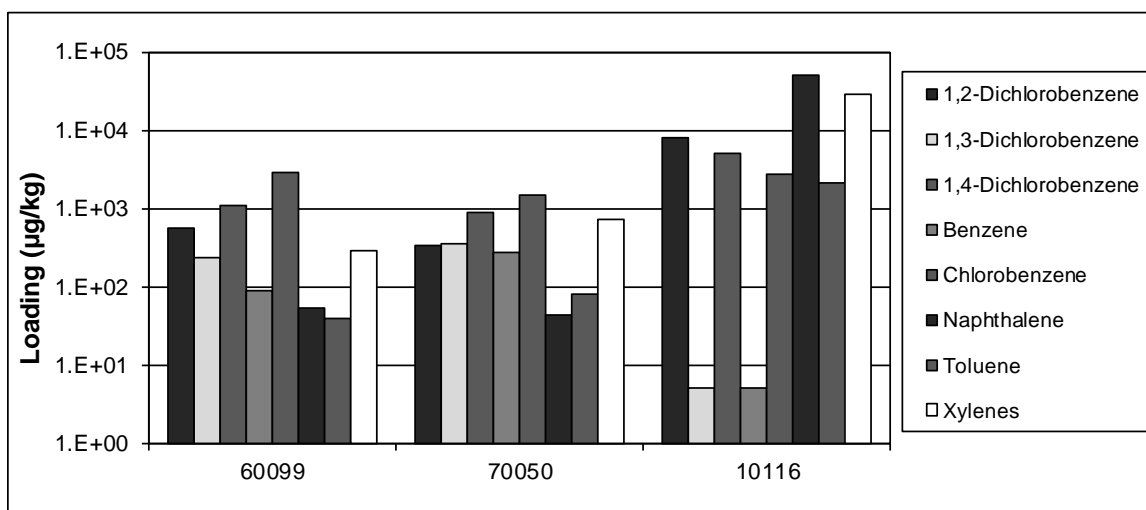


Figure 3.5: Contaminant loadings on sediments representative of each SMU.

Porewater from SMU 6 and SMU 7 sediment cores were near neutral-pH while the ILWD porewater had pH values greater than 10. Solids analysis of Solvay waste material from the ILWD indicated that the minerals ettringite and hydrocalumite buffer ILWD porewater near pH 11. Cap amendments capable of porewater pH neutralization,

such as siderite, have been evaluated (Vlassopoulos et al., 2011) with the goal of encouraging downstream COI biotransformation within the cap.

Ion concentrations in porewater obtained by sediment centrifugation showed dissolved manganese and iron in SMUs 6 and 7 up to 27.3 and 190 μM , respectively. Neither species was detected in SMU 1 porewater (minimum detection limit = 0.27 μM). Sulfate was detected in SMU 1 up to 3.5 μM , while in SMUs 6 and 7 it was typically around 0.10 μM but as high as 1.0 μM (Figure 3.6). The absence of dissolved manganese and iron in ILWD porewater, despite Mn- and Fe-oxide content of 0.03% and 1.0%, respectively, suggests that dissimilatory metal reduction was not occurring. Furthermore, sulfate concentrations in excess of ~ 30 μM have been shown to inhibit methanogenesis in fresh water sediments (Lovley and Klug, 1986), suggesting that the ILWD may exhibit minimal anaerobic bacterial metabolism. The detection of dissolved metal species in porewater from SMUs 6 and 7 indicate anaerobic metabolic activity, either direct bacterial metal reduction or reaction of biogenic sulfide with metal oxides.

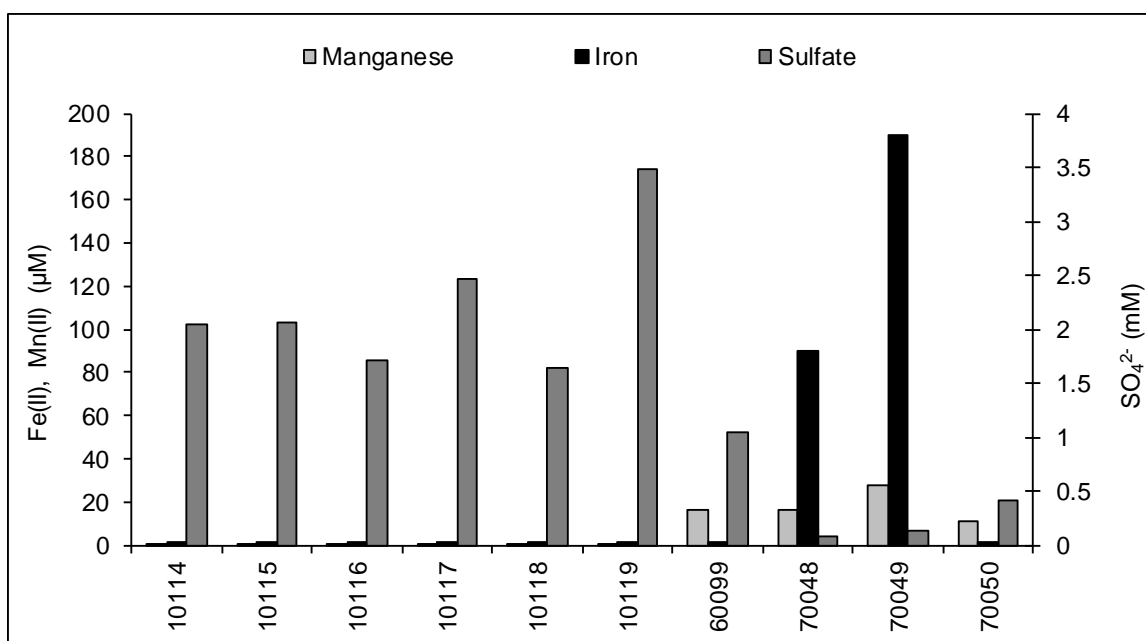


Figure 3.6: Dissolved concentrations of biogeochemical indicators of anaerobic metabolism.

APW was prepared using average concentrations of sediment porewater constituents from six sampling locations within SMU 1 and three sampling locations within each SMU 6 and SMU 7 (Table 3.1). The prepared waters were supplemented with 50 mM K_2HPO_4 , as a source of phosphorus for bacterial growth, and used in biotransformation and gas production experiments.

Table 3.1: Composition of APW used for sediment slurries to test COI biotransformation and gas production. Concentrations are in g/L.

Chemical	SMU1	SMU6	SMU7
NaCl	1.75	2.51	0.63
Na ₂ SO ₄	0.31	0.071	--
CaCl ₂	2.79	1.85	0.54
NH ₄ Cl	0.35	0.77	0.75
MgCl ₂	--	0.86	0.97
KCl	0.63	0.060	0.036
K ₂ PO ₄	8.66	8.66	8.66
pH	11.0	6.8	7.4

3.3.2 Sediment Slurries

Microcosms for assessing the potential of native sediment bacteria to degrade COIs were used to examine the impact of sediment source, temperature, and the presence or absence of oxygen. Under site conditions (i.e., 12°C and anaerobic), BTEX was biotransformed most rapidly followed by naphthalene then the chlorobenzenes (Table 3.2). General trends were observed that have been reported previously by others: (1) biotransformation under aerobic conditions began after a shorter lag time and proceeded at a faster rate than under anaerobic conditions (Table 3.2) (Suarez and Rifai, 1999), (2) BTEX and naphthalene were removed more quickly than were the chlorobenzenes under both aerobic and anaerobic conditions (Table 3.2) (Suarez and Rifai, 1999), (3) toluene biotransformation proceeded faster than did that of other substrates (Table 3.2) (Bruce et al., 2009), and (4) dichlorobenzenes were biotransformed by reductive dehalogenation under anaerobic conditions (Figure 3.7) (Ramanand et al., 1993; Fung et al., 2009). Autoclaving was not universally successful at sterilizing sediments because contaminant

loss was observed in some control vessels (e.g., sediment 10118 with SMU 7 APW, Table 3.2). The extent of biotransformation varied between sampling locations within and between SMUs 6 and 7 while biotransformation was not observed in the pH-impaired SMU 1. Benzene degradation at pH 10.0 has been reported by bacteria isolated from alkaline zones in a BTEX-contaminated aquifer (Fahy et al., 2008), but COI biodegradation was not observed in the current study.

Table 3.2: Extent of biotransformation of COI under anaerobic conditions.

Sediment Location	Temperature (°C)	1,2-Dichlorobenzene	1,3-Dichlorobenzene	1,4-Dichlorobenzene	Benzene	Chlorobenzene	Ethylbenzene	Naphthalene	Toluene	Xylene
60098	12	-	-	-	-	-	+	+	+	+
60099	12	-	-	-	-	-	-	-	+	+
60100	12	-	-	-	-	+	+	+	+	+
70048	12	-	-	-	++	++	++	++	++	++
70049	12	+	+	+	+	+	+	+/-	+	+
70050	12	-	-	-	-	-	-	-	-	-
10118, SMU 1 APW (pH 7.0)	22	-	-	-	+/-	+/-	+/-	-	+/-	+/-
10118, SMU 7 APW	22	+/-	+/-	+/-	-	+/-	+/-	-	-	+/-
10118+70049 SMU 1 APW (pH 7.0)	22	+	+	+	-	+	+	-	+	+

++ > 50% removal in fewer than 400 days

+ > 50% removal in 600 days

- < 50% removal in 600 days

+/- Removal observed in both sample and control bottles

The impact of site temperature on biotransformation rate is illustrated clearly by the concentration time series for chlorobenzenes with sediment from location 70049 (Figure 3.7). At 22°C, dichlorobenzenes were completely dehalogenated to monochlorobenzene.

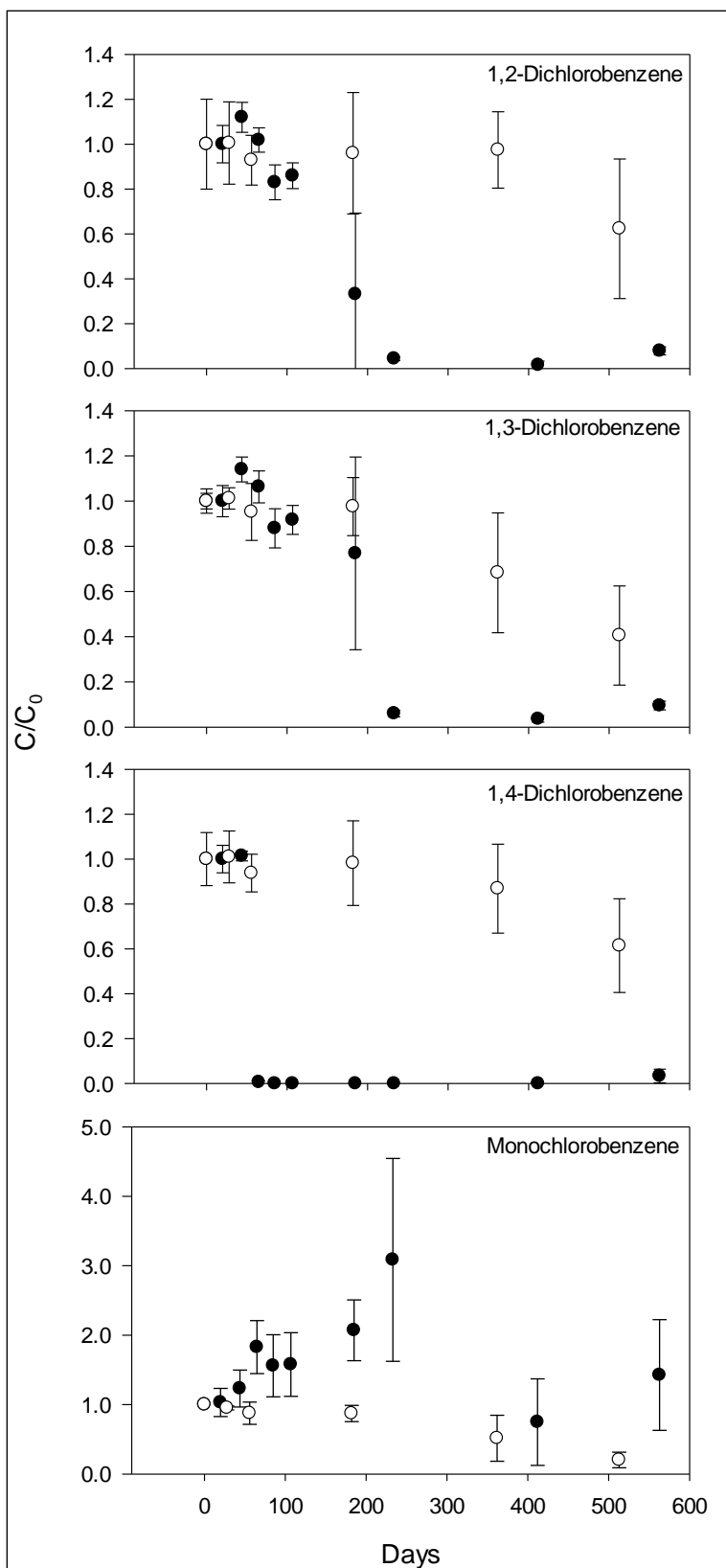


Figure 3.7: Identical slurries with sediment from location 70049 incubated at 22°C (solid) and 12°C (hollow). Error bars indicate one standard deviation from three biological replicates.

Transformation of 1,2-dichlorobenzene occurred within 60 days, followed by apparently simultaneous dechlorination of the other two isomers within 230 days. Preference for 1,2-dichlorobenzene over the other isomers has been observed elsewhere (Fung et al., 2009) and is predicted by thermodynamics (Dolfing and Harrison, 1992). Monochlorobenzene accumulated until the DCBs were completely removed, then gradually approached the starting concentration. Dehalogenation of monochlorobenzene to benzene, as reported by Fung et al. (2009), could not be confirmed because benzene accumulation was not observed. Monochlorobenzene might have been biotransformed by a pathway other than dehalogenation, or removal of monochlorobenzene and benzene might have proceeded at similar rates. Very different profiles were observed at 12°C. Only about half of each of the dichlorobenzenes and 80% of the monochlorobenzene were removed after 500 days. Transformation of monochlorobenzene and all dichlorobenzene isomers seemed to occur simultaneously. These results suggest the presence of bacteria capable of transforming chlorobenzene in sediment at location 70049 and indicate that site conditions, namely porewater temperature, might not be conducive to rapid biotransformation. Other researchers are conducting follow-up studies to examine whether amendment with electron donor, electron acceptor, nitrogen, and phosphorus can expedite pollutant biotransformation at 12°C.

Results were mixed in biotransformation tests by sediment bacteria from location 10118 in pH-neutral APW, designed to test whether biotransformation was likely in the field following the adjustment of porewater pH from 11.0 to near pH 7.0. For the first two tested conditions, (i.e. 10118 sediment in SMU 1 APW adjusted to 7.0 and 10118

sediment with SMU 7 APW, respectively), similar contaminant disappearance was observed in biotic sample slurries and autoclaved controls. However, the third condition, sediment from location 10118 seeded with sediment from location 70049 in SMU 1 APW with the pH adjusted to 7.0, demonstrated rapid removal of several of the contaminants of interest as compared with both the autoclaved controls and the slurries with 10118 sediment without bioaugmentation (Table 3.2). This was observed under both aerobic and anaerobic conditions, and although these slurries were incubated at 22°C, results suggest that biotransformation could proceed at site temperatures. In SMU 1, biological contaminant removal appears to be limited by porewater pH and the absence of bacteria capable of degrading the COI under site conditions. These obstacles might be overcome in a sediment cap by neutralizing porewater pH with a cap amendment such as siderite (Vlassopoulos et al., 2011) and seeding the cap with sediment from a location with contaminant biotransformation capability.

Sediment slurries were used to determine whether the sediment-borne bacterial community was capable of transforming pollutants of interest at the site. They also provided an indication of which chemicals were likely to persist under field conditions and which sediment locations should be studied further for biotransformation enhancement by neutralization of porewater pH or addition of nutrients. The potential for translation of biotransformation activity from sediments to a sand cap in the field was evaluated with sand-capped sediment column tests.

3.3.3 Sand-Capped Sediment Columns

Porewater solutes and bacteria were transported from the sediment columns to the cap columns, simulating sediment porewater advection through a sand cap in the field. COI concentrations in influent samples were variable with time, indicating heterogeneity in the COI concentration profiles in the sediment columns. COI influent concentrations to the sand cap columns were represented in the model as a series of pulse inputs to account for this time-dependency. In simulating sand column effluent, biotransformation was initially set to zero to fit retardation and dispersion to the breakthrough portion of the effluent profile. It was assumed that some time would be required for the bacterial biomass to accumulate in the sand cap column prior to measurable pollutant removal. The estimates of retardation and dispersion fit from the breakthrough portion of the effluent profile were then used to simulate the effluent profile through the entire time of column operation. The quality of fit between observed and predicted values, assessed by the coefficient of determination (R^2), indicated whether biotransformation could be considered negligible. This process is described in detail in Section 5.2.4.

Biotransformation of toluene in a sand column receiving porewater from sediments from location 70049 provides an example. Complete toluene breakthrough occurred by elution of 3.2 cap pore volumes and the effluent toluene concentration was unchanged in the sample collected at 4.5 pore volumes (Figure 3.8). The next three samples increasingly deviate from the curve of predicted effluent without a reaction term, suggesting the onset of toluene biotransformation. Over the same time, the concentration of chlorobenzene in sand cap effluent samples continued to increase, suggesting that the

decrease in effluent toluene concentrations was due to reaction and was not a sampling artifact.

Toluene has been shown to be a preferred substrate among the pollutants in this study (Langenhoff et al., 1989; Phelps and Young, 1999), so biotransformation of other solutes was only considered a possibility once the reaction of toluene was evident. Toluene biotransformation appears to cease after the elution of eight pore volumes, possibly due to either competitive or inhibitory effects from a component of the sediment-porewater matrix, or thermodynamic inhibition of fermentation owed to high dissolved hydrogen concentrations in column porewater from the atmosphere of the anaerobic chamber (Edwards and Grbic-Galic, 1994). Though apparently short-lived, this is believed to be the first demonstration of biotransformation of a sediment-borne contaminant in a sand cap by native sediment bacteria under anaerobic conditions and has significant implications for the potential of sediment caps to serve as “biobarriers” for a variety of biodegradable hydrocarbon contaminants. Details of column operation, characterization of hydraulics, measurement of geochemical indicators of anaerobic metabolism, and explanations of possible reasons for the termination of activity are presented in Chapter 5.

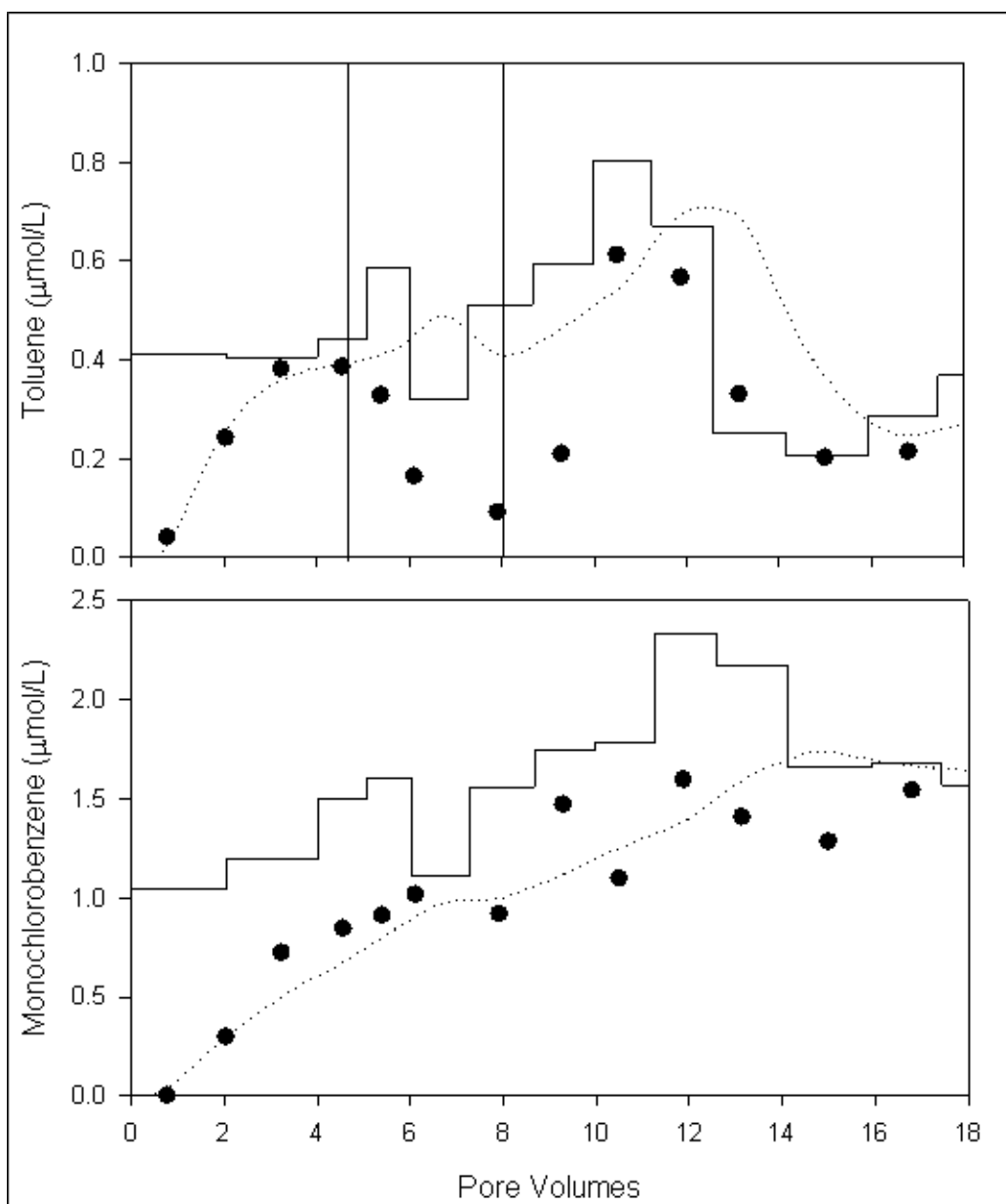


Figure 3.8: Breakthrough curves for toluene and monochlorobenzene in a sand column connected in series to a column containing sediment from location 70049. The influent concentration profile is represented by the solid line, effluent observations by the markers, and simulated effluent assuming no reaction by the dotted line. Note that effluent toluene concentrations deviate from prediction for pore volumes 4.5 – 8 while chlorobenzene effluent continues to trend upward during this time, suggesting biotransformation of toluene in the sand cap.

3.3.4 ¹⁴C-Toluene Microcosms

To confirm that the apparent reactivity of toluene observed in sand-capped sediment columns was due to biotransformation (Section 3.3.3) slurries with either sand or sediment were spiked with ¹⁴C-labeled toluene. Biotransformation of ¹⁴C-toluene in microcosms was not observed after 70 days of incubation. The activity of fractions at pH 14, which includes non-purgeable intermediates and CO₂, did not differ significantly between sample and control slurries for any of the sample conditions as determined by the student's t-test at a level of $\alpha = 0.05$ (Table 3.3). Biotransformation of toluene in sediment slurries (Section 3.3.2) was not observed until after 260 days when analyzed by gas chromatography, so the radio-labeled microcosms likely require additional time for a critical substrate-degrading biomass to develop (Corseuil and Weber Jr., 1994). Although biodegradation of the ¹⁴C-labeled substrate was not observed in these tests, the ability to demonstrate mineralization of only a few percent of the parent compound has been shown in similar tests (e.g., Vogel and Grbic-Galic, 1987).

Table 3.3: The mean and standard deviation of counts per minute (CPM) per mL for the pH 14 fraction (i.e., non-purgeable intermediates and CO₂) of aqueous slurry samples after 70 days. P-values are from a student's t-test comparing the sample condition with controls (n = 3 for all).

Description	CPM/mL	P ($\alpha = 0.05$)
Sand, unamended	758 (372)	0.30
Sediment, unamended	720 (163)	0.13
Sand, amended	1161 (265)	0.30
Sediment, amended	798 (32.8)	0.17
Controls	1043 (227)	--

3.3.5 Gas Production

Gas production trends with respect to location largely mirrored the microbial activity trends from the biotransformation tests. Gas production in SMU 1 was negligible, suggesting that the pore water chemistry, specifically the high pH and sulfate concentrations, is not conducive to methanogenesis. The volume and rate of biogenic gas produced was greatest in sediment from location 70049, though all SMU 6 and SMU 7 locations generated measurable volumes. Analysis of a headspace sample by GC-FID confirmed the presence of methane, indicating development of reduced conditions in sediment slurries. As observed by Viana et al. (2007), both proximity to the wastewater treatment plant effluent discharge point (a consistent source of labile organic carbon) and experimental temperature noticeably affected the maximum gas production rate and the cumulative volume of gas produced, an indicator of the duration of gas production (Figure 3.9).

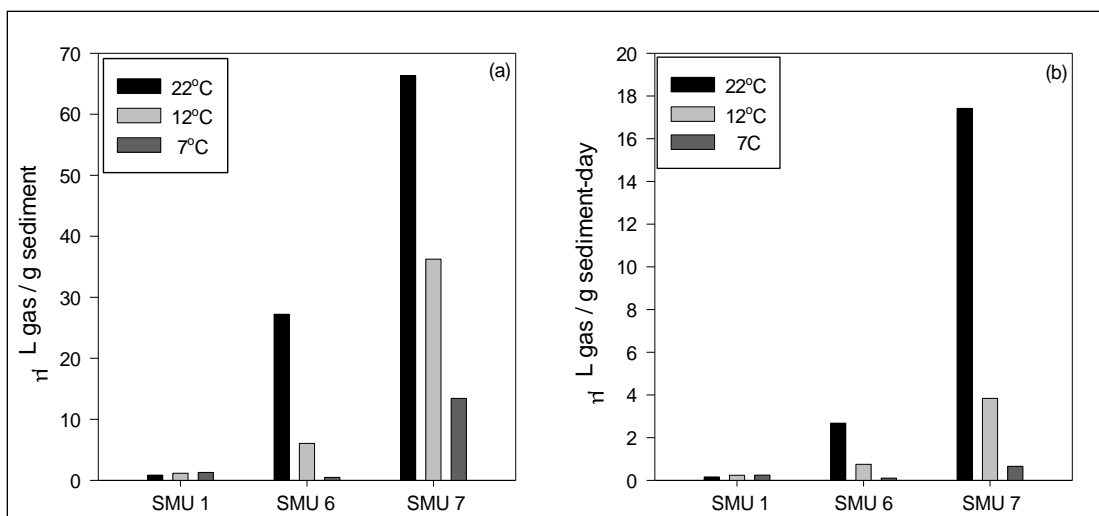


Figure 3.9: Maximum values for (a) the cumulative volume of gas produced (μL of gas per gram of sediment) and (b) the rate of gas production (μL of gas per gram of sediment per day) in each SMU at three incubation temperatures.

Rates of gas production were used to estimate upper bounds on gas flux from the sediment. Based on field data from a 1995 study by Matthews et al. (2005), methane production contributing to flux out of the sediment was assumed to occur in the top 12 cm of the sediment bed. Also assuming a sediment dry bulk density on the order of 1.0 g/cm^3 , theoretical gas flux maxima, observed for location 70049, were 1.71, 0.37, and $0.06 \text{ L m}^{-2} \text{ d}^{-1}$ for temperatures of 22°C , 12°C , and 7°C , respectively. Field deployed seepage meters in SMU 7 measured an average gas flux of $0.25 \text{ L m}^{-2} \text{ d}^{-1}$ at an average temperature of 12°C (unpublished data), in reasonable agreement with laboratory results. Gas ebullition is a function of hydrostatic pressure (Fendinger et al., 1992), but microcosms were designed to measure total gas production in sediments with negligible hydrostatic pressure and thus likely overestimate gas fluxes in the field.

A long-term study of methane flux in Onondaga Lake provides an indication of gas production trends after placement of a cap. Following closure of the soda ash facility, the dissolved calcium ion concentration decreased, which, in turn, reduced coagulation and the rate of deposition of phytoplankton (Jackson & Lochmann, 1992). The result was a 37% reduction in the downward flux of particulate organic matter (Matthews et al., 2005). The methane flux at the deepest point in the lake, considered generally representative of conditions throughout the lake, decreased from 0.16 to 0.02 L m⁻² d⁻¹ after five years, demonstrating the importance of the deposition of fresh labile carbon for methanogenesis, but also showing that accumulated recalcitrant organic carbon can support methanogenesis over several years (Matthews et al., 2005). Placement of a sediment cap completely and abruptly separates particulate organic matter from sediment methanogens, and a similar reduction in methane flux is anticipated.

Similar laboratory and field tests show a wide range of values for gas flux at contaminated freshwater sites. Gas fluxes exceeding 16 L m⁻² day⁻¹ during summer months were reported for sediments from the Collateral Channel in Chicago, IL, for which a one-meter thick zone of gas production was assumed (Yin et al., 2010). A gas collection system was included in the cap design to prevent damage to the cap resulting from gas ebullition. With sediments from the Anacostia River in Washington, D.C., methane fluxes of 0.34 L m⁻² day⁻¹ at 22°C were reported (Himmelheber and Hughes, 2005). This rate of gas production is of concern only for low permeability cap amendments, such as swelling clays, and is not expected to compromise the integrity of sand or gravel caps (Reible et al., 2006).

3.3.6 Gas-Phase Contaminant Transport

Biogenic gas advection could contribute substantially to chemical transport given the volatility of these sediment contaminants. Transport from sediment to overlying water by gas advection has been demonstrated in laboratory columns with polychlorinated biphenyls (McDonough and Dzombak, 2005) and polycyclic aromatic hydrocarbons (Yuan et al., 2007). The maximum gas flux calculated previously (i.e., $\sim 1 \text{ L m}^{-2} \text{ d}^{-1}$) was applied to estimate the maximum gas-phase flux of sediment contaminants due to gas ebullition in the field. The change in mass of contaminant in the hexane trap over time was used to compute the contaminant flux, accomplished by normalizing the COI concentration in the trap by the column cross-sectional area, then performing a linear regression with time as the independent variable. For example, the flux of 1,4-dichlorobenzene from a column with sediment from location 10118 was estimated to be $0.30 \text{ } \mu\text{mol m}^{-2} \text{ d}^{-1}$ at this rate of gas flow (Figure 3.10). The analytical detection limit corresponded to an area-normalized mole density of $2 \text{ } \mu\text{mol m}^{-2}$.

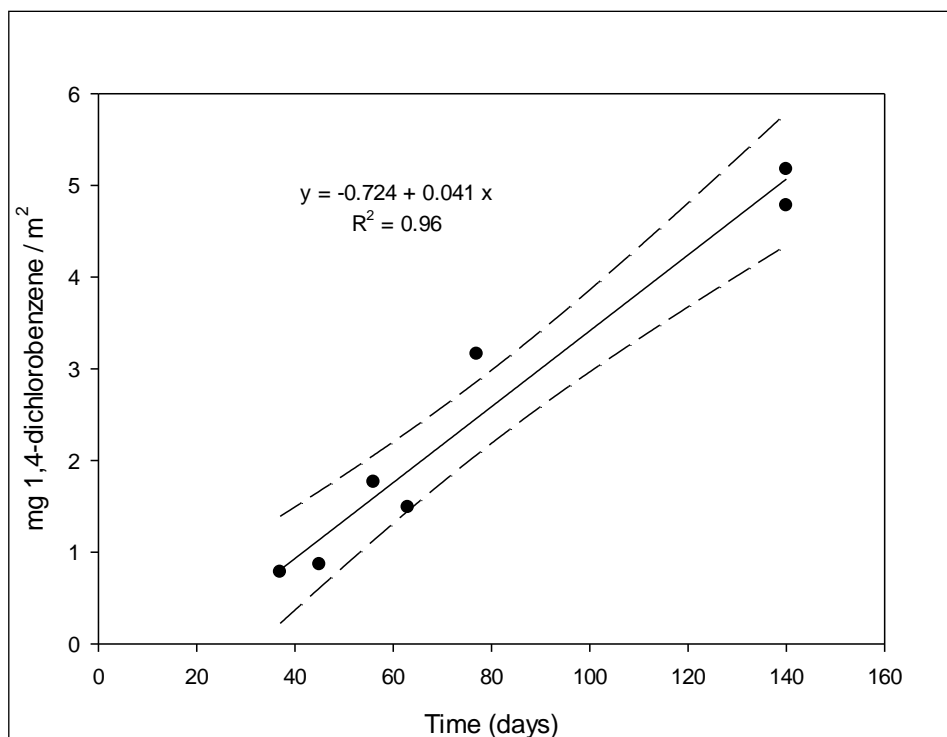


Figure 3.10: Gas-phase flux of 1,4-dichlorobenzene from a column packed with sediment from location 10118. The solid line shows the best-fit slope by linear regression and dashed lines define the 95% confidence interval.

Based on concentrations measured in replicate cores from the same locations, gas-phase contaminant fluxes were generally lower than those predicted by equilibrium aqueous-gas phase partitioning (Figure 3.11). Contaminant fluxes predicted from aqueous-phase concentrations and Henry's Law constants (Table 2.2) represent theoretical upper bounds that assume negligible mass transfer limitations across the particle-water and water-gas interfaces (Adams et al., 1990). In practice, transfer limitations do exist and field solute fluxes are expected to be lower than predicted theoretically.

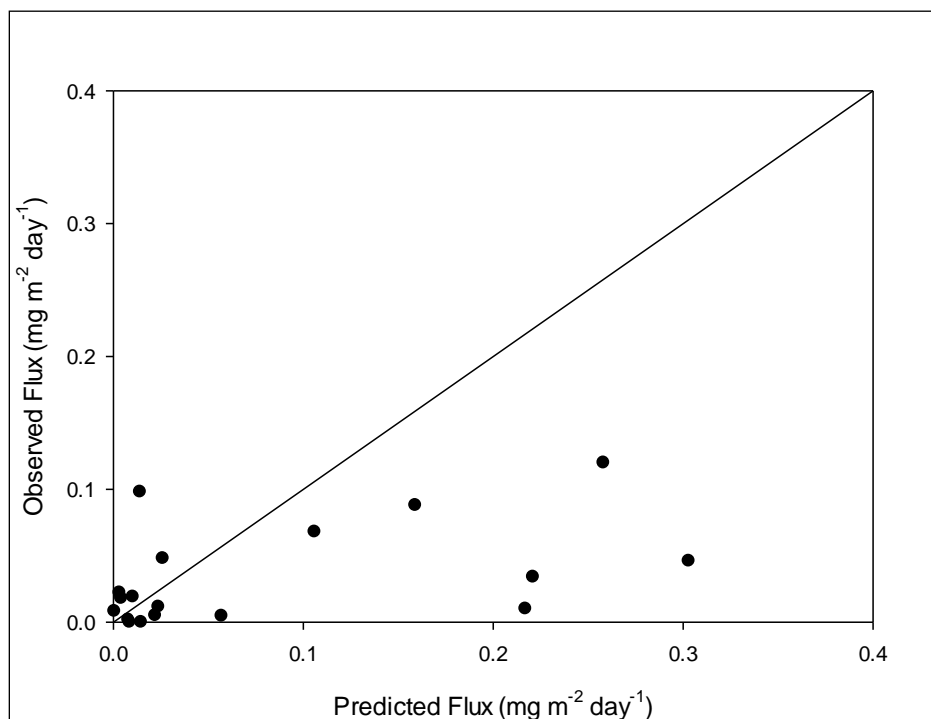


Figure 3.11: Gas-phase contaminant fluxes observed in column tests (ordinate) and predicted from aqueous-phase concentrations and equilibrium partitioning to the gas phase (abscissa).

The flux of benzene from the sediment could not be quantified because chromatographic separation of benzene and the trap solvent (i.e., hexane) was not achieved. Despite the high loading of naphthalene on SMU 1 sediments (observed in the cores that were analyzed), it was rarely detected in the hexane trap, which likely was due to mass transfer kinetics limitations. Prediction of theoretical fluxes could have been improved by measuring the actual contaminant concentration profiles in the sediment cores rather than using concentrations from replicate cores collected from the same location.

For the upper bound condition of gas flux of $1 \text{ L m}^{-2} \text{ d}^{-1}$, gas-phase contaminant transport would be of nearly equivalent significance to dissolved contaminant transport. At this gas flux, solute flux is

$$1 \frac{\text{cm}}{\text{d}} C_{aq} \frac{\mu\text{g}}{\text{L}} H = C_{aq} H \frac{\mu\text{g}}{\text{m}^2 \text{d}}$$

where H is the appropriate Henry's Law constant, equal to or less than $0.2 \text{ L}_{aq}/\text{L}_g$ for the chemicals of interest (Schwarzenbach et al., 2003). For groundwater seepage with a Darcy velocity of approximately 0.02 cm/d , the theoretical dissolved solute flux is on the order of

$$0.02 \frac{\text{cm}}{\text{d}} C_{aq} \frac{\mu\text{g}}{\text{L}} = 0.2 C_{aq} \frac{\mu\text{g}}{\text{m}^2 \text{d}}$$

and roughly equivalent to the theoretical gas phase flux. The experimental results suggest that gas phase fluxes in the field will generally be smaller than predicted and that dissolved solute convection is likely the dominant transport mechanism.

At least two methods exist for suppressing gas flux at sites where cap integrity is potentially threatened or gas-phase contaminant transport is determined to be significant: installation of a gas diversion system with optional treatment and/or amendment of the cap with NO_3^- , Fe(III) -, or SO_4 -bearing minerals. Yin et al. (2010) proposed placement of a membrane of low permeability atop a layer of sand in a cap design for Collateral Channel in Chicago, IL. Biogenic gas produced in sediments was intended to be dispersed laterally in the highly-permeable sand layer, thereby protecting the overlying vegetative zone of the cap from vertical gas ebullition. As an alternative to diverting biogenic gas, the rate of methanogenesis could be suppressed by amending the cap with

minerals that provide an energetically-preferred electron acceptor. Because carbon dioxide has a much higher aqueous solubility than does methane (560 mM and 2.0 mM, respectively, at 12°C), reduced methane production corresponds to a decrease in the volume of gas produced. Methanogenesis was reduced in sediment slurries with the addition of amorphous iron oxide (Lovley and Phillips, 1986), in rice paddies fertilized with ferrihydrite (Jackell and Schnell, 2002) and in peatland soils subjected to periodic addition of an ammonium sulfate solution (Dise and Verry, 2001). In addition to suppressing gas production, amendment of a cap with energetically-preferred terminal electron acceptors might encourage contaminant biotransformation, as discussed in section 3.3.2.

It is recommended that future tests incorporate (1) a water trap to humidify the gas before it enters the column, as done by Yuan et al., (2007); (2) a tracer to confirm the gas flow rates reported by gas flow controllers and to allow for estimation of the gaseous void fraction; and (3) measurement of contaminant loadings on column solids subsequent to experiment termination to relate pollutant mass released to the total pollutant mass in the column.

3.4 CONCLUSIONS

In support of the sediment cap design for Onondaga Lake, bench-scale tests of COI biodegradation (i.e., sediment slurries, sand-capped sediment columns, and slurries with sediment and sand spiked with ^{14}C -substrate), biogenic gas production, and gas-phase contaminant transport were employed to improve prediction of COI fate and transport. Results from Onondaga Lake show how these tests, which are applicable to

other sites, provide complementary insight into sediment bacterial activity and its implications for pollutant mobility. For example, the absence of intrinsic contaminant biotransformation in batch slurries with ILWD sediment led to consideration of cap amendments including porewater-neutralizing minerals, such as siderite, and bioaugmentation with sediment containing COI-degrading bacteria. Batch and column tests showed that bacteria capable of contaminant biotransformation are present in sediment, but that site conditions might not be favorable for rapid removal.

Additionally, microcosm tests facilitated assessment of biogenic gas production, which was moderate in Onondaga Lake sediments. Gas production rates measured in the laboratory were of the same magnitude as those observed in the field and are not believed to pose a threat to sand cap integrity. In fact, gas production is expected to cease almost completely once labile carbon is depleted near the cap/sediment interface. Finally, the gas-phase fluxes of the pollutants in this study were determined to be minor as compared with the aqueous contaminant fluxes, even at the maximum observed rate of gas production.

Cap design considerations follow directly from laboratory test results (Figures 3.12 and 3.13). Improved laboratory characterization of field processes will aid in optimizing parameters for sediment cap design.

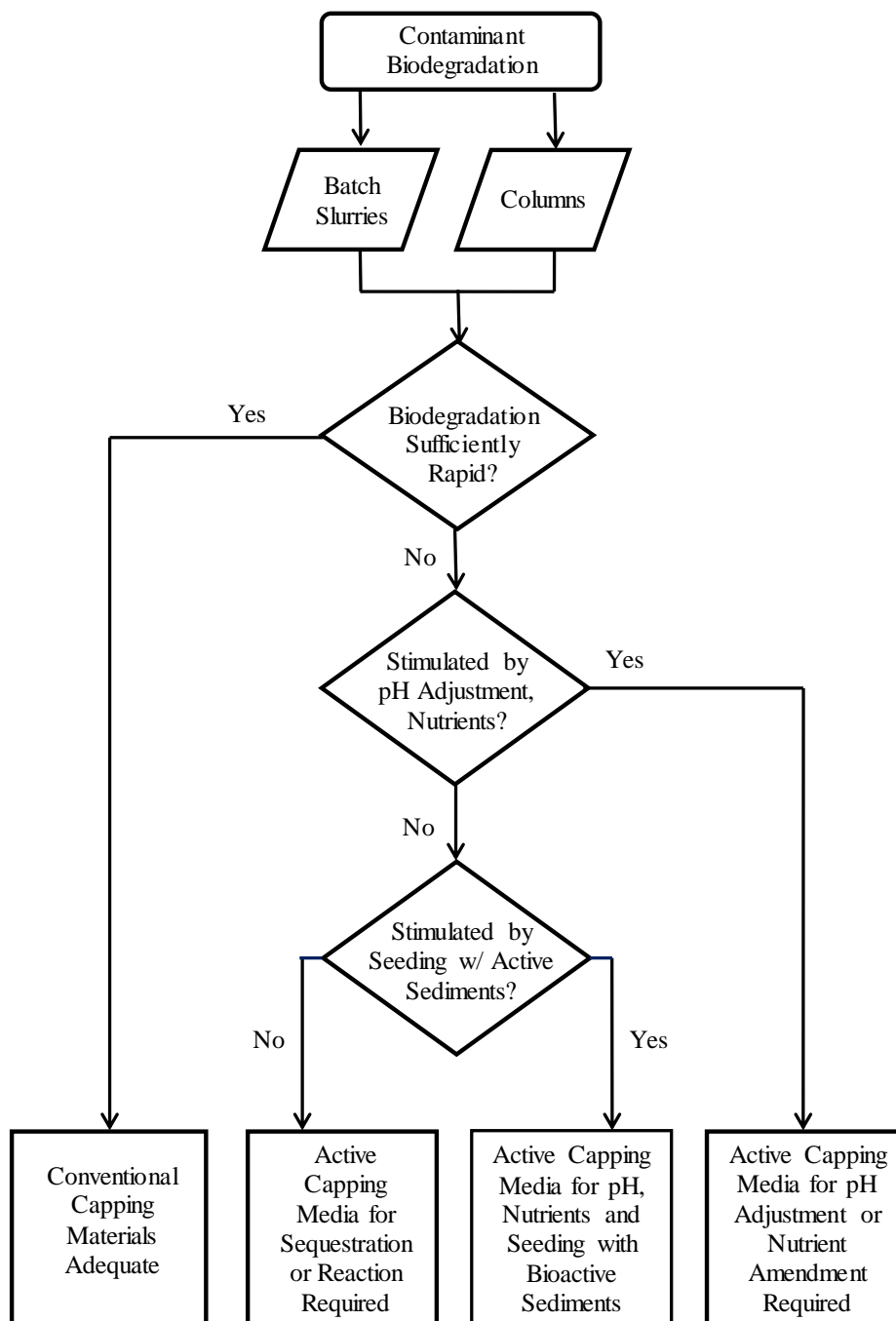


Figure 3.12: Theoretical flow diagram showing cap design considerations based on laboratory tests of contaminant biotransformation.

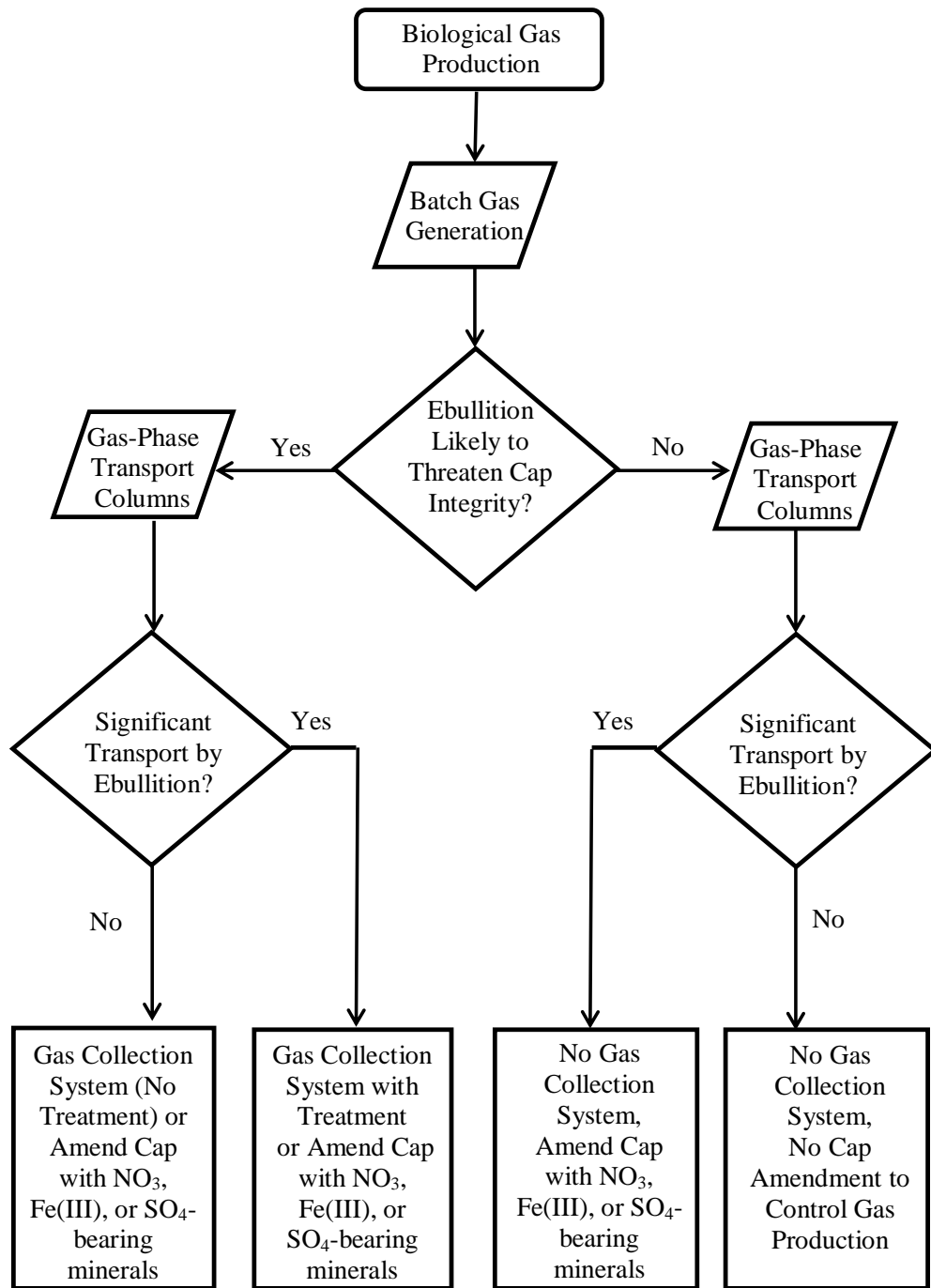


Figure 3.13: Theoretical flow diagram showing cap design considerations based on laboratory tests of gas production and contaminant transport.

Chapter 4. Insights into Bacterial Community Composition and Contaminant Catabolism Potential in Sediment Caps

4.1 INTRODUCTION

Recent research suggests that in situ sediment caps can become colonized by sediment bacteria and function as zones of hydrocarbon contaminant biotransformation (Himmelheber et al., 2009). Such a contaminant sink in a sediment cap would be particularly significant for sites polluted by low-sorbing, highly bioavailable pollutants, such as methylated and chlorinated benzenes. Benzene, toluene, ethylbenzene, and xylenes (BTEX), as well as chlorobenzene and dichlorobenzenes, have been shown to be biotransformed under a range of anaerobic conditions (Vogel and Grbic-Galic, 1986; Wilson et al., 1986; Grbic-Galic and Vogel, 1987; Ramanand et al., 1993; Edwards and Grbic-Galic, 1994; Lovley et al., 1995; Masunaga et al., 1996; Kazumi et al., 1997; Anderson et al., 1998; Kunapuli et al., 2008; Fung et al., 2009). While the potential for communities of sediment bacteria to biotransform pollutants is easily assessed by studying field samples, whether that activity will be translated to the cap is not known. Common considerations for predicting bacterial metabolic activity include the presence of catabolic genes, bacterial community structure, and biomass density.

The detection of genetic biomarkers, genes that code for enzymes that catalyze a particular reaction, is a common method of demonstrating the potential for pollutant biotransformation and complement community analysis by elucidating possible metabolic pathways. One of the genes encoding the enzyme that activates toluene by addition of fumarate to produce benzylsuccinate has proven useful as a genetic biomarker.

Specifically, the presence of the gene coding for the α -subunit of the enzyme benzylsuccinate synthase, *bssA*, would provide a line of evidence supporting anaerobic toluene biotransformation of toluene in sediments or in a sediment cap. The presence of *bssA* in groundwater samples from BTEX-contaminated aquifers has been similarly proposed as a line of evidence for anaerobic toluene biotransformation (Beller et al., 2002; Oka et al., 2011).

Bacterial community analysis has proven a useful tool for identifying responses by bacterial communities to environmental pollution (Osborn et al., 2000). For example, Vinas et al. (2005) observed shifts in community dominance from members of the α -Proteobacteria to members of the γ -Proteobacteria as bioremediation progressed in a creosote-contaminated soil. Similarly, the iron-reducing bacterial community was found to be enriched in *Geobacteraceae* in aquifer zones where benzene oxidation occurred as compared with zones where benzene was not oxidized (Rooney-Varga et al., 1999; Röling et al., 2001). Rooney-Varga et al. (1999) further emphasized the relationship between phylogeny and function, claiming that the “specific enrichment of *Geobacter* spp. is the only variable which has been found to be associated with the capacity for anaerobic benzene degradation at this site”. Given that examples exist where differences in metabolic activity have been attributed exclusively to bacterial community structure, it follows that a high degree of bacterial community similarity implies a high likelihood of similarity in metabolic capability (e.g., benzene oxidation).

At early times following placement of a sediment cap, the biomass concentration in the cap is likely insufficient to noticeably reduce contaminant concentrations. Corseuil

and Weber (1994) speculated that a critical microbial population size must develop for biotransformation to commence based on observed biomass-dependent delays in the degradation of benzene, toluene, and xylenes in aquifer sand. Over time, however, the biomass density in a sediment cap is expected to increase until a stable density is reached. Contaminant biotransformation might occur provided that the number of contaminant-degrading bacteria exceeds the critical population size and that the other requirements for biodegradation (Section 2.3) are satisfied. Because not all bacteria are metabolically active, measurements of total bacterial biomass in sediments are not reliable indicators of bacterial activity (Mosher et al., 2006). However, total microbial biomass can be indicative of environmental stimulation or stress, as evidenced by a doubling in bacterial biomass density in sediments polluted by PAHs of moderate concentration (i.e., $\sim 30 \mu\text{g PAH} / \text{g dry sediment}$) and a decrease in bacterial biomass in sediments polluted by PAHs at high concentrations (i.e., $\sim 80 \mu\text{g PAH} / \text{g dry sediment}$) with respect to the biomass at an unpolluted station (Langworthy et al., 2002). Development of a typical biomass density in a sediment cap (i.e., $10^6 - 10^9 \text{ cells} / \text{g dry sediment}$) would further indicate the potential for contaminant biotransformation within the cap.

Himmelheber et al. (2009) observed that the microbial community structure was highly correlated with the dominant terminal electron accepting process (TEAP) in a sediment column capped with sand. A steep redox gradient was established in their column, with oxygen diffusing into the top of the sand cap and the cap becoming increasingly reduced with depth. These conditions simulate the zone of redox transition near the cap/water interface but do not represent conditions at depth within a cap. For

instance, an aerobic boundary facilitates redox cycling and the oxidation of terminal electron acceptors such as manganese and iron, whereas under fully reduced conditions, electron acceptors are consumed by abiotic reactions with bisulfide (van Cappellan and Wang, 1996). Additionally, the experiment of Himmelheber et al., (2008) was conducted near 20°C, a temperature more favorable for bacterial growth than is common in many surface water sediments. Further study is required to characterize the bacterial colonization of a sand cap at site-representative temperatures and under strictly anaerobic conditions.

To determine the extent to which contaminant biotransformation observed in sediments polluted with BTEX, chlorobenzenes, and naphthalene is indicative of the potential for biotransformation in a sand cap, both sediment and cap were incubated in an anaerobic chamber while fluxes of indicators of dominant TEAPs were measured. Following colonization of the sand cap by sediment bacteria, both sediment and cap were analyzed for the presence/absence of the *bssA* gene, bacterial community diversity, the degree of similarity of the bacterial community composition at different depths in the sediment and the sand cap, and bacterial biomass density in both media. Further understanding of bacterial colonization and biotransformation activity in a sand-based sediment cap could improve pollutant fate and transport modeling and lead to more effective management of contaminated sediments.

4.2 MATERIALS AND METHODS

4.2.1 Upflow Columns

Surficial sediment cores were collected from Onondaga Lake locations 60105 and 70049 in 5-cm diameter polycarbonate tubes on July 3, 2009, shipped on ice to the University of Texas, and stored in the dark at 4°C until use. Cores were extruded into glass columns (15-cm length, 4.8-cm inner diameter) (Kimble-Kontes, Vineland, NJ). Sand was sieved through a 2-mm sieve and packed into glass columns (15-cm length, 4.8-cm inner diameter) with site surface water that was passed through a 0.45 µm filter. Each sediment column was connected in series to a single sand column by 1/8-inch inner-diameter Teflon tubing that was substituted by polyether-ether-ketone (PEEK) tubing (VICI Valco, Houston, TX) in November, 2009, to minimize hydrogen intrusion (Figure 4.1). Sediment porewater was pumped from the sediment column through the cap column, thereby exposing the sand cap to indigenous bacteria and pollutants. Stainless steel three-way valves (Arthur Fluid System Technologies, Austin, TX) were installed for sample collection at two locations: (1) between the sediment and sand columns, and (2) at the downstream end of the sand cap column. A peristaltic pump (Watson-Marlow-Bredel, Wilmington, MA) induced flow at a rate corresponding to a Darcy velocity of 0.25 cm/day. Flow was recirculated from sand cap columns to sediment columns except during sample collection, during which time sample volumes were replaced by withdrawal from a reservoir of deaerated surface water. Columns were incubated inside an anaerobic glovebox (Coy Laboratories, Grass Lake, MI) with an atmosphere of 0.2 – 3.0% H₂, make-up N₂, at 12°C.

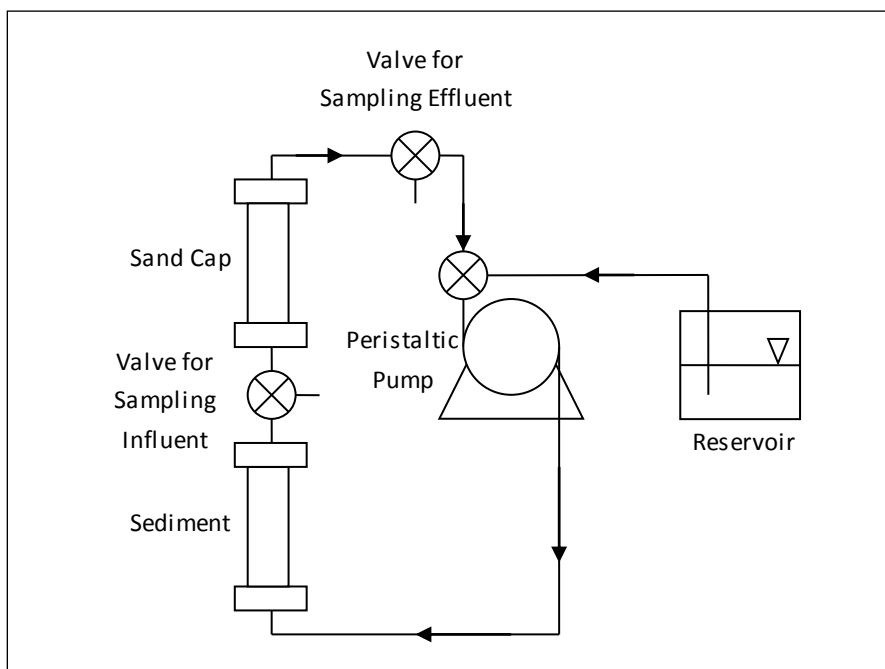


Figure 4.1: Laboratory column set-up for simulating sand-capped sediment.

4.2.2 Column Sampling and Analytical Methods

Sand cap influent and effluent were collected in 2-mL amber vials that were pre-filled with 0.5 mL of purge-and-trap grade methanol for analysis of volatiles by EPA method SW-826 8260B, performed by DHL Analytical (Round Rock, TX). Sample volumes were determined gravimetrically, and samples were stored without headspace at 4°C until analysis. Anions, specifically chloride, phosphate, and sulfate were measured on a 700 Series ion chromatograph with a 15-cm MetroSep A Supp 5 column (Metrohm USA, Inc. Riverview, FL) (Method 4110, Eaton et al., 2005). Ferrous iron was measured by the phenanthroline method (Method 3500B, Eaton et al., 2005). For methane and sulfide (Cline, 1969), 1.0 mL of eluent was collected in Teflon tubing then transferred to

either a 9-mL headspace vial for methane analysis by gas chromatography with flame ionization detection (Appendix B) or a 0.7-mL polypropylene microcentrifuge tube for sulfide analysis (Appendix B).

After 18 and 28 pore volumes had passed through cap columns 60105 and 70049, respectively, solid samples were collected for characterization. For column 60105, flow was terminated and both sediment and sand columns were dissected for biomass quantification and bacterial community characterization. For column 70049, approximately 10 grams each of sediment from the top of the sediment column and sand from the bottom of the sand column were removed for *bssA* gene detection and further biodegradation studies with ¹⁴C-labeled toluene (Section 3.2.6).

4.2.3 DNA Extraction, T-RFLP, and *bssA* Screening

DNA was extracted from sediment slurries with the FastDNA Spin Kit for Soil (MP Biomedicals, Solon, OH), according to the manufacturer's instructions. Extracted DNA was diluted 1:5 and 1:10 in 1X Tris-EDTA. DNA was amplified by PCR with primer sets for the 16S rRNA gene (FAM-labeled 8f/1492r) (Reardon et al., 2004) or the *bssA* gene (7772f/8546r) (Winderl et al., 2007) (Appendix B). To 0.2-mL PCR tubes, 2X PCR MasterMix (Fermentas/Thermo-Fisher Scientific), primers, bovine serum albumin (BSA), template DNA, and DNA-free water were added to give a reaction volume of 50 µL. The final concentrations were 2 mM MgCl₂, 0.2 mM dinucleoside triphosphates (dNTP), 1.25 Units of Taq polymerase, 0.4 g/L BSA, 500 nM forward and reverse primers, and 5 µL of diluted DNA template. Temperature programs were executed on an MJ Research thermal cycler (Hercules, CA), which was heated to 95°C before sample

tubes were added. Temperature programs for both 16S rRNA and *bssA* gene PCR were (1) initial template denaturation at 95°C for 5 minutes, then 30 cycles of (2) template denaturation at 95°C for 1 minute, (3) primer annealing for 1 minute, and (4) extension at 72°C for one minute. A final extension of 72°C for 10 minutes followed cycle completion. The size of the PCR products was checked by agarose gel electrophoresis. To minimize amplification of non-target sequences, a “touchdown” annealing temperature method was adapted from Burr et al. (2006) for T-RFLP, which consisted of five cycles at each 60°C, 58°C, and 56°C, then 15 cycles at 55°C. For *bssA*, 35 temperature cycles were completed at three different annealing temperatures tested in parallel: 54°C, 56°C, and 58°C. PCR products were checked by electrophoresis in a 1.5 % agarose gel in 1X Tris-Acetate-EDTA buffer at a current of 70 mA for 40 minutes. Gels were stained in 1X SybrGold for 15 minutes and viewed on an ultraviolet light box.

For T-RFLP, amplicon from three PCR reactions were pooled and purified with the MinElute PCR Clean-up kit (Qiagen, Valencia, CA) to remove remaining primers and nucleotides. Purified amplicon concentrations were measured by spectrophotometer (NanoDrop, Wilmington, DE), and 100 ng of purified amplicon was digested with 5 units of restriction enzyme *RsaI* (New England BioLabs, Ipswich, MA) in 20 µL of 1X NEB Buffer 4 at 37°C for 3 hours followed by enzyme inactivation at 65°C for 20 minutes. Digested amplicon was purified by MinElute, and fragments were separated by fragment length on an Applied Biosystems 3130 DNA sequencer (Life Technologies, Carlsbad, CA) at the Institute for Cellular and Molecular Biology at the University of Texas-Austin.

To account for differences in signal intensity between samples, electropherogram peak areas were normalized according to Kaplan et al. (2001). Briefly, the smallest relative peak area (i.e., the ratio of the peak area to the total area) from the sample with the smallest total area was used as the new relative peak area threshold. Relative peak areas in other samples that were smaller than this threshold were discarded, the total areas were recalculated for each sample, and normalized relative peak areas were computed.

Several widely used indices were applied to quantify species richness, community evenness, and community similarity. The species richness was reported as the number of distinct peaks, each representing an operational taxonomic unit (OTU), in each profile following normalization (Liu et al., 1997). Community evenness, an indication of whether OTUs are evenly distributed (high value) or highly skewed (low value), was assessed within each dissection zone using Simpson's index ($E_{1/D}$) and the Smith-Wilson index (E_{var}) (Equations 4.2 and 4.3, respectively) (Smith and Wilson, 1995; Blackwood et al., 2007). $E_{1/D}$ demonstrates higher sensitivity to more abundant operational taxonomic units (OTUs) than to less abundant OTUs while E_{var} is reportedly indiscriminate (Smith and Wilson, 1995). Both the Jaccard index (1912) and the Bray-Curtis similarity index (Equations 4.4 and 4.5) (Bray and Curtis, 1957; Bloom, 1981) were computed between all dissection zones to provide a quantitative estimate of bacterial community self-similarity within sediment and sand as well as the similarity across sediment and sand samples. The Jaccard index considers only the presence or absence of species within a community while the Bray-Curtis index accounts for the relative abundance of individual species.

Evenness:

$$E_{1/D} = \frac{1}{\sum_{j=1}^S x_j^2} \frac{1}{S} \quad \text{Equation 4.2}$$

$$E_{var} = 1 - \frac{2}{\pi} \arctan \left\{ \frac{\sum_{i=1}^S (\ln(x_i) - \sum_{j=1}^S \ln(x_j)/S)^2 / S}{\sum_{j=1}^S x_j} \right\} \quad \text{Equation 4.3}$$

Similarity:

$$J = \frac{A \cap B}{A \cup B} \quad \text{Equation 4.4}$$

$$BC_{A,B} = \frac{2 \sum_{j=1}^{S_{A,B}} \min(x_{A,j}, x_{B,j})}{\sum_{j=1}^{S_{A,B}} (x_{A,j} + x_{B,j})} \quad \text{Equation 4.5}$$

where A and B are two T-RFLP electropherograms, x is the area of peak j, which corresponds to a particular fragment length, S is the number of peaks in a given profile, and $S_{A,B}$ is the total number of unique peaks in profiles A and B. Note that evenness and similarity indices are bound by (0,1).

4.2.4 Biomass Density Determination

Phospholipids were extracted from sediment slurries according to Findlay et al. (1989). Approximately two grams of sediment or sand was transferred to a 50-mL glass centrifuge tube, to which 7.4 mL of chloroform, 14.3 mL of methanol, and 5.9 mL of 50 mM potassium phosphate were added. Tubes were shaken and then incubated statically at room temperature (approximately 22°C) for three hours. An additional 7.4 mL each of chloroform and phosphate solution were added and the tubes were again shaken vigorously. Suspensions were centrifuged at 3000 rpm for five minutes and then

incubated statically at room temperature for 24 hours. The aqueous (top) layer was aspirated and discarded, and the chloroform layer was passed through glass fiber filter paper and collected in a clean 50-mL glass centrifuge tube. The chloroform volume was reduced to 1-2 mL under a nitrogen stream; then 100 μ L was transferred to a 2-mL amber vial and completely removed under a nitrogen stream. Phospholipids were digested by addition of 0.45 mL of potassium persulfate (50 g/L in 0.36 N H_2SO_4) and incubated at 95°C overnight. After samples cooled, 0.1 mL of an ammonium molybdate solution (2.5% in 5.72 N H_2SO_4) was added and vials were incubated at room temperature for ten minutes. Molybdophosphate was reacted with 0.45 mL of a solution of polyvinyl alcohol (0.11%) and malachite green (0.011%) for 30 minutes at room temperature, after which time the absorbance of 0.3 mL of reactant was measured at 610 nm in a clear 96-well plate on a Biomek plate reader (Appendix B). Molybdophosphate concentrations were calculated from a standard curve prepared with glycerol phosphate (Sigma-Aldrich, St. Louis MO). All glassware was washed with phosphate-free detergent, and a blank (i.e., sand from the same source as that used for column tests) was processed in parallel with samples. The surface area of sediment and sand samples was determined on an Autosorb 1-MP (Quantachrome, Boynton Beach, FL) at the Jackson School of Geosciences (Appendix B).

4.2.5 Statistical Analysis

Differences between concentrations of TEAP indicators in sand cap column influent and effluent as well as differences between biomass densities in sand and sediment columns were assessed using the Wilcoxon Rank Sum Test. The student's t-test

was used to determine whether species richness and community evenness differed significantly between the sand cap and the sediments at a level of $\alpha = 0.05$. The similarity in bacterial community composition was computed pairwise for each profile with all other profiles in both columns (i.e., five sections from the sand cap column and six sections from the sediment column giving a symmetrical 11 x 11 similarity matrix). Only similarity scores above the diagonal were considered, thus eliminating redundant elements and the scores of unity reflecting perfect self-similarity. Three groups of similarity scores were considered: (1) both profiles were from the sediment column ("S:S", N = 15), (2) both profiles were from the sand cap column ("C:C", N = 10), and (3) one profile was from the sediment column and the other was from the sand cap column ("S:C", N = 30). The null hypothesis, that the three datasets did not differ significantly at a level of $\alpha = 0.05$, was tested by the Kruskal-Wallis one-way analysis of variance on ranks. Were the null hypotheses rejected, a pairwise comparison (Dunn's test) was used at a significance level of $\alpha = 0.05$. All statistical analysis was performed with the program SigmaPlot 11.0 (Systat Software Inc., San Jose, CA).

4.3 RESULTS AND DISCUSSION

4.3.1 Upflow Columns – Fluxes of Contaminants and Geochemical Indicators of Anaerobic Metabolism

Only half of the contaminants in porewater from sample 60105 were of concentrations exceeding the analytical detection limit of 3.2 $\mu\text{g/L}$, and none were above the minimum reporting limit (Table 4.1). In contrast, concentrations were 1-2 orders of

magnitude higher in porewater from sample 70049. A student's t-test found that differences were not significant between sand cap column influent and steady-state effluent concentrations at a level of $\alpha = 0.05$ (Table 4.1), although biotransformation of toluene was observed in column 70049 after steady effluent concentrations were reached. The low concentrations in sample 60105 might not be sufficient to induce gene expression for contaminant biotransformation. For instance, induction for aerobic toluene degradation reportedly occurs at concentrations near 50 $\mu\text{g/L}$ (Robertson and Button, 1987); threshold concentrations for anaerobic toluene degradation could not be found. Failure to induce gene expression likely contributes to the observed absence of contaminant biotransformation in the sand cap column of sample 60105 (Table 4.1).

Table 4.1: Sand cap column influent and steady-state effluent concentrations for columns 60105 and 70049, reported as "mean (one standard deviation)" in $\mu\text{g/L}$ except pH. P-values computed by student's t-test at significance level of $\alpha = 0.05$ except where noted. Effluent concentrations of naphthalene in column 60105 and 1,3-Dichlorobenzene in column 70049 did not reach steady state.

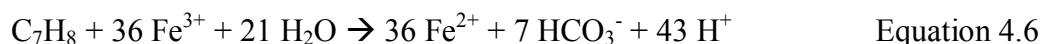
Analyte	60105			70049		
	Influent	Effluent	p-value	Influent	Effluent	p-value
1,2-Dichlorobenzene	<3.2	<3.2	--	48.0 (16.5)	39.7 (0.07)	0.50
1,3-Dichlorobenzene	<3.2	<3.2	--	7.1 (2.6)	--	--
1,4-Dichlorobenzene	<3.2	<3.2	--	85.6 (32.1)	59.2 (2.5)	0.27
Benzene	4.9 (1.1)	5.2 (0.7)	0.99	63.6 (26.3)	59.9 (25.0)	0.66
Chlorobenzene	5.6 (2.0)	5.8 (0.5)	0.13 ^a	182 (52)	164 (14)	0.46
Ethylbenzene	<3.2	<3.2	--	20.1 (6.7)	17.3 (1.9)	0.38 ^a
Naphthalene	9.5 (3.0)	--	--	384 (134)	343 (29)	0.56
Toluene	8.4 (7.3)	7.0 (2.9)	0.59 ^a	35.9 (16.3)	33.5 (3.0) ^b	0.80
Total Xylenes	5.1 (0.8)	9.0 (0.1)	<0.001	142 (51)	118 (18)	0.32
pH	7.7 (0.4)	8.1 (0.3)	0.13	8.2 (0.1)	8.0 (0.1)	0.07

^a Test of normality failed, p-value was computed by the Wilcoxon rank sum test

^b The steady-state effluent concentration was computed before the onset of biotransformation

Despite a lack of detectable contaminant biotransformation in column 60105, anaerobic metabolic activity was suggested by geochemical TEAP indicators. Dissolved iron and methane concentrations of 20 – 40 μM and up to 800 μM , respectively, confirmed that the sediment bacterial community was metabolically active. Sulfate reduction was confirmed by the presence of sulfide at a concentration of approximately 10 μM .

Biotransformation of toluene was observed in the sand column of sample 70049 between cap pore volumes 4 – 8. The average influent toluene concentration was reduced from 0.43 μM at the influent to 0.11 μM at the effluent (Figure 4.2). Over the same period of time, the concentration of dissolved iron increased from $7.7 \pm 5.3 \mu\text{M}$ (mean \pm one standard deviation) at the inlet to $16.8 \pm 6.0 \mu\text{M}$ at the outlet of the sand cap column (Figure 4.3). Coupled with iron reduction, complete oxidation of 0.32 μM toluene theoretically yields 12.5 μM Fe^{2+} (Lovley and Lonergan, 1990) (Equation 4.6):



Due to the presence of other electron donors in the sediment cap and the fact that the influent and effluent ferrous iron concentrations were not well-defined prior to the initiation of toluene biotransformation, toluene oxidation cannot be conclusively coupled with iron reduction. However, evidence of iron reduction in the cap and the documented importance of iron-reducers in toluene biotransformation (e.g., Coates et al., 1999) suggest that the two processes might have been coupled.

The microbially-reducible iron oxide content of the sand was determined to be 1.4 $\mu\text{mol/g}$ by the method of Lovley and Phillips (1987a) (Appendix B). Oxidation of other electron donors could have been coupled with either iron- or sulfate-reduction resulting in the precipitation of iron sulfides in the cap column, but this could not be confirmed. Toluene biotransformation appeared to stop after elution of 8 cap pore volumes for reasons that are discussed in Section 5.3.4.1.

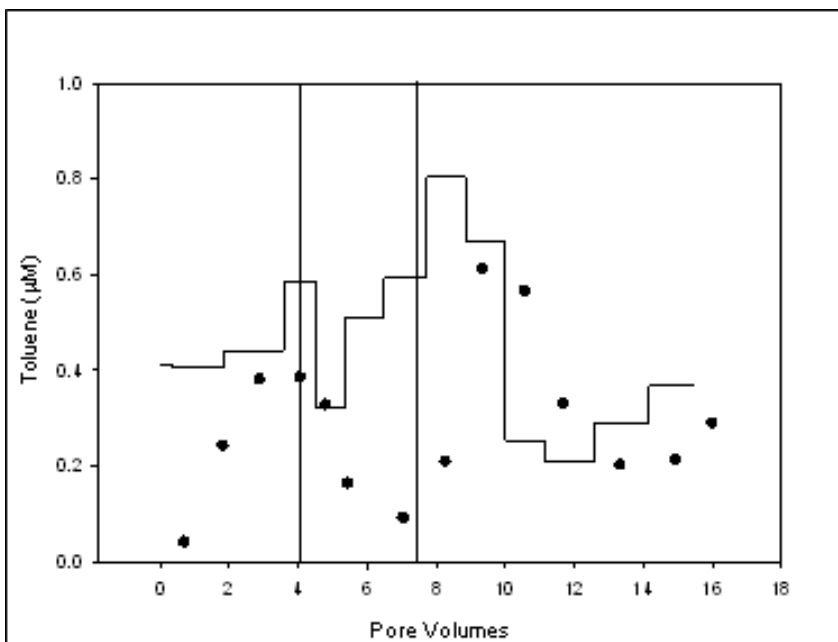


Figure 4.2: Toluene influent (solid line) and effluent observations (circles) in column 70049. The vertical lines denote the time that toluene biotransformation occurred.

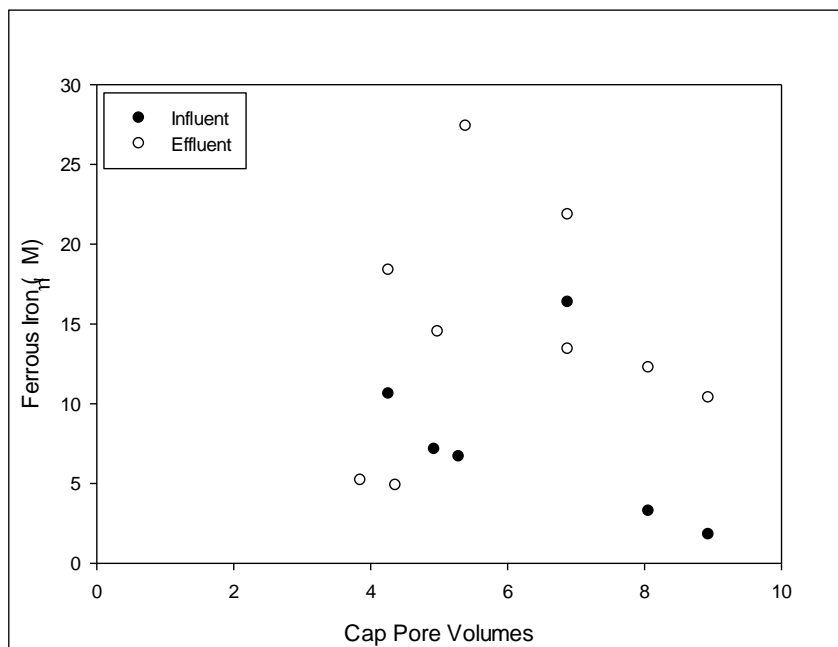


Figure 4.3: Ferrous iron concentrations in sand cap column influent and effluent samples from column 70049.

4.3.2 Detection of *bssA* in Sediment and Sand from Column 70049

The *bssA* gene was detected in both sediment and sand samples from column 70049 (Figure 4.4), indicating the potential for anaerobic toluene biotransformation in both media. Detection of *bssA* provides a line of evidence for anaerobic biotransformation as the mechanism of toluene removal in the sand cap column (Figure 4.2). Similarly, the presence of the *bssA* gene was proposed as a line of evidence for ongoing natural attenuation in BTEX-contaminated aquifers (Oka et al., 2011). The nearly stoichiometric production of ferrous iron concomitant with toluene removal suggests possible biotransformation by iron-reducing bacteria, several of which have been implicated in the degradation of monoaromatic contaminants (Coates et al., 1996). The benzylsuccinate pathway for toluene degradation has been reported for strains of the iron-reducers *Desulfitobacterium aromaticivorans*, *Geobacter toluenoxydans* (Kunapuli et al., 2010), *Geobacter grbiciae* and *Geobacter metallireducens*, with detection of the *bssA* gene with primers 7772f/8546r in the latter two species (Winderl et al., 2007).

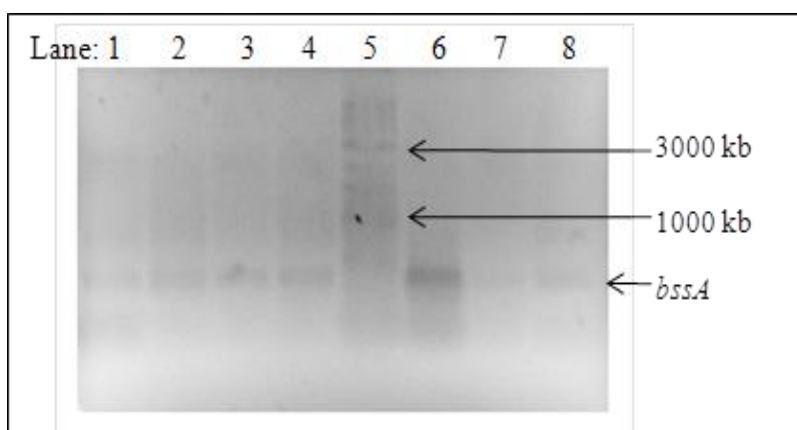


Figure 4.4: Amplification of the *bssA* gene. Ten ng of template DNA from sand was added to the reactions in lanes 1, 3, and 7; 20 ng was added to reactions in lanes 2, 4, and 8; sediment DNA was the template in lane 6 (30 ng). Twenty μL of PCR product were added to each sample well. The annealing temperature was 54°C in lanes 1-2, 56°C in lanes 3-4, and 58°C in lanes 6-8. Lane 5 contains 5 μL of a 2-log DNA ladder (New England Biolabs, Ipswich, MA).

4.3.3 Bacterial Community Diversity and Community Similarity in Column 60105

Fragment patterns from T-RFLP analysis indicated that bacterial communities in the sediment and sand cap were complex throughout each column (Figures 4.5 and 4.6). Species richness, given by the number of distinct peaks in each normalized profile, averaged 41.8 ± 3.9 ($n = 5$) in sand sections and 45.2 ± 6.2 ($n = 6$) in sediment sections; species richness was not significantly different in the two media ($p = 0.32$).

The two evenness indices, indicators of the degree to which the density is evenly distributed among OTUs in an electropherogram (e.g., 0 means uneven and high skew within the community whereas 1 means perfect evenness), were contradictory on whether the communities were similarly skewed in sand and sediment, perhaps owing to their difference in bias toward abundant species. The Simpson's index was significantly

different between sand and sediment ($p < 0.001$) with index averages and standard deviations of 0.26 ± 0.04 in sand and 0.47 ± 0.05 in sediment, suggesting greater skew in the sand distributions. Conversely, the Smith-Wilson index (0.56 ± 0.05 in sand and 0.60 ± 0.06 in sediment) suggested insignificant differences in community evenness ($p = 0.31$). The same conclusion was reached by Himmelheber et al. (2009), who reported Smith-Wilson evenness values between 0.23 and 0.53 and concluded that OTU distributions were similar across all dissection zones. By inspection of the electropherograms in Figures 4.5 and 4.6, community skew appears more severe in sand than in sediment: in nearly all sand profiles, 1-2 large peaks account for the majority of the peak area whereas in sediment profiles, the area is largely distributed among nearly half a dozen peaks. Thus, one or two OTUs appear to dominate the bacterial community in the sand cap, while the sediment community has several dominant members.

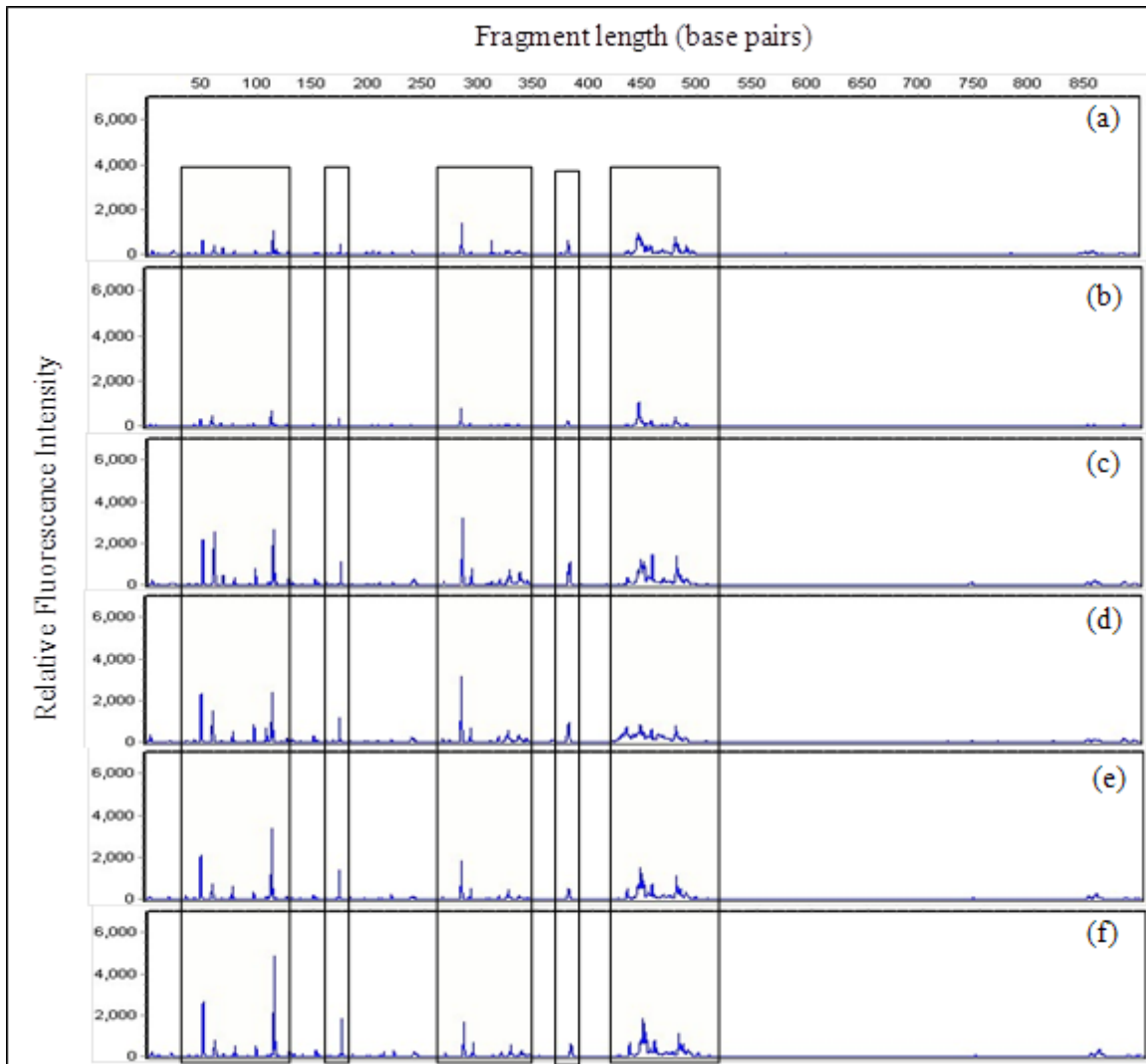


Figure 4.5: T-RFLP electropherograms from sediment DNA at midpoint-depths of (a) 2.5 cm, (b) 7.5 cm, (c) 12.5 cm, (d) 17.5 cm, (e) 22.5 cm, and (f) 27.5 cm. Boxes outline peak patterns that were consistently present in all samples though changes in relative area were observed.

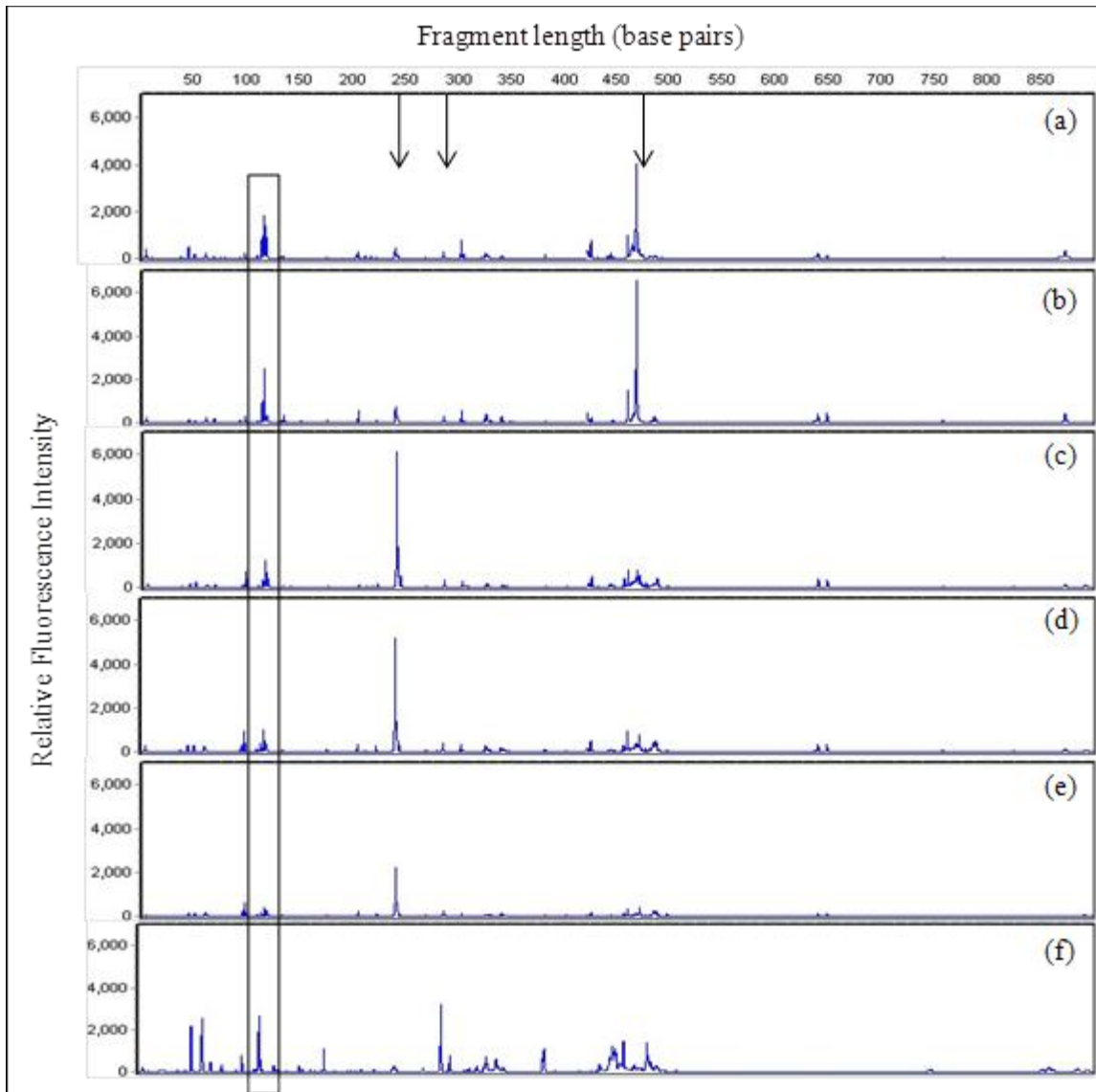


Figure 4.6: T-RFLP electropherograms for sections of the sand column at midpoint-depths of (a) 3.75 cm, (b) 6.25 cm, (c) 8.75 cm, (d) 11.25 cm, (e) 13.75 cm, and (f) from the sediment column at a midpoint-depth of 12.5 cm. Boxes outline peak patterns that were consistently present in all samples though changes in relative area were observed. Arrows highlight peaks that were prominent in either some sand samples or some sediment samples but not both, indicating shifts in bacterial community structure.

Both Jaccard and Bray-Curtis indices showed greater similarity between two sections from the same column (i.e., two profiles from sediment or two profiles from sand) than the similarity between two profiles from different columns (i.e., one profile from sediment and one profile from sand) (Figure 4.7). The Kruskal-Wallis one-way analysis of variance on ranks found differences to be significant for both Jaccard and Bray-Curtis similarity matrices. Pairwise comparison by Dunn's method determined that, for both the Jaccard index and the Bray-Curtis index, similarity scores for two profiles from the sediment column ("S:S") were not significantly different from similarity scores for two profiles from the sand cap column ("C:C"). However, scores for one profile from the sediment column and one profile from the sand cap column ("S:C") did differ significantly with both S:S scores and C:C scores.

The Jaccard index, based on species presence/absence, and the Bray-Curtis index, based on relative species abundance, both suggest that bacterial community structures in sediment and sand are largely dissimilar. Possible explanations for community dissimilarity include differences between sediment and sand mineralogy (Boyd et al., 2007), grain size distribution (Jackson and Weeks, 2008), and carbon content (Polymenakou et al., 2005). Given the dissimilarity between bacterial communities in sediments and in the sand cap, bacterial community structure is not likely to be a useful tool for predicting the translation of a certain metabolic capability (e.g., benzene oxidation) to a sediment cap from the underlying sediments.

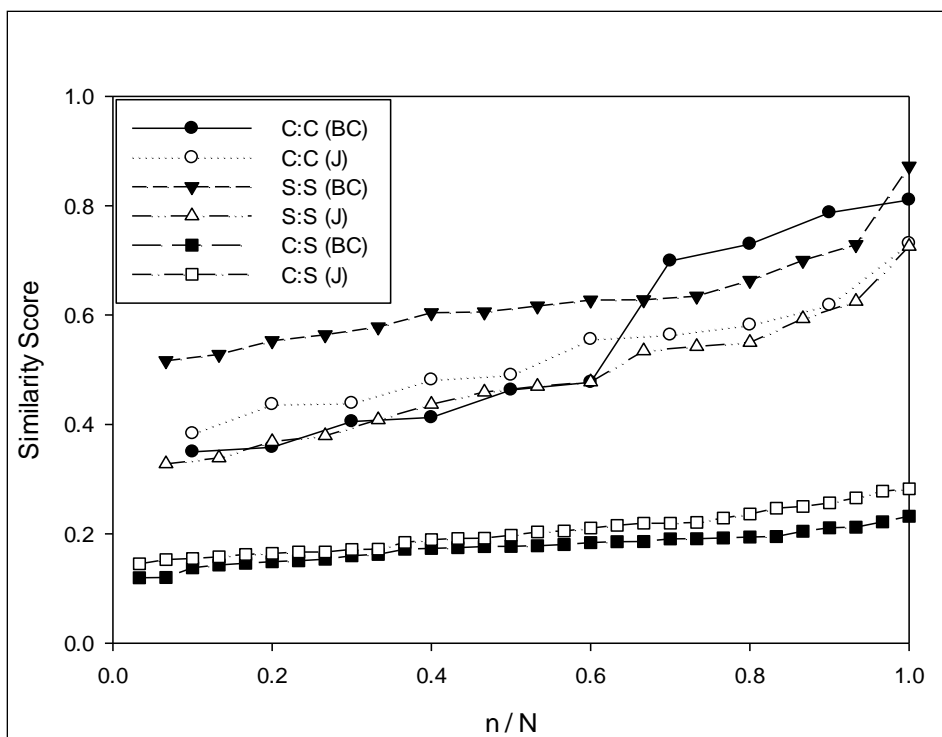


Figure 4.7: Similarity indices ranked from lowest ($n=1$) to highest ($n=N$). Pairwise similarity between profiles from the cap (C:C) and sediment (S:S) are represented by circles and triangles, respectively, and similarity between profiles from each the sediment and the cap columns (S:C) are shown as squares. Bray-Curtis (BC) and Jaccard (J) indices are represented by solid and hollow markers, respectively.

The distance between analyzed sections did not strongly influence bacterial community similarity. The highest correlation observed between distance and community similarity was for paired profiles from the sand cap column using the Bray-Curtis index ($R^2 = 0.45$) and the lowest correlation observed was for comparisons between the sediment and sand columns using the Jaccard index ($R^2 = 0.02$). This result suggests that differences in community composition within each column are due to natural variability

rather than the development of concentration gradients with respect to energy sources, electron acceptors, or nutrients, along the vertical axis.

4.3.4 Biomass Quantification in Column 60105

Phospholipid densities per gram of sediment were approximately 20 times higher in sediments than in the sand cap in column 60105 (Table 4.2). Applying a conversion factor of 3.43×10^9 cells per 100 nmol of phosphate (Findlay et al., 1989), cell densities were on the order of 10^8 cells per gram of dry sand and 10^9 cells per gram of dry sediment, within the range of densities commonly found in the literature (Dale, 1974; Findlay et al., 1989; Jiang et al., 2006). Cell density was not found to be correlated with depth in either the sediment or the sand column ($R^2 < 0.1$ for both). The phospholipid density measured on clean sand was indistinguishable from the experimental blank.

Table 4.2: Physical properties of sand and sediments and bacterial cell densities normalized by mass or surface area. Specific surface area is reported as “mean (% error)” (n = 2) while all others are “mean (one standard deviation)”

	Sand	Sediment
Dry solids bulk density (g cm^{-3}) (n=3)	1.67 (0.24)	0.80 (0.03)
Specific surface area ($\text{m}^2 \text{g}^{-1}$) (n=2)	1.7 (8.6)	5.7 (1.8)
Cell density per mass of solids ($\times 10^{-7}$ cells g^{-1})	8.82 (6.06) ^a	144 (46.1) ^b
Cell density per area of solids ($\times 10^{-7}$ cells m^{-2})	5.04 (3.46) ^a	25.1 (8.03) ^b

^a n = 11

^b n = 12

One factor contributing to the smaller biomass density in sand than in sediments is the difference in surface area available for colonization by bacteria. The bulk density

and specific surface area of sediments and sand (Table 4.2) indicate that the grain surface area available for colonization by bacteria is three times greater in sediment than in sand on a mass basis and two times greater for a given volume of media. The differences in cell densities between sediment and sand were significant on both a mass and surface area basis ($p < 0.001$).

Detection of substantial biomass in a sand cap supports the hypothesis that a sand cap becomes colonized by bacteria and could therefore become a zone of contaminant biotransformation. Sand cap colonization by sediment bacteria was reported previously (Himmelheber et al., 2009) but this study expands upon those findings by demonstrating biomass development under conditions that are less conducive to bacterial growth (i.e., strictly anaerobic and at low temperature), representing a cap at depth. It must be noted that this result was obtained in a hydrogen-rich environment so the supply of an energy source was likely unlimited. With regard to contaminant biotransformation, a high biomass density shows that a sand cap can support bacterial growth, but further characterization is required to determine whether specific contaminant-degrading populations are among the bacterial community and are actively metabolizing pollutants.

4.4 CONCLUSIONS

The apparent biotransformation of toluene and possible coupling with dissimilatory iron reduction in a sand column demonstrates the potential for biological pollutant mass removal in sediment caps and suggests an important role for iron-reducing bacteria, such as members of the family *Geobacteraceae*, in the oxidation of hydrocarbon

contaminants in sand caps. Detection of the *bssA* gene in a sand cap sample provides further evidence of pollutant-biotransformation potential. Possible explanations for the termination of toluene biotransformation in column 70049 are explored in Chapter 5.

The development of a complex bacterial community in a sand column simulating a sediment cap was demonstrated under strictly anaerobic conditions at a temperature representative of surface water sediments (i.e., 12°C). This study complements the simulation of a near-surface zone of a sediment cap by Himmelheber et al. (2008, 2009) in which one boundary of a sand column was aerobic and a steep redox gradient existed across the column. An aerobic boundary facilitates redox cycling and increases the availability of high-potential electron acceptors (van Cappellan and Wang, 1996) and, in conjunction with elevated temperatures (i.e. 20°C), creates thermodynamic conditions that are more favorable for bacterial growth than are commonly found in the field. The observation by Himmelheber et al. (2009) that sand caps become colonized by bacteria and can become zones of contaminant biotransformation was shown to be true even under strictly anaerobic conditions and at a temperature representative of lake sediments. However, molecular hydrogen, an important energy source for bacteria, was present in the experiment at greater than normal concentrations for natural sediments and likely contributed to enhanced bacterial growth.

Under strictly anaerobic conditions, the bacterial biomass normalized to mass of solids was smaller in sand than in sediments by a factor of 20. Bacterial community richness was similar, but indices of community evenness were contradictory, with the sand and sediment communities being either comparably even or more even (i.e., less

skewed) in sediment than in sand. The bacterial community similarity in sediments and sand was found to be significantly higher within a medium than across media, as determined by both a presence/absence index (i.e., the Jaccard index) and an index that weighs OTUs according to relative abundance (i.e., the Bray-Curtis index). This finding suggests that, despite examples of the use of bacterial community structure for predicting contaminant biodegradation potential (Rooney-Varga et al., 1999; Röling et al., 2001), it is likely not useful for predicting whether potential activity observed in sediments is translated to a cap. Methods that target specific bacterial populations with known functional capabilities (i.e., benzene oxidation), such as DNA hybridization, would provide a more definitive indication of the potential for contaminant degradation by confirming the presence of bacteria capable of degradation. Additionally, characterization of bacterial communities from both the sediment and the sand, including identification by sequencing 16S rRNA for comparison against a database of known pollutant degraders, is recommended. Additional suggestions are discussed in detail in Section 7.2.3.

Collectively, these results complement previous studies suggesting the potential for a sand cap to function as a zone of contaminant biotransformation, demonstrated specifically by the observation of anaerobic toluene biotransformation. Although the removal of toluene was not continuous, the reasons are believed to be due to experimental conditions that would not exist in the field (Chapter 5). Predicting rates of metabolic processes in sediment caps remains a challenge that may eventually be surmounted by improved understanding of the interdependency of bacterial community structure and metabolic activity.

Chapter 5. Thermodynamic and Kinetic Considerations for Contaminant Biotransformation in Sand-Capped Sediment Column Experiments

5.1 INTRODUCTION

Laboratory column tests have long been used to examine pollutant fate and transport in sediments and soils and were recently applied to studies of biological solvent dechlorination (Himmelheber et al., 2007) and polycyclic aromatic hydrocarbon (PAH) oxidation (Hyun et al., 2008) in sediment caps. In the current study, column tests were employed to assess the potential for biotransformation in a sand cap of the contaminants of interest in Onondaga Lake sediments, namely BTEX, chlorobenzenes, and naphthalene.

Toluene biotransformation in an anaerobic sand cap column in series with a column of sediment from location 70049 in Onondaga Lake was documented in Sections 3.3.3 and 4.3.1. Biotransformation started after elution of four cap pore volumes and ceased after elution of eight cap pore volumes. The description of sand-capped column tests in Chapter 4 will be expanded to columns containing sediments from different sampling locations with details pertaining to operating conditions, the range of detectable degradation rates, the biogeochemical processes occurring in the column, and the corresponding thermodynamics of biotransformation.

5.2 METHODS

5.2.1 General Column Operation

Sediment cores (5-cm inner diameter) were collected from Onondaga Lake sediment management unit (SMU) six (locations 60103, 60105, 60216) and SMU seven (70087) and 10 liters of Onondaga Lake surface water (OLSW) were sent to the University of Texas at Austin on ice on October 8, 2008. Additional 5-cm diameter cores were collected from SMU seven (locations 70024, 70049, 70050, 70123) and shipped to the University of Texas at Austin on ice on July 3, 2009. Cores and water were stored in the dark at 4°C until use.

Columns were prepared and operated in an anaerobic chamber (Coy Labs, Grass Lake, MI) with an atmosphere of ~3% H₂, 97% N₂ at 12°C as described in Section 4.2.1. Flow to columns 60103, 60105, 60216, and 70087 began on March 9, 2009; columns 70024A, 70049A, 70050, and 70123 began on August 6, 2009; and columns 70024B and 70049B began on September 8, 2009, giving ten columns total. Initially, all columns were connected by Teflon tubing except for the peristaltic pump tubing. The week of November 10, 2009, all Teflon tubing was replaced with polyether-ether-ketone (PEEK) tubing (VICI Valco, Houston, TX) to reduce the transfer of hydrogen gas from the glovebox atmosphere into the water that was recirculated through the columns.

Between November and late December, 2009, a leak in the chamber allowing hydrogen to escape and oxygen to enter was evident from the accumulation of moisture and the rate at which the volume of the inflatable chamber decreased. The chamber atmosphere required replenishment 2 – 3 times per week rather than weekly, as was

typical during normal operation. Oxygen concentrations up to 500 ppm were occasionally detected during this time. A slit in the vinyl was sealed in mid-January, 2010, and chamber operation returned to normal with steady hydrogen concentrations of 2 – 3%.

5.2.2 Model description and identification of relevant transport parameters

Transport of a conservative tracer through the sand cap column was described by a one-dimensional transport equation with advection and diffusion:

$$R \frac{\partial C}{\partial t} = D \frac{\partial^2 C}{\partial z^2} - v \frac{\partial C}{\partial z} \quad \text{Equation 5.1}$$

where R is the retardation factor [--],
 C is the aqueous phase concentration [M/L³],
 t is time [T],
 D is dispersion [L²/T],
 z is position (positive in the direction of flow) [L],
and v is the interstitial (i.e., pore water) velocity [L/T].

Dispersion, D , is the sum of the effective diffusion coefficient and the product of the dispersivity and the interstitial velocity (v):

$$D = D_{\text{eff}} + \alpha v \quad \text{Equation 5.2}$$

where D_{eff} is the effective diffusion coefficient [L²/T] and
 α is the hydrodynamic dispersivity [L].

D_{eff} describes molecular diffusion in a porous medium and is commonly estimated as the product of the diffusion coefficient in water (D_w , [L²/T]) with a correction for the tortuosity of the diffusive path. Relations defining D_{eff} as a function of D_w and porosity (ϵ , [--]) that successfully described experimental data in sandy sediments with porosity 0.35 – 0.40 were proposed by Lerman (1979)

$$D_{\text{eff}} = D_w \epsilon^2 \quad \text{Equation 5.3}$$

and by Weissberg (1963)

$$D_{eff} = D_w \frac{\varepsilon}{1 - 2\ln(\varepsilon)} \quad \text{Equation 5.4}$$

The value of D_{eff}/D_w is similar for both of these relations for the porosity range under consideration. The above expressions are defined in terms of Darcy velocity and must be divided by ε for calculations in terms of pore water velocity.

The parameters velocity and dispersivity are properties of the medium and are thus constant in a given column for all solutes. These were estimated by injection of bromide, a non-reactive and non-sorbing hydraulic tracer.

5.2.3 Breakthrough of hydraulic tracer and parameter fitting

5.2.3.1 Hydraulic Tracer Test

Potassium bromide was dissolved in OLSW at a final concentration of 40 mM, and the solution was deaerated. The tracer was introduced between the sediment and cap columns (Chapter 4, Figure 4.1) with a syringe pump at a rate of 0.2 $\mu\text{L}/\text{min}$ from March 15 to March 21, 2010. The concentration of tracer entering the cap column was described by a material balance (Figure 5.1) and was assumed constant for a given column. Influent bromide concentrations differed between columns because Q_{sediment} was not equal for all peristaltic pump channels.

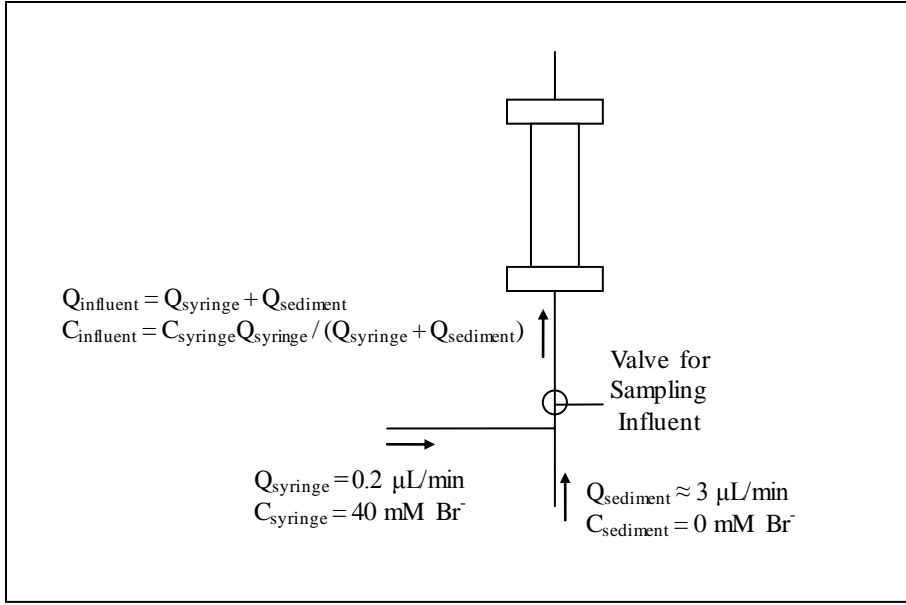


Figure 5.1: Material balance on bromide for the sand cap column, where Q is volumetric flow rate and C is molar concentration.

The sand cap column was modeled as a semi-infinite domain with constant influent concentration and constant initial concentration (assumed to be zero):

Initial condition: $C(t=0, z) = 0 \text{ mg/L}$
 Boundary condition 1: $C(t, z \rightarrow \infty) = 0 \text{ mg/L}$
 Boundary condition 2: $C(t, z=0) = C_{\text{influent}}$

A general solution to Equation 5.1 subject to the above conditions is reported by

van Genuchten and Alves (1982) (after Lapidus and Amundson, 1952; Ogata and Banks, 1961):

$$\begin{aligned}
 C(z, t) &= C_i + (C_0 - C_i) A(z, t) & \text{for } 0 < t \leq t_0 & \quad \text{Equation 5.5} \\
 C(z, t) &= C_i + (C_0 - C_i) A(z, t) - C_0 A(z, t - t_0) & \text{for } t > t_0
 \end{aligned}$$

where

$$A(z, t) = \frac{1}{2} \operatorname{erfc} \left[\frac{Rz - vt}{2\sqrt{DRt}} \right] + \frac{1}{2} \exp \left(\frac{vz}{D} \right) \operatorname{erfc} \left[\frac{Rz + vt}{2\sqrt{DRt}} \right]. \quad \text{Equation 5.6}$$

5.2.3.2 Hydraulic Parameter Estimation

Equation 5.5 was used to estimate the pore water velocity, dispersion, and influent bromide concentration in each column given bromide effluent and initial concentrations in the program CXTFIT (U.S. Department of Agriculture's Salinity Laboratory). The Levenberg-Marquardt algorithm for non-linear minimization of the sum of squared errors was used to generate 95% confidence intervals around the best fit parameter (Toride et al., 1999). The influent concentration was fit because it was not known exactly; flow varied between sediment columns (i.e., Q_{sediment}) and diluted the bromide solution to uncertain concentrations. The values for velocity that were fit from tracer data were compared with velocity estimates from flow rate measurements.

5.2.4 Contaminant Transport and Biotransformation

5.2.4.1 Development of relevant equations

Two of the processes under examination, namely (1) the transport of solutes from a “generator” sediment column with an non-homogeneous vertical concentration profile, and (2) microbial colonization of a sand cap column and the onset of biotransformation of the contaminants of interest (COIs), introduce time dependencies into the transport equation. The first process is addressed in the formulation of the boundary-value problem while the second is addressed in the formulation of the initial-value problem. The general solution is the superposition of the two.

First consider the time-variable bottom boundary condition for the sand cap column ($z = 0$). The solute concentration exiting the sediment column and entering the sand cap column was sampled in 3-week intervals and was represented as a series of

pulse inputs assumed to start and stop at midpoints between sampling events. For a time-dependent boundary represented as a series of pulses, the boundary-value transport equation, C^B , is given by

$$C^B(z, t) = \sum_{j=1}^n (f_j - f_{j-1}) \Psi(z, t - t_j) \quad \text{Equation 5.8}$$

where $f_j = C(z = 0, t)$ for pulse j and n is the total number of pulses over the time period of interest. In the case that reaction is negligible, Ψ is Equation 5.5. When reaction is included, Equation 5.1 becomes

$$R \frac{\partial C}{\partial t} = D \frac{\partial^2 C}{\partial z^2} - v \frac{\partial C}{\partial z} - k C \quad \text{Equation 5.7a}$$

where k is the first-order degradation rate constant and the other variables are as previously defined. Equation 5.7a can be expressed in non-dimensional variables as

$$R \frac{\partial C}{\partial T} = \frac{1}{P} \frac{\partial^2 C}{\partial Z^2} - \frac{\partial C}{\partial Z} - \mu C \quad \text{Equation 5.7b}$$

where P is the Peclet number (column length x velocity / dispersion), Z is dimensionless position (position / column length) and μ is the Damköhler number (rate constant x column length / velocity). Inclusion of a reaction term in the transport equation over a semi-infinite domain gives

$$\Psi(Z, T, \mu) = \left[\begin{aligned} &\frac{1}{2} \exp\left[\frac{P(1-w)Z}{2}\right] \operatorname{erfc}\left(\frac{RZ - w(T - T_j)}{\sqrt{4R(T - T_j)/P}}\right) \\ &+ \frac{1}{2} \exp\left(\frac{P(1+w)Z}{2}\right) \operatorname{erfc}\left(\frac{RZ + w(T - T_j)}{\sqrt{4R(T - T_j)/P}}\right) \end{aligned} \right] \quad \text{Equation 5.9}$$

where $w = (1 + 4\mu/P)^{0.5}$ (Toride et al., 1999).

To simulate solute breakthrough with reactivity starting at time $t = t'_{k>0}$, solutions over the time intervals $0 < t < t'_{k>0}$ and $t \geq t'_{k>0}$ must be superimposed. The initial condition over the first time interval is given by $C(z, t = 0) = 0$, so the general solution is equal to the solution to the boundary-value problem without reaction. For $t \geq t'_{k>0}$, transport is described by the equation including reaction, and the vertical concentration profile in the sand column at time $t = t'_{k>0}$ becomes the initial condition for this solution. A solution to the initial value problem on a semi-infinite domain with $C(z = 0, t) = 0$ is given by

$$C^I(Z, T) = \sum \left\{ (U_i - U_{i-1}) \frac{1}{2} \exp\left(-\frac{\mu T}{R}\right) x \right. \\ \left. \begin{aligned} & \left[2 - \operatorname{erfc}\left[\frac{R(Z - Z_i) - T}{\sqrt{4RT/P}}\right] - \right. \\ & \left. \exp(PZ) \operatorname{erfc}\left[\frac{R(Z + Z_i) + T}{\sqrt{4RT/P}}\right] \right. \\ & \left. - \sqrt{\frac{R}{\pi PT}} \exp\left[-\frac{P[R(Z - Z_i) - T]^2}{RT}\right] \right] + \\ & \left. \sqrt{\frac{R}{\pi PT}} \exp(PZ) \times \right. \\ & \left. \exp\left[-\frac{P[R(Z + Z_i) + T]^2}{4RT}\right] \right] \end{aligned} \right\} \quad \text{Equation 5.10}$$

where U_i is the COI pore water concentration at a position in “step” i (Toride et al., 1999). The solution to the transport equation with reaction, applicable at times $t > t'_{k>0}$, is the superposition of the solutions to the boundary value and initial value problems (i.e., $C(Z, T) = C^I(Z, T) + C^B(Z, T)$). Solutions for $t < t'_{k>0}$ (without reaction) and for $t \geq t'_{k>0}$

(with reaction) were joined to construct a contaminant breakthrough curve over the entire time domain.

5.2.4.2 Procedure for simulating solute effluent profiles

The procedure for simulating solute effluent profiles was as follows:

- (1) Fit transport parameters to breakthrough data assuming no reaction;
- (2) Assess whether concentration profiles are well-described without a sink term and identify solute breakthrough profiles that would be better described with a sink term;
- (3) Estimate the time at which biotransformation started (i.e., $t'_{k>0}$). Repeat simulation up to that time without reaction and store the vertical concentration profile at time $t'_{k>0}$;
- (4) Represent the vertical solute concentration profile in the column as a series of discretized steps and use that profile as the initial condition for modeling over the domain $t > t'_{k>0}$;
- (5) fit a reaction rate to effluent observations over the domain $t > t'_{k>0}$.

5.2.5 Measurement of Biogeochemical Indicators of Metabolism

Analysis of sand cap column influent and effluent samples for methane, ferrous iron, sulfate and sulfide were described in Chapter 4, Section 4.2.2. After elution of 18 cap pore volumes through column 60105, flow was terminated and the sediment and sand columns were transferred to an anaerobic chamber with a nitrogen atmosphere. Solids were cored with a plastic syringe that had the tip removed and were transferred to 9-mL glass headspace vials that were sealed with butyl-rubber stoppers and aluminum crimp

caps. Within 30 minutes of sample collection, headspace H_2 was measured on a Trace Analytical reducing gas analyzer (Menlo Park, CA) (Appendix C) in the Jackson School of Geosciences.

5.3 RESULTS AND DISCUSSION

5.3.1 Hydraulic Transport Parameters

Porewater velocity and dispersion were fit for the bromide breakthrough curve for each column (Figure 5.2, Table 5.1). Velocities that were fit from tracer curves generally agreed with estimates based on volumetric flows (data not shown) from sampling events; however columns 60103 and 60216, both of which demonstrated high methanogenic activity, were exceptions.

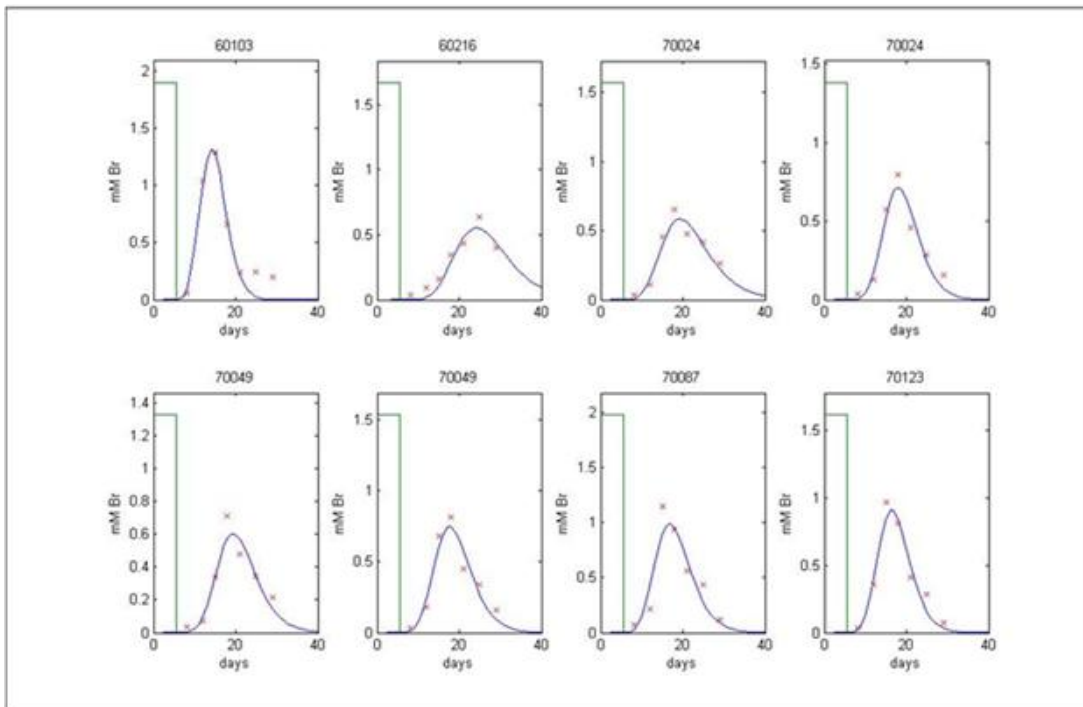


Figure 5.2: Tracer influent profile (rectangle), effluent observations (x), and best-fit effluent profile (smooth line).

Longitudinal dispersion was estimated in each column by Equations 5.2 – 5.4. The diffusion coefficient for bromide in 12°C water was interpolated from data at other temperatures and determined to be $1.52 \times 10^{-5} \text{ cm}^2/\text{s}$ (Li and Gregory, 1974; Lerman, 1979). The effective diffusion coefficient for bromide, D_{eff} , was found to be $0.40 \text{ cm}^2/\text{d}$ by averaging the results of Equations 5.3 and 5.4, allowing computation of the longitudinal dispersivity in each column from Equation 5.2 (Table 5.1). In general, the hydraulic tracer tests showed flow through the sand columns to be devoid of irregularities and confirmed that Darcy velocities for all columns were within 38% of the target velocity of 0.25 cm/d .

Table 5.1: Fit pore water velocity (v), fit dispersion (D), calculated dispersivity (α), calculated influent bromide concentration (C_0), and the coefficient of determination (R^2) for tracer breakthrough curves fit to data. Reported as “fit parameter (0.5 x 95% confidence interval)”.

Column	v (cm/d)	D (cm^2/d)	α (cm)	C_0 (mM)	R^2
60103	1.24 (0.12)	0.51 (0.51)	0.11	1.90 (0.57)	0.96
60105 ^a	0.94 (0.15)	--	--	--	--
60216	0.62 (0.13)	0.40 (0.35)	0.02	1.67 (0.74)	0.94
70024A	0.78 (0.12)	0.65 (0.47)	0.32	1.57 (0.49)	0.92
70024B	0.91 (0.10)	0.44 (0.35)	0.05	1.38 (0.41)	0.93
70049A	0.82 (0.11)	0.45 (0.41)	0.07	1.33 (0.48)	0.90
70049B	0.92 (0.12)	0.53 (0.46)	0.16	1.54 (0.51)	0.91
70050 ^b	0.81 (0.26)	--	--	--	--
70087	0.97 (0.17)	0.59 (0.59)	0.20	1.98 (0.90)	0.85
70123	1.02 (0.10)	0.50 (0.41)	0.12	1.62 (0.46)	0.94

^a Tracer not performed, velocity computed from flow measured during sampling

^b Missed maximum concentration of tracer breakthrough curve, high uncertainty in estimated parameters, velocity estimated from flow measured during sampling

5.3.2 Contaminant Biotransformation

Biotransformation of toluene was apparent in columns from locations 70049A, 70050, and 70123 (Figure 5.3). For all, complete toluene breakthrough occurred during elution of the initial 4 – 6 cap pore volumes, then successive sampling events reflected decreasing concentrations in column effluent until pore volumes 8 - 10. The rate of reaction required to fit the effluent curve to effluent observations during this time was the same in all three columns at 0.1 day^{-1} (Damköhler number of 1.6). For reasons that are examined below, toluene activity stopped after the elution of eight cap pore volumes. During this time, similar trends were not observed in the other seven columns, suggesting that toluene biotransformation was specific to these locations.

Two lines of evidence support biotransformation as the explanation for reduced toluene in effluent from sand cap column 70049A during the elution of pore volumes 4 – 8. First, toluene was biotransformed under anaerobic conditions at 12°C in dilute slurries with sediments from location 70049 (Section 3.3.2). Second, a gene encoding the α -subunit of the enzyme benzylsuccinate synthase (*bssA*), which catalyzes the initial reaction of anaerobic toluene biotransformation, was detected in both sediment and sand cap samples taken from column 70049A. These results suggest that toluene biotransformation is possible in a sand cap above sediment from location 70049. Apparently similar behavior in columns 70050 and 70123 suggest biotransformation in those columns, as well. Biotransformation was not observed in the replicate column with sediment from location 70049 (i.e., 70049B) for reasons examined in Section 5.3.4.1.

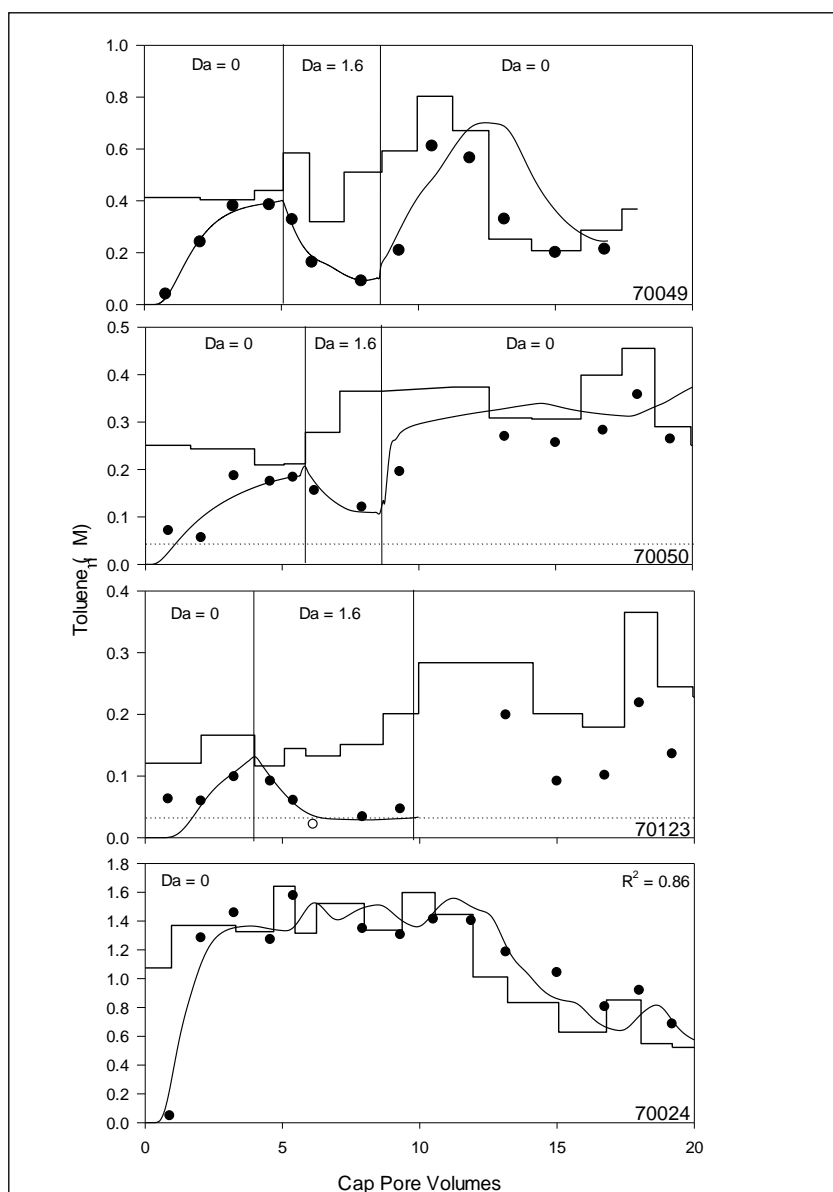


Figure 5.3: Toluene concentration profiles in columns with sediments from four distinct locations. Influent is represented as a series of pulses, modeled effluent is shown as a smooth line, markers represent effluent observations, the dashed line shows the detection limit, and the hollow marker in profile 70123 indicates a sample below the detection limit. The fit is improved by inclusion of a reaction term between pore volumes 5 and 10 in the top three profiles, while reaction was not observed in the plot for 70024.

The other contaminants of interest were not subject to quantifiable biotransformation. With the exception of dichlorobenzenes and naphthalene, all other contaminants (i.e., BTEX and monochlorobenzene) achieved complete breakthrough from the sand column and were well-described by the transport equation without reaction (Appendix C). Based on the flow rate and column length, deviation from the simulated breakthrough representing “no reaction” by at least 10% corresponds to a half-life of 0.3 years and a first-order degradation rate of $k_1 = 2.19 \text{ yr}^{-1}$ (Figure 5.4), taken to be the smallest rate detectable in these tests. Many of the biotransformation rates estimated from batch slurry tests with sediments described in Section 3.3.2, such as those for chlorobenzene transformation by sediment from location 70049, were smaller than this minimum detectable rate.

Figure 5.4 also shows little sensitivity in the ratio of effluent-to-influent concentrations to the dispersion coefficient. Standard errors for estimates of dispersion with CXTFIT were often of the same magnitude as the best-fit estimate, further suggesting that transport is advection-dominated. Peclet numbers, which indicate the magnitude of advection to dispersion, ranged from 10 – 20 and support the notion of advection-controlled transport.

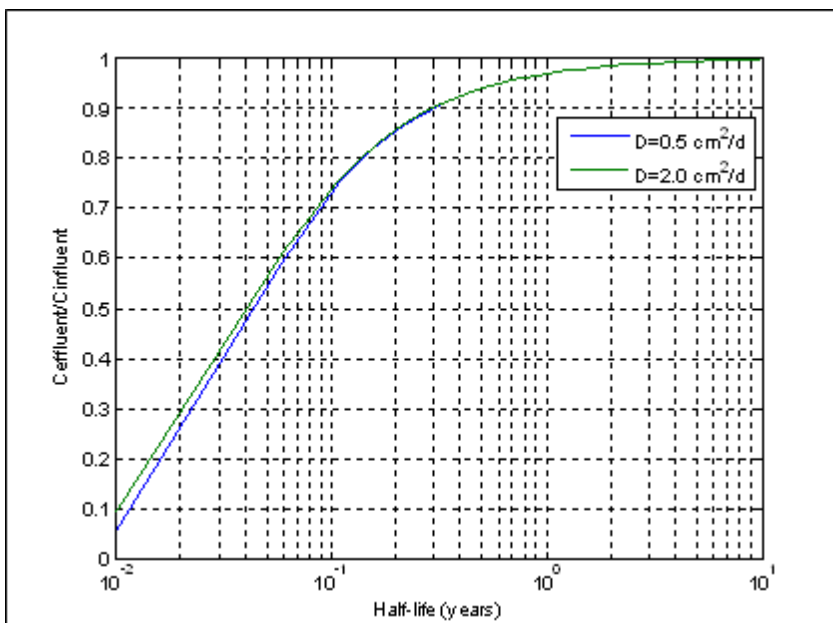


Figure 5.4: Effluent-to-influent ratio against contaminant half-life at steady-state for two different values of dispersion.

The first-order reaction rate constant estimated for toluene biotransformation in column 70049 proved largely insensitive to dispersion and retardation. (Note that the third parameter in the advection-dispersion-reaction equation (Equation 5.7a), porewater velocity, is related to the estimate of retardation. In advection-controlled systems, the chemical velocity is defined by the product of porewater velocity and retardation; thus retardation can be isolated as an uncertain variable while porewater velocity is assumed to be known exactly.) Independently changing each parameter to its upper or lower 95% confidence limit produced no more than a 20% change in the estimated rate of toluene biotransformation in column 70049 (Table 5.2), thereby validating the attribution of

observed decreased effluent concentrations to reaction rather than transport variable uncertainty.

Table 5.2: Response of reaction rate constant, k , to dispersion coefficient (D) and retardation factor (R) for column 70049.

D (cm ² /d)	R (--)	k (1/day)
2.1	2.0	0.103
2.1	1.4	0.087
2.1	2.5	0.119
0.5	2.0	0.094
5.0	2.0	0.122

5.3.3 Geochemical Indicators of Anaerobic Metabolism

Indications of anaerobic metabolism, namely methanogenesis, sulfidogenesis, and iron-reduction were observed in all columns. In two of the three columns in which toluene biotransformation was observed, the concentration of dissolved iron was significantly greater in the sand cap effluent than in the influent. Toluene oxidation might have been coupled to dissimilatory iron reduction in the sand cap in columns 70049 (7.7 ± 5.3 μM influent, 16.8 ± 6.0 μM effluent, $p\text{-value} = 0.012$) and 70050 (13.6 ± 5.5 μM influent, 34.0 ± 20.0 μM effluent, $p\text{-value} = 0.026$) as determined by a student's t -test at a level of $\alpha = 0.05$. A dominant terminal electron accepting process (TEAP) in the sand cap column 70123 could not be determined from geochemical data as significant differences were not observed between influent and effluent concentrations of ferrous iron, sulfate, or methane (Appendix B). For the 7 columns in which toluene biotransformation was not observed, the dissolved iron concentration was either greater in the influent than in the effluent or the difference was not statistically significant (Figure 5.5).

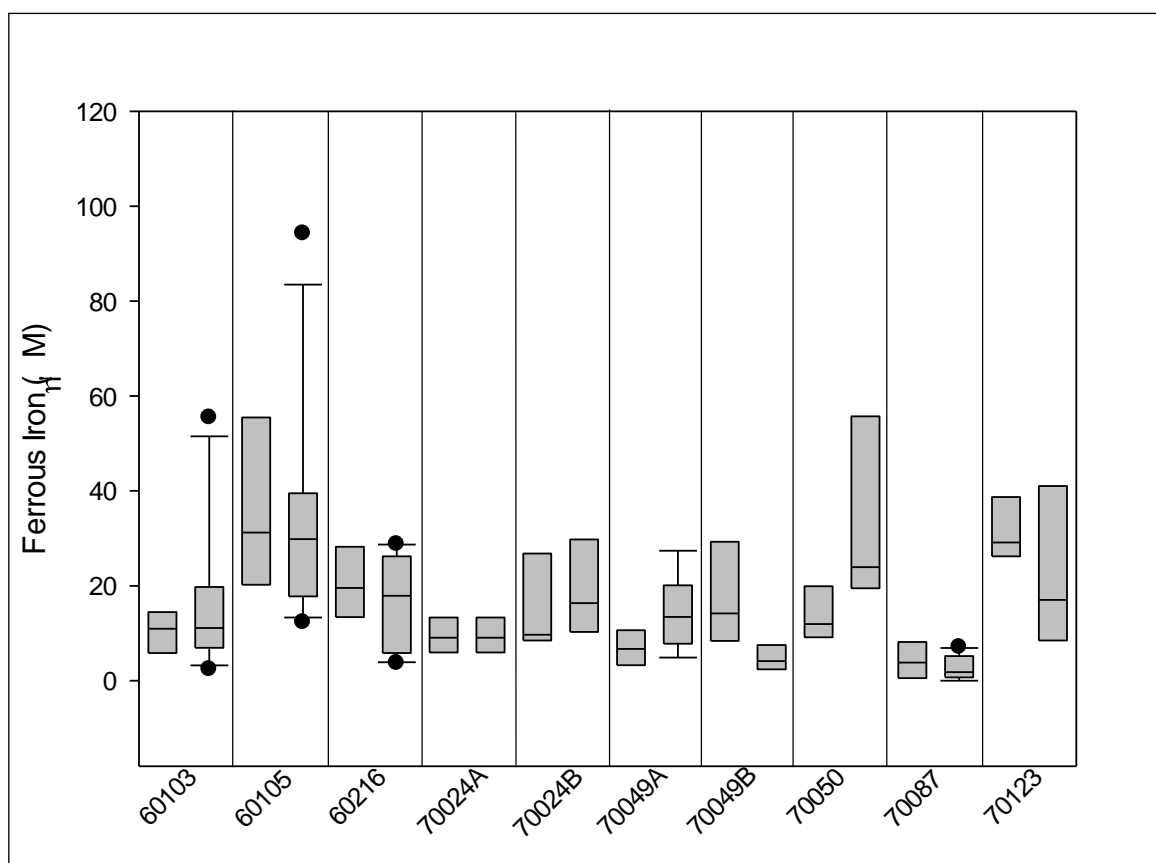


Figure 5.5: Ferrous iron concentrations in sand cap column influent (left) and effluent (right). Effluent concentrations were significantly greater than influent concentrations only for columns 70049A and 70050.

Over time, columns became pressurized due to the production of biogenic gas between sampling events. When sampling valves were opened after 3 – 4 weeks, up to 2 mL of water was regularly expelled. Methane concentrations from sediment and sand cap columns generally increased over time (Figure 5.6), indicating increasing activity by methanogens. At temperatures below 15°C, acetogenic bacteria and hydrogenotrophic methanogens compete for dissolved hydrogen with acetogens expected to dominate

(Kotsyurbenko, 2005). Acetoclastic methanogens consume the produced acetate but grow slowly (Kotsyurbenko, 2005). The apparent increase in methane production indicates anaerobic conditions and might reflect a growing acetoclastic methanogen population over time.

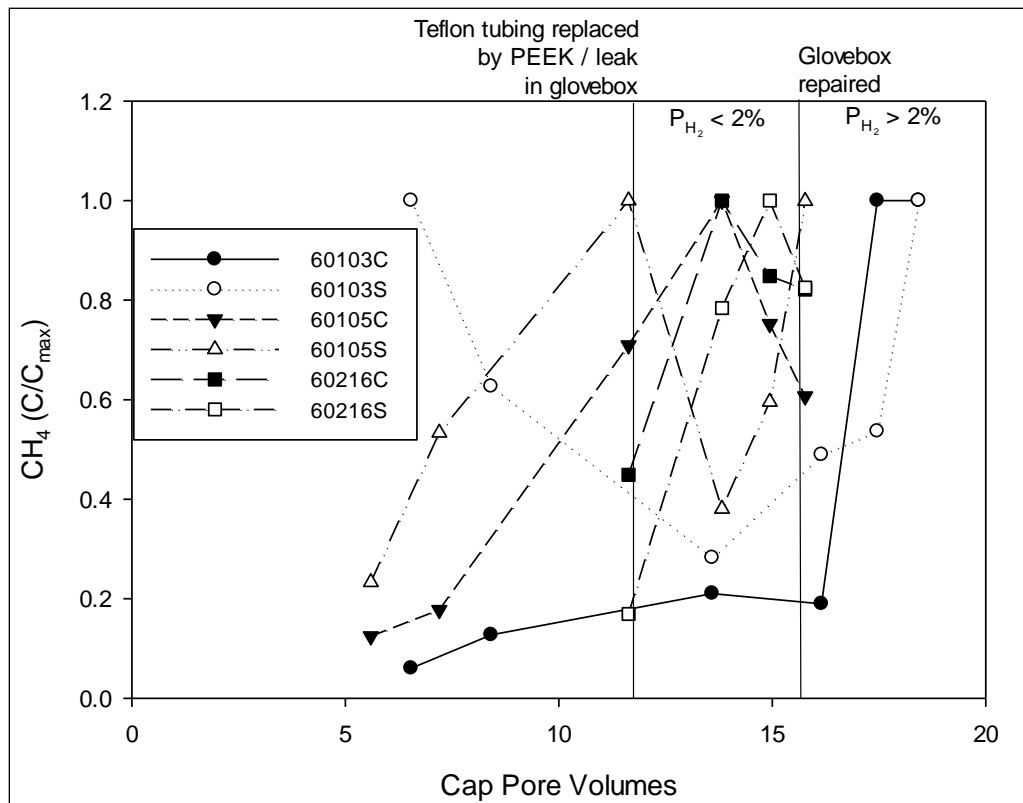


Figure 5.6: Dissolved methane concentrations normalized to maximum concentration in effluent from cap (C) and sediment (S) samples from columns 60103, 60105, and 60216. Concentrations generally increase over time suggesting experimental conditions favorable for methanogenesis.

Although there is some variability in the time interval over which toluene biotransformation occurred in columns 70049A, 70050, and 70123, they all closely correspond to the two-month period of November and December, 2009, when the hydrogen concentration in the anaerobic chamber was highly variable. As described in Section 5.2.1, the chamber was refilled frequently, and although oxygen was detected in the chamber atmosphere at several hundred ppm, geochemical indicators (i.e., the presence of ferrous iron in the influent and effluent of all cap columns and the increasing trend in methanogenesis depicted in Figure 5.6) suggest that the columns remained anaerobic (Section 5.3.3). Following repair of the glovebox in late December, 2009, toluene biotransformation appears to cease in all columns. The concentration of hydrogen in the glovebox atmosphere, which varied from <0.2% (i.e., the minimum concentration detectable by the Coy gas analyzer) to >2% with rapid fluctuation during that two-month period, stabilized at 2 – 3% after the glovebox was repaired. This stable hydrogen concentration exceeds those typical of sediment environments and is believed to have caused the termination of toluene biotransformation.

5.3.4 Hydrogen, Reaction Thermodynamics, and Biochemical Kinetics

5.3.4.1 The Thermodynamic Feasibility of Toluene Fermentation

Although some bacteria have been identified that can completely biodegrade toluene and other contaminants of interest under anaerobic conditions, metabolic cooperation by a consortia of bacteria is far more common in the environment (Schink, 1988). Regardless of the terminal electron accepting process, complex organic substrates

are sequentially decomposed to metabolic products that often can be utilized as substrates by other members of the bacterial community. Hydrogen is one such metabolite, produced in fermentation reactions and widely utilized as an electron donor. The concentration of dissolved hydrogen is strictly controlled by sediment bacteria seeking to prevent hydrogen oxidation by competitors. Additionally, the hydrogen concentration dictates the thermodynamic feasibility of many biotransformation reactions in anaerobic environments. For example, the dissolved hydrogen concentration has been identified as a sensitive indicator of system performance in anaerobic digestion. Hydrogen partial pressures of 2 – 6.5 Pa (approximately 15 – 50 nM) were found to indicate normal digester performance, but pressures exceeding 6.5 Pa signaled system failure (Cord-Ruwisch et al., 1997).

Although iron-reduction is theorized to have been the TEAP coupled to toluene biotransformation in columns 70049A and 70050, a sharp increase in the hydrogen concentration inside the glovebox, which would cause in an increase in the dissolved hydrogen concentration inside the columns, would likely favor sulfate reducers and methanogens over iron-reducing bacteria (Lovley and Phillips, 1987b). Under methanogenic conditions, hydrogen and acetate are produced from toluene fermentation and their concentrations must be maintained below threshold concentrations that would make toluene fermentation thermodynamically infeasible. Hydrogen and acetate are produced from toluene by pathways such as Equation 5.11a and 5.11b.



Equation 5.11a (Meckenstock, 1999)



Equation 5.11b (Heider et al., 1998)

For either reaction 5.11a or 5.11b to be thermodynamically feasible, the dissolved hydrogen partial pressure must be maintained on the order of 1 Pa (Heider et al., 1998), similar to anaerobic digestion reactors (Cord-Ruwisch et al., 1997). Toluene mineralization coupled to methanogenesis has been demonstrated (Vogel and Grbic-Galic, 1987); this is thermodynamically feasible given that the characteristic hydrogen concentration for methanogenesis is typically 10 - 50 nM (Lovley and Goodwin, 1988). In the current study, the sediment column tests were conducted in an anaerobic chamber containing 2-3% hydrogen. At equilibrium with a 2% hydrogen atmosphere, the concentration of dissolved hydrogen in APW would be 16,800 nM, and the reaction under consideration would not be feasible.

Following elution of 18 cap pore volumes to column 60105, flow was stopped, the sand and sediment columns were cored at various depths, and the dissolved hydrogen concentrations were measured on a reducing gas analyzer (Trace Analytical, Menlo Park, CA). In general, dissolved hydrogen concentrations in column 60105 were 100 – 250 nM with a few observations below this range (Figure 5.7), well above concentrations typical of methanogenic environments. Such a high dissolved hydrogen concentration is likely inhibitory to fermentation and might explain the termination of toluene biotransformation in columns 70049A, 70050, and 70123 following stabilization of the hydrogen atmosphere inside the anaerobic chamber. Edwards and Grbic-Galic (1994) reported a

similar inhibitory effect by exogenous hydrogen addition on toluene fermentation under methanogenic conditions, though a threshold hydrogen concentration was not identified. Toluene biotransformation was not observed in the replicate core from location 70049 (i.e., 70049B) which was started one month later than column 70049A. It is believed that, due to the later start date for column 70049B, the biomass in the sand cap column was insufficient to detectably biotransform toluene during the time that the hydrogen concentration was depressed. Like the other columns, biotransformation was thermodynamically inhibited once the hydrogen concentration was restored.

In hydrogen-rich environments at low temperatures (i.e., $<15^{\circ}\text{C}$), homoacetogens, bacteria that produce acetate from hydrogen and carbon dioxide, are believed to outcompete hydrogenotrophic methanogens (Conrad et al., 1989; Kotsyurbenko et al., 2001). This theory is supported by observations that acetoclastic methanogenesis (i.e., fermentation of acetate to methane and carbon dioxide) dominates hydrogenotrophic methanogenesis (i.e., production of methane from hydrogen and carbon dioxide) at low temperatures, as determined by relative rates of production of methane and carbon dioxide (Kotsyurbenko, 2005). Although acetate concentrations have not been measured in column porewater, it is possible that they are sufficiently high such that the fermentation of toluene to acetate is thermodynamically infeasible. It is believed that the concentrations of both hydrogen and acetate became inhibitory to toluene fermentation once the hydrogen concentration in the anaerobic chamber stabilized above 2%.

The hydrogen concentration inside the glovebox was reduced from $>2\%$ to 0.2 – 0.4% in November, 2010 (0.2% hydrogen being the lowest concentration detectable by

the hydrogen meter), but toluene biotransformation was not restored as of May, 2011. It is unclear whether the capability to biotransform toluene was retained in bacterial communities in the sand caps of columns 70049A, 70050, and 70123, or whether the concentrations of hydrogen and acetate can be reduced to the point that toluene biotransformation becomes thermodynamically feasible.

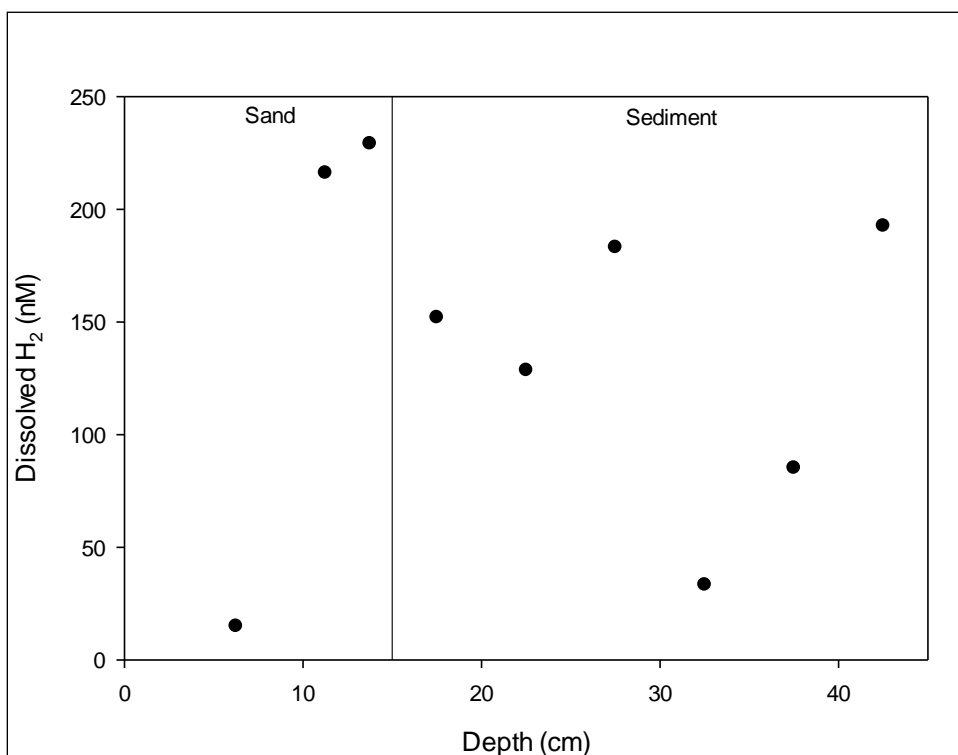


Figure 5.7: Dissolved hydrogen concentrations in cores from column 60105. Samples collected at depths of 1.25, 3.75, and 8.75 cm in the sand column were indistinguishable from background and are not shown.

5.3.4.2 Microbial Dehalogenation and Competition with Methanogens

While reduced environments are a requirement for reductive dehalogenation, substrate reactivity is once again controlled by the concentration of dissolved hydrogen.

Unlike hydrocarbon oxidation discussed above, dehalogenation is thermodynamically feasible under these experimental conditions using standard free energies reported by Dolfing and Harrison (1992). Assuming that the appropriate bacterial populations are present, the lack of biotransformation activity is owed to biochemical kinetics rather than thermodynamics.

In anaerobic sediments, TEAPs are spatially stratified because of control of the dissolved hydrogen concentration. As such, each TEAP has a corresponding characteristic hydrogen concentration, as mentioned above, with iron reduction occurring around 0.2 nM hydrogen, sulfate reduction around 2 nM hydrogen, and methanogenesis greater than 10 nM hydrogen (Lovley and Goodwin, 1988). The threshold hydrogen concentration for dehalogenating bacteria seems to be similar to that for sulfate reduction based on dehalogenation of pentachlorophenol by a mixed culture (Madsen and Aamand, 1991). This was corroborated by studies of dehalogenation of the solvents perchloroethylene (PCE) and trichloroethylene (TCE), which was most successful at dissolved hydrogen concentrations of 2 – 11 nM (Yang and McCarty, 1998). Additionally, Smatlak et al. (1996) reported that the half-velocity constant for hydrogen was ten-fold smaller for PCE-dechlorinating bacteria than for methanogens, suggesting a kinetic strategy for dehalogenating bacteria of maintaining hydrogen concentrations below the threshold concentration at which methanogens become competitive.

While methanogenesis might slow dechlorination, it does not appear to completely inhibit dechlorination, as exemplified by concomitant methane production and dehalogenation of chlorobenzene and chlorotoluene dehalogenation (Ramanand et

al., 1993; Fung et al., 2009). At the hydrogen concentrations measured in column 60105, dehalogenating bacteria are competing not only with methanogens but also with homoacetogens, which are believed to out-compete methanogens for hydrogen at temperatures below 15°C (Kotsyurbenko et al., 2001). As with the oxidation of toluene and the other non-chlorinated pollutants used in this study, the dehalogenation of chlorobenzenes might have been slowed by elevated concentrations of dissolved hydrogen.

5.4 SUMMARY AND CONCLUSIONS

Sand-capped sediment columns proved effective at demonstrating anaerobic contaminant biotransformation in a sand cap, though toluene was the only pollutant that was biotransformed and only over a limited period of time. Challenges imposed by time-dependent boundary conditions and biotransformation rates were overcome by superimposing solutions to the appropriate transport equation.

Excess hydrogen in the anaerobic chamber is suspected of creating unfavorable conditions for continuous contaminant biotransformation. As hydrogen is a product of fermentation, hydrogen forcing by the chamber atmosphere is believed to have made conversion of toluene to fermentation products thermodynamically infeasible. Additionally, the activity of homoacetogens, which can out-compete methanogens for hydrogen at low temperatures, likely resulted in elevated acetate concentrations that made toluene fermentation to acetate thermodynamically infeasible.

With regard to dechlorination, the dissolved hydrogen concentration in columns was above the threshold concentrations for both methanogenesis and homoacetogenesis, and it is possible that the activity of dechlorinating bacteria was diminished as a result of

competition. The rates of dehalogenation of the chlorobenzenes observed in sediment slurries (Section 3.3.2) were near the limit thought to be detectable in sand-capped column tests, so inhibition of dehalogenation by exogenous hydrogen cannot be evaluated. Stimulation of dehalogenation at increased hydrogen concentrations was not observed. It is hypothesized that prevailing conditions selected for acetogens and methanogens in columns at the expense of competing metabolic niches. Whether contaminant biotransformation activity can be restored following elimination of all exogenous hydrogen is unknown.

In addition to thermodynamic constraints imposed by elevated hydrogen concentrations, it is possible that toluene biotransformation stopped due to the development of toxicity in the sand cap column. The migration of toxic organics into the sand column at rates slower than toluene might have inhibited the biotransformation of toluene that had occurred over the preceding two months. Additional data is required to evaluate this hypothesis.

Provided that exogenous hydrogen concentrations can be controlled in future experiments, the methods described in this chapter are broadly applicable to other sites and can be used to simulate transport through a variety of capping media to evaluate contaminant retardation and the potential for biotransformation.

Chapter 6. Organophilic Clay Slows the Migration of Volatile Organic Pollutants Through Sand-Based Sediment Caps

6.1 INTRODUCTION

In-situ capping is an increasingly attractive option for the management of impaired sediments (Forstner & Aritz, 2007). Conventional capping materials, such as sand and gravel, are often adequate for isolating benthos from common hydrophobic sediment pollutants such as polycyclic aromatic hydrocarbons (PAHs) and polychlorinated biphenyls (PCBs). However, contaminant properties and site hydraulics may render conventional capping materials ineffective. For sites affected by relatively water-soluble contaminants, negligible biodegradation, advection-dominated transport, or a combination thereof, traditional sediment caps can be amended to improve contaminant sequestration and reduce the rate of chemical migration. Activated carbon, coke, and organophilic clays are potential cap amendments that can be applied in a thin layer and substantially improve sequestration of hydrophobic pollutants (Murphy et al., 2006; McDonough et al., 2007). Despite having the smallest theoretical sorption capacity of these three media, the ability of organophilic clays to sorb dissolved phase contaminants, retard migration of non-aqueous phase liquids, and largely resist fouling makes it an effective amendment in sediment caps. Furthermore, they appear to be non-toxic to benthic organisms (Paller and Knox, 2010). In-situ performance of organophilic clays for controlling dissolved-phase contaminant migration is currently being evaluated at a capping demonstration in the Anacostia River (Reible et al., 2006).

To better predict the site-specific performance of an organophilic clay in a sediment cap, the sorption of BTEX, chlorobenzenes, and naphthalene was evaluated in batch microcosms and upflow columns with actual sediment porewater as the solvent. The use of real porewater allows for performance evaluation reflecting competitive sorption effects and interference by porewater constituents such as humic acids, which reportedly affect PCB adsorption to organophilic clays (Sharma et al., 2009). The high aqueous solubilities of these contaminants of interest (COIs), relative to more common sediment pollutants like PAHs and PCBs, suggest that sediment cap amendments may be necessary to reduce COI fluxes to acceptable levels. Improved understanding of their performance in natural waters is necessary.

6.2 MATERIALS AND METHODS

6.2.1 Batch isotherms

Two-inch diameter surficial sediment cores were collected from the in-lake waste deposit (ILWD) from Onondaga Lake on July 3, 2009. Sediment pore water was extracted by centrifugation, then sparged with nitrogen to remove volatile pollutants. Sparged pore water was analyzed for remaining volatiles and dissolved organic carbon (DOC) by TestAmerica (Pittsburgh, PA), shipped to the University of Texas-Austin (UT-Austin) on ice, and stored at 4°C until use. Sparged porewater was analyzed for aromatic content of DOC by specific ultraviolet absorbance (SUVA) according to U.S. EPA Method 415.3 at UT-Austin.

Depending upon the desired aqueous concentration of the COIs at equilibrium, either 0.1 or 1.0 g of PM-199 organoclay (CETCO, Hoffman Estates, IL) was added to

50-mL glass centrifuge tubes. PM-199 is a bentonite clay modified with di(hydrogenated tallow) dimethyl-ammonium chloride and has a particle diameter $0.3 \text{ mm} < d < 1.0 \text{ mm}$. The tubes were filled with sparged pore water to minimize headspace and the volume of water added was recorded. The threads of the tube were wrapped with Teflon tape; then the tubes were capped with Mininert valves (Restek Corp., Bellefonte, PA), spiked with a custom standard (AccuStandard, New Haven, CT) containing COIs at various concentrations in methanol (Table 6.1), and tumbled in the dark at 12°C. Note that the concentration of methanol, which never exceeded 1.6%, likely did not have a large effect on the partitioning behavior of the COIs (Nzengung et al., 1997). After seven days, supernatants were decanted to completely fill 40-mL volatile organics analysis (VOA) vials that were analyzed by EPA SW-846 Method 8260B by DHL Analytical (Round Rock, TX). The difference between the starting contaminant mass and the aqueous-phase mass after 7 days was attributed to adsorption to organoclay:

$$q = \frac{V_{aq}(C_0 - C_e)}{M_{sorbent}} \quad \text{Equation 6.1}$$

where q is the adsorbed contaminant mass per mass of adsorbent, V_{aq} is the aqueous volume, C_0 is the initial contaminant concentration, C_e is the contaminant concentration at equilibrium, and $M_{sorbent}$ is the mass of sorbent. Freundlich isotherm parameters were estimated for each curve by least-squares non-linear curve-fitting in Matlab:

$$q = K_f C_e^{1/n} \quad \text{Equation 6.2}$$

where K_f and $1/n$ are empirically determined, chemical-specific constants for a particular temperature. Linear partitioning coefficients were also fit using non-weighted least squares regression:

$$q = K_d C_e \quad \text{Equation 6.3}$$

where K_d is the distribution coefficient describing linear two-phase partitioning.

Table 6.1: Relevant properties and stock concentrations for sorption isotherms.

Chemical	C _{solubility} (mM) ^a	log K _{oc} ^b	D _w (x10 ⁻⁵ cm ² /s) ^c	Dipole Moment (Debyes) ^d	Spike Standard (mM)
1,2-Dichlorobenzene	0.891	3.08	0.55	2.50	203.8
1,3-Dichlorobenzene	0.832	3.23	0.552	1.72	203.8
1,4-Dichlorobenzene	0.501	3.04	0.55	0	204.3
Benzene	22.4	2.00	0.68	0	12.83
Chlorobenzene	4.07	2.55	0.61	1.69	267.1
Ethylbenzene	1.58	2.94	0.55	0.59	282.5
Naphthalene	0.251	2.97	0.5	0	233.5
Toluene	6.03	2.53	0.6	0.36	108.5
m-Xylene	1.51	2.89	0.55	0.30	282.7
o-Xylene	1.78	2.89	0.55	0.62	283.3
p-Xylene	1.70	2.89	0.55	0	282.2

^a at 20°C (Schwarzenbach et al., 2003)

^b determined from field data by Parsons

^c computed at 12°C according to Hayduk and Laudie (1974), using 1.22 centipoise as the viscosity of water

^d all measured in gas state, except m-xylene measured in aqueous state (Yaws, 1999)

6.2.2 Upflow columns

Duplicate sediment cores from two locations in Onondaga Lake were extruded into the bottom half of a 30-cm tall, 4.8-cm diameter glass column (Kimball-Kontes, Vineland, NJ). Columns both with and without cap amendment were operated (Table 6.2). For baseline columns (i.e., sand only), the top 15 cm of the column was filled with sand and Onondaga Lake surface water. For amended-cap columns, a one-cm thick layer of bulk PM-199 organoclay was placed atop the sediment followed by placement of a 14-cm thick layer of sand (Figure 6.1). Upward flow was recirculated with positive displacement pumps (Fluid Metering Inc., Syosset, NY) except during sample collection,

at which time sparged Onondaga Lake surface water (OLSW) was drawn from a reservoir into the bottom of the column to replace the effluent that was collected for analysis. Effluent samples were collected in 2-mL amber vials that were pre-filled with 0.5 mL purge-and-trap grade methanol. Samples were stored without headspace and sample volumes were determined gravimetrically. Samples were analyzed by EPA SW-846 Method 8260B by DHL Analytical (Round Rock, TX). Analytical detection limits for this sample volume were 4.0 µg/L.

Table 6.2: Upflow column hydraulic parameters and sediment depth at the top of the core.

Column	Description	Darcy Velocity (cm/d)	Dispersivity (cm)	Depth at Top of Core (cm)
1A	Amended	0.66	0.67	84
1B	Baseline	0.076	0.46	41
2A	Amended	0.24	0.30	53
2B	Baseline	0.075	0.55	36

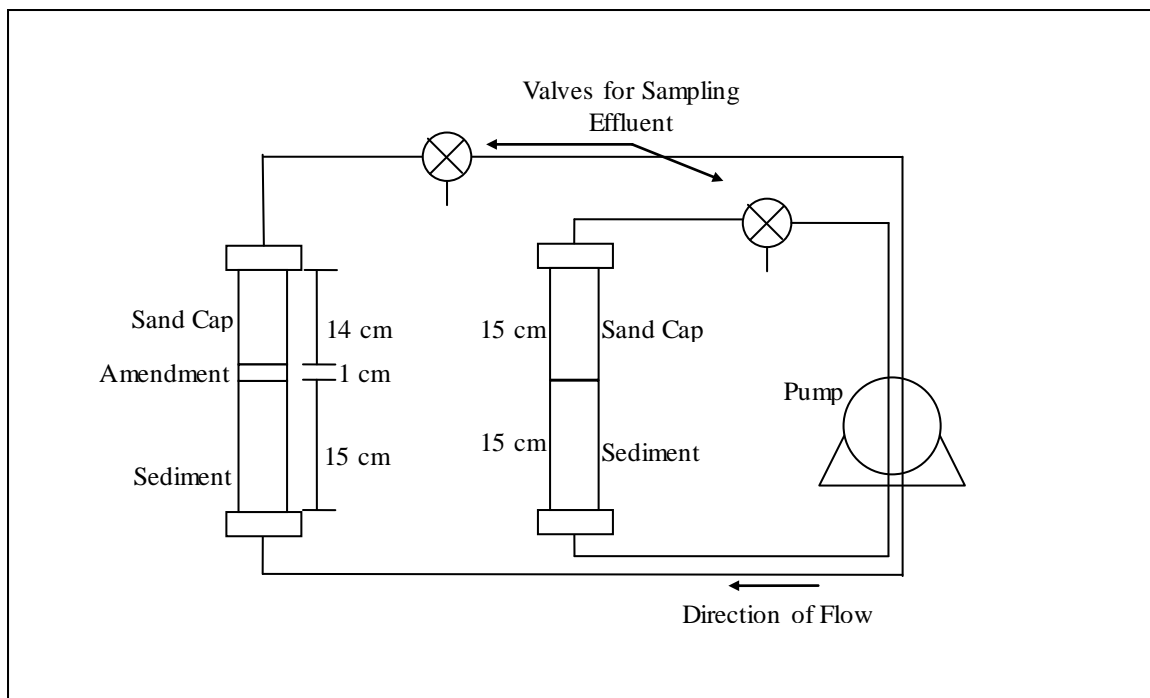


Figure 6.1: Schematic for organoclay-amended sand cap columns and sand only (“baseline”) cap columns.

Hydraulic tracer tests were conducted at the start of flow for all columns and again in amended-cap columns immediately before stopping flow. For baseline columns, 10 mg/L of fluorescein (VWR, Radnor, PA) prepared in site water was injected for 24 hours. Fluorescein concentrations in 100- μ L effluent samples were quantified by fluorescence excitation/emission of 485/528 nm (Appendix D) in a Biotek plate reader (Winooski, VT). Fluorescein sorbed to PM-199, so the tracer for amended-cap columns was 75 mM potassium bromide dissolved in OLSW and injected for four hours. Bromide concentrations were measured by electrode (Cole-Parmer, Vernon Hills, IL).

Before shutdown of amended-cap columns, tritiated water (American Radiolabeled Chemicals, St. Louis, MO) of activity 25 nCi/mL was injected continuously for 30 days. One-mL effluent samples were added to 20-mL scintillation vials containing 10 mL of ScintSafe Plus 50% (Fisher Scientific), and activity was measured on a Beckman LS-5000 liquid scintillation counter (Beckman-Coulter, Waltham MA) with settings according to Putz (2004).

6.2.3 Hydraulic parameter estimation and breakthrough simulation

Solute transport was described by the one-dimensional advection-diffusion equation (Equation 6.4). The domain was modeled as semi-infinite with a constant concentration at the bottom boundary and a uniform initial concentration in the sand cap of zero:

$$R \frac{\partial C}{\partial t} = D \frac{\partial^2 C}{\partial z^2} - v \frac{\partial C}{\partial z} \quad \text{Equation 6.4}$$

where R is the retardation factor [--], C is the aqueous phase concentration [M/L³], D is the dispersion coefficient [L²/T], z is the vertical displacement [L], and v is the interstitial velocity [L/T]. The program CXTFIT (Toride et al., 1999) was used to estimate hydraulic properties from tracer profiles and retardation factors from solute breakthrough curves. In short, CXTFIT employs the Levenberg-Marquardt algorithm to minimize the error between prediction and observation in the least-squares sense.

6.3 RESULTS AND DISCUSSION

6.3.1 Isotherms

ILWD sediment porewater is high in contaminant load (Table 6.3) and has a pH of 10-12. The porewater chemistry, specifically pH, is suspected of completely inhibiting biotransformation of contaminants by sediment bacteria, as discussed in Sections 3.3.1 and 3.3.2. The measured concentration of dissolved organic carbon was 760 mg/L, and SUVA indicated an organic carbon aromaticity of 5.1%, much lower than the humic acid concentration of 1.0 g/L that reduced PCB adsorption to organophilic clays (Sharma et al., 2009).

Table 6.3: Residual analyte concentrations in sparged pore water and best-fit parameters for Freundlich and linear isotherms.

Analyte	Concentration in Sparged Porewater ($\mu\text{g/L}$)	Organoclay Batch Isotherm		
		Kf ($\mu\text{g}^{1-1/n} \text{L}^{1/n} \text{kg}^{-1}$)	1/n	Kd (L/kg)
1,2-Dichlorobenzene	550	2092.5	1.25	2412.3
1,3-Dichlorobenzene	<20	793.2	0.98	777.4
1,4-Dichlorobenzene	490	236.8	0.96	218.1
Benzene	500	55.9	0.94	64.9
Chlorobenzene	1200	255.7	1.29	447
Ethylbenzene	65	240.7	1.11	290.2
Naphthalene	2700	3797.4	1.22	4140.7
Toluene	290	137.8	1.14	161.1
Total Xylenes	840	218.0	1.21	394.2

Trends observed for isotherms with PM-199 were similar to those reported for these solutes sorbing to other organophilic clays (Figure 6.2).

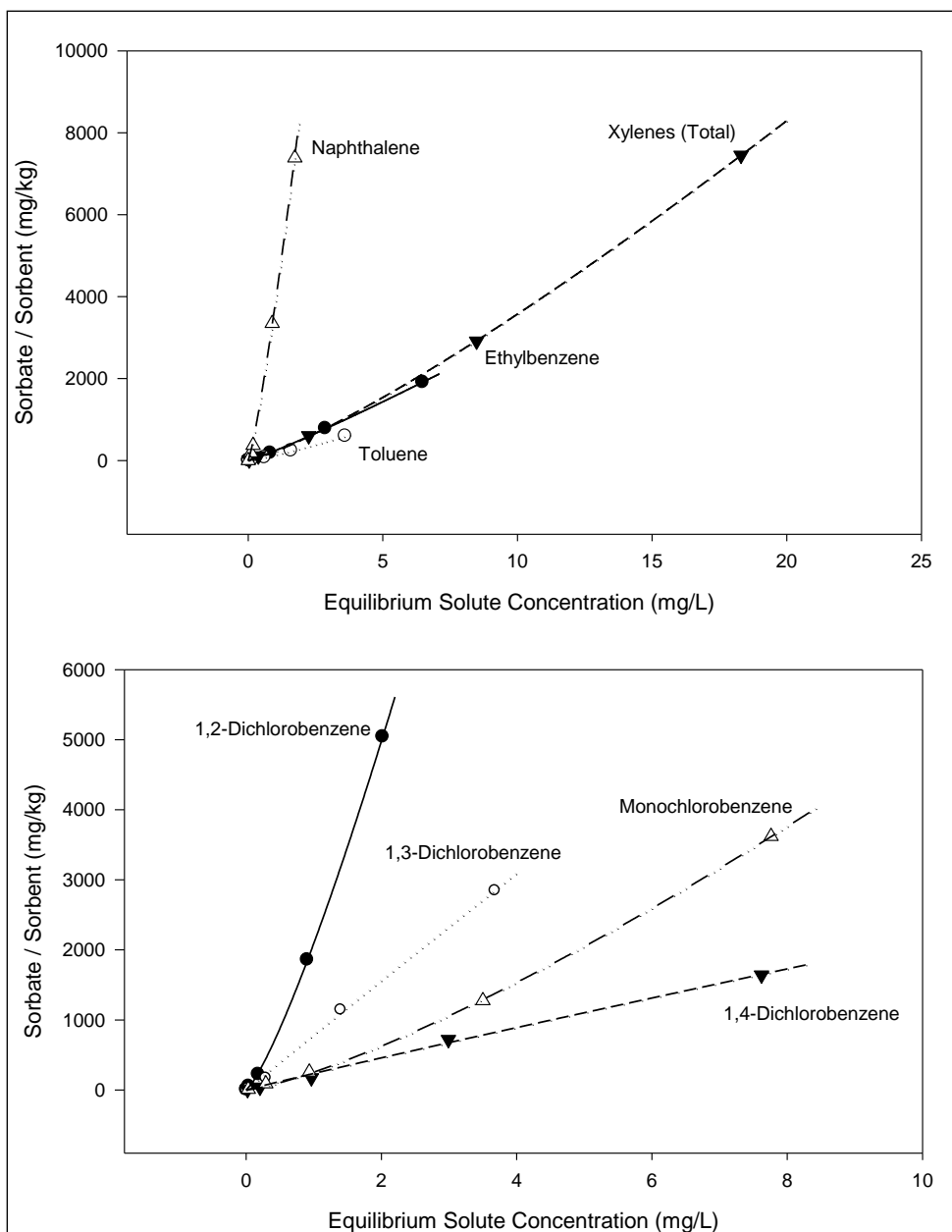


Figure 6.2: Freundlich isotherms for ethylbenzene, naphthalene, toluene, and total xylenes (top) and monochlorobenzene and the three dichlorobenzene isomers (bottom)

The logarithm of K_f for BTEX demonstrated a negatively-sloped linear dependence on solubility, suggesting that absorption into the organic matrix of the organophilic clay was the dominant sorption mechanism (Figure 6.3a). Contrarily, sorption actually increased with increasing water solubility for dichlorobenzenes, indicating that mechanisms other than absorption into the hydrophobic region were dominant. A positive linear relationship between $\log K_f$ and molecular dipole moment was observed for the dichlorobenzenes (Figure 6.3b), indicating that electrostatic interactions between the molecule and charged sites on the clay surface likely contribute to sorption (Sheng and Boyd, 2000). A combination of organic-phase sorption and surface-cation solvation might explain why monochlorobenzene demonstrates greater sorption relative to its solubility than observed for BTEX. Qu et al. (2007) proposed interactions between the π -electrons of PAHs with surface cations as an explanation for the large K_f for naphthalene compared with monoaromatics.

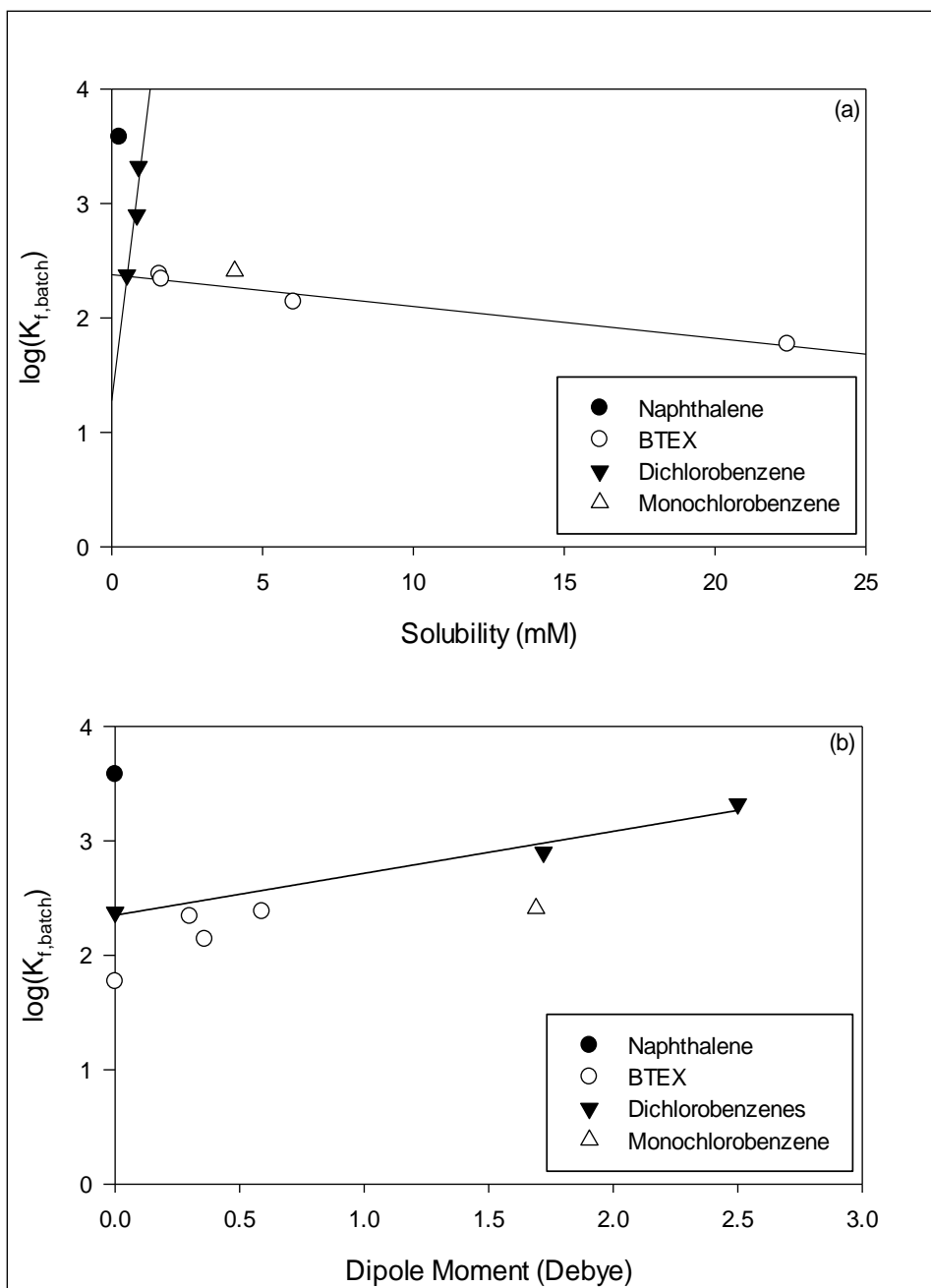


Figure 6.3: Solute adsorption to PM-199 organoclay as a function of (a) solubility and (b) dipole moment.

Freundlich isotherms provided the best fits to batch adsorption data, producing coefficients of determination, R^2 , greater than 0.99 for all compounds except for benzene, for which $R^2 = 0.94$. Adsorption is nearly linear for 1,3-dichlorobenzene, 1,4-dichlorobenzene, and benzene; however, for the other compounds, the adsorption capacity appears to increase with increasing aqueous phase concentration (Figure 6.3), indicated by values of $1/n$ greater than one. While linear adsorption isotherms are commonly reported in the literature for aromatic compounds with various organophilic clays (Boyd et al., 1988; Qu et al., 2007), others have observed enhanced sorption to aliphatic-modified montmorillonite with increasing aqueous concentrations of BTEX (Sharmasarkar et al., 2000), chlorobenzenes (Sheng and Boyd, 2000) and PCBs (Sharma et al., 2009). Having observed increased BTEX sorption to clay substituted with trimethylphenylammonium than with aliphatics, Sharmasarkar et al., (2000) hypothesized that the growing aromatic content of the organic phase enhances sorption of BTEX to the aliphatic-substituted clay with increasing aqueous solute concentration. Additionally, the role of cosolvents in controlling the interlayer spacing of clays and the solvation of surface ions is believed to contribute to enhanced sorption with increasing solute concentration (Sheng et al., 1996).

6.3.2 Column Breakthrough Curves

Two effects of amending a conventional sand cap with PM-199 organoclay were observed from column effluent. First, the time to breakthrough for most chemicals was about one order of magnitude greater with a 1-cm thick layer of organoclay than without

amendment. The retardation factor in baseline columns was greatest for 1,2-dichlorobenzene at 2.1, while in organoclay-amended columns the largest value was 61.8 for naphthalene (Table 6.4). The decrease in migration velocity imparted by organoclay will be significant in field applications because the deposition of sediment to the top of the cap with time will extend the effective cap thickness and increase the distance that a chemical must migrate to reach the benthic zone (Lampert, 2010).

Table 6.4: Summary of retardation factors (R) and coefficients of determination (R^2) in upflow columns with sediments from two locations with either a 15-cm thick cap of only sand (i.e., “Baseline 1B” and “Baseline 2B”) or a cap with a 1-cm thick layer of organoclay topped by 14 cm of sand (i.e., “Amended 1A” and “Amended 2A”).

Chemical	<u>Baseline 1B</u>		<u>Baseline 2B</u>		<u>Amended 1A</u>		<u>Amended 2A</u>	
	R	R^2	R	R^2	R	R^2	R	R^2
1,2-Dichlorobenzene	2.1	0.95	1.3	0.89	51.2	0.90	30.0	0.95
1,4-Dichlorobenzene	2.1	0.95	1.4	0.87	18.8	0.86	18.0	0.88
Benzene	1.0	NA	1.0	NA	3.0	-0.2	6.7	0.90
Chlorobenzene	1.7	0.91	1.2	0.75	13.3	0.96	13.5	0.95
Ethylbenzene	2.0	0.87	1.4	0.79	13.8	0.89	16.4	0.91
Naphthalene	2.0	0.93	1.3	0.93	61.8	0.88	32.3	0.93
Toluene	1.6	0.82	1.1	0.93	7.47	0.91	10.0	0.99
Total Xylenes	1.8	0.94	1.3	0.90	16.4	0.99	17.2	0.89

The second effect of amending a sand cap with an organoclay layer was that the maximum concentrations measured in column effluent were substantially reduced for those chemicals with the largest K_f values from the isotherm tests, specifically 1,2-dichlorobenzene, chlorobenzene, and naphthalene (Figures 6.4 and 6.5). Maximum effluent concentrations of BTEX and 1,4-dichlorobenzene were similar in baseline and

amended columns. The small degree of adsorption by 1,4-dichlorobenzene relative to 1,2-dichlorobenzene was observed in batch isotherm testing and is attributable to differences in molecule geometry (Sheng and Boyd, 2000).

The validity of comparing retardation factors and concentration maxima between columns rests on the assumptions that the concentration profiles are similar in the different sediment columns. To estimate retardation factors, a constant concentration was assumed at the bottom boundary, though satisfaction of this condition is uncertain. A high degree of variance in the contaminant concentration with depth would provide misleading results. Similarly, large discrepancies in contaminant loadings on sediments between columns would obviously invalidate comparisons of maximum effluent concentrations.

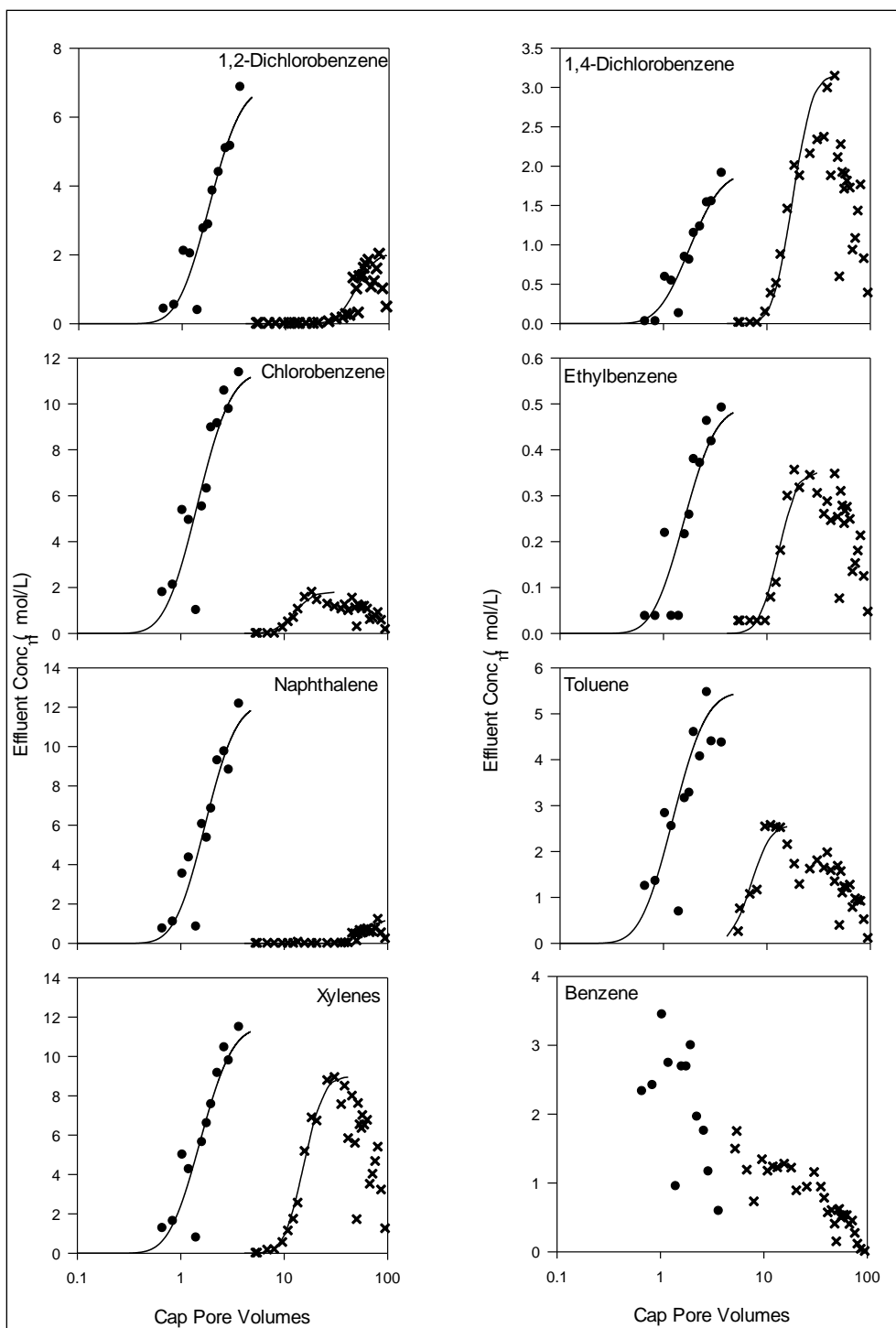


Figure 6.4: Breakthrough curves for baseline column 1A (circles) and organoclay-amended columns 1B (x).

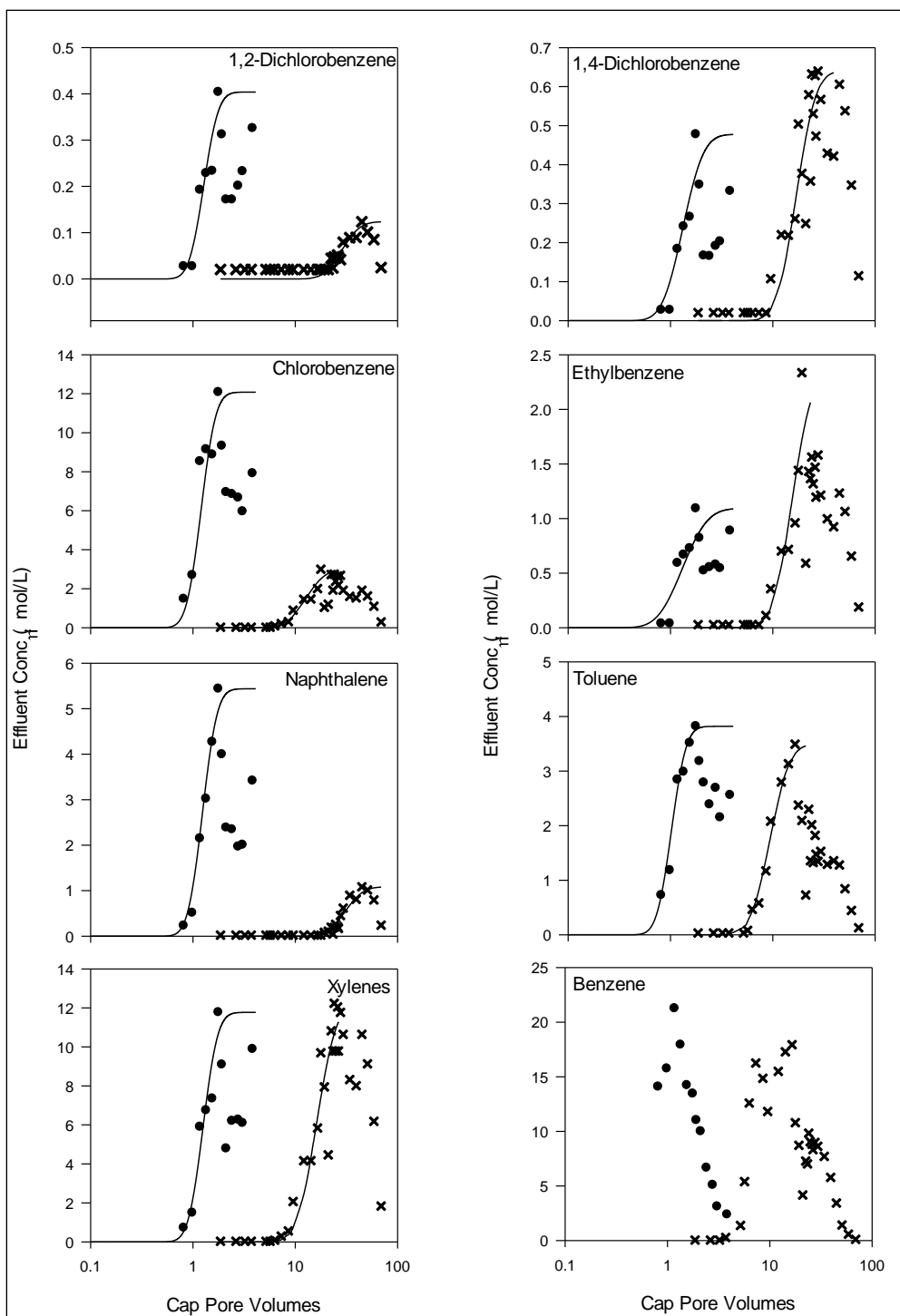


Figure 6.5: Breakthrough curves for baseline column 2A (circles) and organoclay-amended columns 2B (x).

6.3.3 Comparison of Sorption in Batch Isotherms and Column Tests

For computational simplicity, solute sorption to organoclays were assumed to be linear by setting Freundlich exponents to one and equating Freundlich coefficients in Table 6.3 to linear partitioning coefficients, $K_{d,i}$. Clearly this assumption does not affect isotherms with a Freundlich coefficient near one (i.e., 1,3-dichlorobenzene, 1,4-dichlorobenzene, and naphthalene) and approximates isotherms at low solute concentrations while underestimating loading onto organoclay at high concentrations for those chemicals with a Freundlich coefficient greater than one. Assuming a linear isotherm with the Freundlich coefficient provides a conservative estimate of retardation as compared with using the fit linear isotherm values, which were greater in magnitude for all compounds (Table 6.3). Batch isotherm K_d values were compared with those from columns by considering the cap, which consisted of amendment and sand layers, as a single uniform layer. This approximation is possible because solute sorption to both organoclay and sand is assumed to be linear (Barry and Parker, 1987). From the retardation factors fit for the entire column, R_i , the retardation factors for the organoclay layer were found by rearrangement of the weighted sum of retardation in both the organoclay and sand layers:

$$R = \frac{R_1 * \varepsilon_1 * z_1 + R_2 * \varepsilon_2 * z_2}{\varepsilon_1 * z_1 + \varepsilon_2 * z_2} \quad \text{Equation 6.5}$$

where ε_i is the porosity [--], z_i is the layer thickness [L], and subscripts 1 and 2 represent organoclay and sand, respectively. The retardation factor in the organoclay layer, R_1 , was used to estimate the linear partitioning coefficient measured in column tests, $K_{d,column}$, from rearrangement of the relation

$$R = 1 + \frac{\rho K_d}{\epsilon} \quad \text{Equation 6.6}$$

where ρ is the solid bulk density [mass/volume] and the others are as defined previously.

The resulting values of $K_{d,\text{column}}$ were all smaller than partition coefficients from isotherms, $K_{d,\text{isotherm}}$, by as much as one order of magnitude (Figure 6.6). Several possible explanations exist for this discrepancy. First, the effects of cosolvents on interlayer spacing in the organoclay might have differed between isotherm tests and column tests because the ratios of solute concentrations were dissimilar. Sheng et al. (1996) demonstrated that sorption of trichloroethylene was increased by addition of chlorobenzene as a cosolvent and that chlorobenzene controlled the interlayer spacing of the organoclay. In isotherms, concentrations were nearly equal for all analytes excluding benzene and toluene, while in columns, concentrations varied by more than one order of magnitude. Second, the organoclay layer in the column may not have been uniformly one cm thick, resulting in a decreased hydraulic retention time in the organoclay layer along certain streamlines and introducing the possibility that equilibrium partitioning was not achieved. Third, rather than equilibrium solute partitioning occurring uniformly throughout the column, it may be the case that pore water consists of a mobile fraction, which is instantaneously in equilibrium with the solids, and an immobile fraction, with exchange between the two described by a mass transfer coefficient (Pernyeszi et al., 2006). Fourth, sorption equilibrium might not have been achieved in the columns given that the average pore water residence time in the 1-cm organoclay layer was roughly one day while isotherm tubes were incubated for seven days. An examination of sorption kinetics suggests that 0.5 days is sufficient for chlorobenzene and naphthalene to reach

partitioning equilibrium with PM-199 organoclay in deionized water (Dunlap, 2011, unpublished data), but mass transfer resistances might have slowed partitioning in sediment porewater. The possibility of kinetically-controlled sorption should be explored.

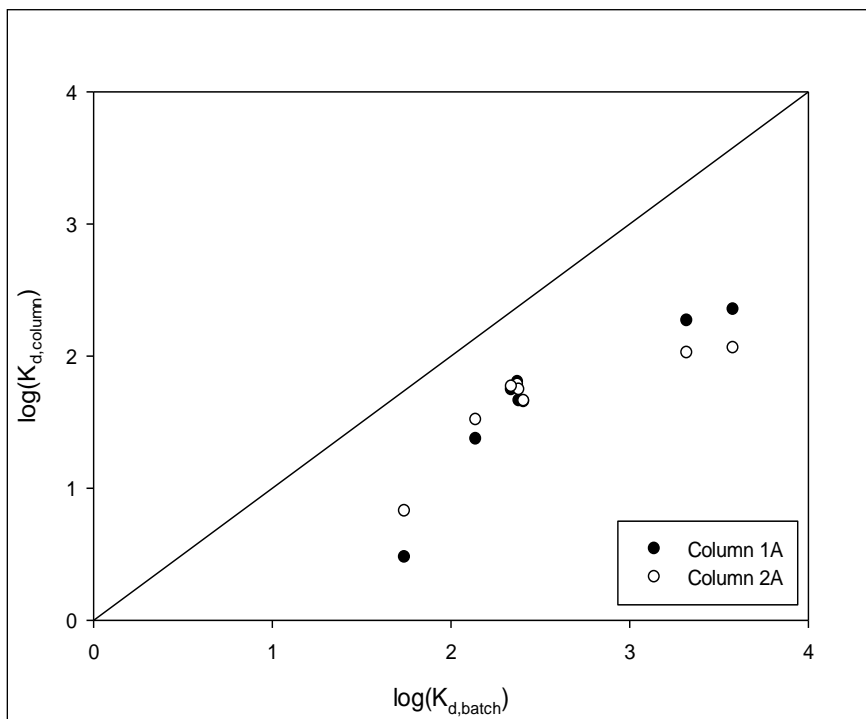


Figure 6.6: Comparison of adsorption in column and batch tests.

6.4 CONCLUSIONS

PM-199 organoclay, a surfactant-modified bentonite clay, sorbed BTEX, chlorobenzenes, and naphthalene to varying degrees. In general, sorption was a function of hydrophobicity and correlated negatively with aqueous compound solubility. However, the three dichlorobenzene isomers demonstrated a positive correlation between

partitioning coefficient and solubility, suggesting that absorption into the inter-layer organic phase was not the only mechanism of sorption to the solid. Partitioning was also positively correlated with dipole moment for the dichlorobenzenes, and it is believed that electrostatic interactions with cations on the clay surface contributed to dichlorobenzene sorption. Enhanced sorption was observed for some solutes with increasing concentration, possibly due to a cosolvent effect. Increasing aromatic content on organoclay particles is believed to further enhance sorption of aromatics (Sharmasarkar et al., 2000).

Slowed contaminant migration achieved by amending a cap with organoclay and coupled with sediment deposition to the top of the cap increases the effective cap length and thus the contaminant migration distance to the benthic zone. PM-199 proved effective, in sediment porewater with greater than 700 mg/L dissolved organic carbon, at retarding the transport of polar halogenated monoaromatics including monochlorobenzene and 1,2- and 1,3-dichlorobenzenes. Naphthalene, the least soluble of the chemicals examined, also was effectively sorbed. PM-199 was less effective with non-polar 1,4-dichlorobenzene and soluble BTEX, but retardation of these solutes could be improved in a cap by using organoclay in conjunction with a more effective sorbent such as activated carbon or by selecting an organophilic clay that was substituted with a surfactant containing an aromatic group.

Contaminants sorbed to organophilic clays are reportedly bioavailable, as indicated by the biodegradation of sorbed chlorobenzene (Witthuhn et al., 2005) and 2,4-dinitrophenol (Witthuhn et al., 2006). To better assess the potential for organophilic clays in the remediation of contaminated sediments, additional work is required to improve understanding of 1) how particular sorbates affect inter-layer spacing, 2) the impact of cosolvent effects with common sediment contaminants, 3) the significance of sorbate

interaction with clay-bound cations, and 4) the effect of sorbate-sorbent interaction on pollutant bioavailability. Amending a sediment cap with PM-199 organoclay appears to be an effective means of sequestering certain volatile contaminants, and the prospect of subsequent biodegradation could improve its efficacy.

Chapter 7: Conclusions and Recommendations for Future Work

7.1 CONCLUSIONS

7.1.1 Bench Scale Tests Aided in the Design of a Sediment Cap for Onondaga Lake

Laboratory tests for quantifying biologically-mediated fate and transport parameters were applied to aid in the design of a sediment cap for Onondaga Lake. Specifically, batch biodegradation tests were used to determine whether (1) indigenous sediment bacteria can degrade the contaminants of concern under site-specific temperatures and redox potentials, (2) amending porewater with energy sources or electron donors stimulates biodegradation of contaminants of concern, (3) bioaugmentation of sediments apparently lacking pollutant biotransformation capability with sediments that have said capability enhances biodegradation of contaminants of concern, (4) pollutants are completely degraded to innocuous products such as CO₂. Additionally, sand-capped sediment columns were used to demonstrate the potential for biodegradation in sand caps under reduced conditions at a site-appropriate temperature.

Gas production was quantified by monitoring the accumulation of gas pressure in sealed anaerobic culture tubes, and gas-phase contaminant transport resulting from biogenic gas production was estimated in sediment-packed gas flow-through columns.

Biological activity in sediments is largely location specific and must be evaluated individually. Using Onondaga Lake as an example, we demonstrated that these methods can aid in the design of a sediment cap.

7.1.2 Contaminant Biotransformation is Possible in Sand-Based Sediment Caps

Results from sand-capped sediment column tests suggest that contaminant biotransformation is possible under environmentally relevant temperatures and redox

potentials. To assess whether activity in a cap is likely for pollutants other than toluene, it is instructive to consider the individual requirements for contaminant biotransformation. In order of decreasing importance, these include microorganisms that produce degradative enzymes, energy sources, electron acceptors, moisture, pH, nutrients, temperature, the absence of toxicity, the removal of metabolites, and the absence of competitive organisms (Cookson, 1995). Each will be considered in order of importance.

The presence of bacteria capable of contaminant biotransformation in a sediment cap seems likely given that sediment-borne bacteria in a cap had previous exposure to sediment pollutants. As a result, some bacteria might have developed the capability to catabolize sediment contaminants prior to translation into the sand cap by porewater advection or cell motility. The presence of bacteria capable of contaminant biotransformation in sediments can be easily verified in batch degradation studies, as described in Chapter 3. It follows that these very bacteria could inhabit a sand cap, as was suggested by sand-capped sediment column tests described in Chapter 5 as well as experiments by Hyun et al. (2006) showing biotransformation of polycyclic aromatic hydrocarbons by sediment-borne bacteria in aerated sand cap columns.

Assessing the availability of energy sources and electron donors requires knowledge of specific biotransformation pathways. For anaerobic toluene biotransformation, toluene serves as the energy source and a number of species might serve as an electron acceptor including ferric iron, sulfate, or carbon dioxide. For reductive dechlorination of chlorobenzene, fermentation products including hydrogen and acetate can serve as energy sources and chlorobenzene as the electron acceptor. The oxidation of aliphatic or aromatic hydrocarbons to fermentation products in sediments and sediment caps is likely thermodynamically feasible even under methanogenic conditions (Dolfing, 2009), suggesting that contaminant biodegradation is possible over a

range of oxidation-reduction potentials. Similarly, reactions such as dehalogenation are thermodynamically feasible in reduced environments such as sediments (Beurskens et al., 1993), though reaction rates might be affected by competition with sand-derived electron acceptors such as ferric oxides.

Moisture, the next requirement cited by Cookson, is of negligible concern in sub-aqueous sediment caps. Porewater pH need only be near-neutral and can be adjusted by inclusion of minerals in a sediment cap if necessary, as discussed in Chapter 3. Sediments are generally considered to be rich in nutrients such as nitrogen and phosphorus (e.g., both were detected at mM concentrations in sediment porewater from column 60100) and nutrient flux from the underlying sediment is expected to prevent nutrient-limiting inhibition of bacterial activity in a cap. Depending upon hydraulics in the cap, nutrients might similarly be transported from the benthic zone above. Site temperature is not expected to be inhibitory to pollutant biotransformation at values typical of surface water sediments (i.e., 10°C – 15°C).

Toxicity to bacteria by sediment pollutants is one reason that biotransformation in a cap could proceed more quickly than in sediments. At sites co-contaminated with metals and hydrocarbons, metals could inhibit hydrocarbon metabolism in sediments, while their relative immobility compared with hydrocarbons would make them either largely absent or present at reduced concentrations, and thus unable to impart toxicity on hydrocarbon-metabolizing bacteria in the cap. As a conservative estimate, inhibition of bacterial activity by toxicity would not be any greater in a cap than in the underlying sediment.

In a complex microbial community with diverse metabolisms, the utilization of a product of one organism as a substrate by another is common, as evidenced by inter-species hydrogen transfer and the syntrophic relationship between acetogenic fermenters

and acetotrophic methanogens. Metabolite removal is an important process for maintaining thermodynamic feasibility for the biotransformation of hydrocarbon contaminants as discussed in Chapter 5. Studies of microbial community diversity presented here as well as results reported by Himmelheber et al. (2009) suggest that the bacterial community that develops in a sand cap is indeed complex and therefore likely to facilitate metabolite removal.

Finally, biotransformation requires that contaminant-degrading bacteria are not at a competitive disadvantage with respect to energy sources, electron donors, and nutrients. This principle might also have been demonstrated in the sand-capped sediment columns discussed in Chapter 5, in which it was hypothesized that methanogens and acetogens out-competed bacteria capable of dehalogenating chlorobenzenes, although sediment slurry results suggest that this reaction might not have proceeded quickly enough to be detected in columns even without microorganism competition. It seems possible that the energy sources (e.g., hydrocarbon contaminants) and electron donors (i.e., iron oxides) available in a cap could select for bacteria, such as members of the *Geobacteraceae* that can degrade aromatic compounds and reduce ferric iron. In two of the three columns that demonstrated toluene removal, the flux of ferrous iron increased from the inlet to the outlet of the cap indicating microbial iron reduction. In the columns operated by Himmelheber et al. (2008), iron reduction was the dominant TEAP throughout most of the cap. Sediments and sand caps can become limited in bioavailable carbon sources, so bacteria capable of biodegradation of hydrocarbon contaminants in the porewater of a sand cap might have a competitive advantage.

All requirements for contaminant biotransformation can be satisfied in a sand cap as demonstrated by this work as well as previous studies. Although toluene was the only pollutant quantifiably biotransformed in column tests, reaction rates much lower than the

minimum detectable rate in these tests would contribute to a substantial reduction in contaminant mass in the field over typical design lifetimes for sediment caps (i.e., tens to hundreds of years). It therefore seems likely that over the designed life of a sediment cap, pollutant biotransformation could represent an important contaminant sink.

7.1.3 Bacterial Community Structure Differs Significantly Between Sediment and Sand and Thus Can Not Be Used to Predict Potential Metabolic Activity in Sand Caps Based on Activity Observed in Sediments

Examples of correlation between the occurrences of benzene oxidation with bacterial community structure (Rooney-Varga et al., 1999; Röling et al., 2001) suggest that a high degree of similarity between bacterial communities suggests a high likelihood of similarity in pollutant degradation capability. Bacterial community profiling by terminal-restriction fragment length polymorphism (T-RFLP) revealed little similarity between the communities in a sand cap and in sediments. The implications of this observation are two-fold. For the case that contaminant biotransformation is occurring in sediments, similar biotransformation potential cannot be assumed in a cap, although it is possible. Contrarily, a lack of evidence of biotransformation in sediments does not preclude biotransformation in a cap; in fact, for reasons discussed above, activity might be more likely in a cap than in sediments. Bacteria capable of degrading a certain pollutant could be present as a minor population in sediments without actively degrading the pollutant because of factors that might include toxicity or preference for a different energy source, for example. Upon translation to the cap, the factors that prevented pollutant biotransformation in the sediment might not be present, and these bacteria could utilize the pollutant as an energy source and become a dominant population within the community in the sand cap.

7.1.4 Organoclays Can Be Effective Cap Amendments for Select Single- and Double-ring Aromatics

Sorption isotherms with benzene, ethylbenzene, toluene, xylenes (BTEX), chlorobenzene, dichlorobenzenes, and naphthalene to PM-199 organoclay in extracted sediment porewater were nearly linear but some compounds exhibited enhanced adsorption with increasing concentration as indicated by a Freundlich exponent greater than one. Amendment of a sand cap with PM-199 organoclay substantially delayed contaminant breakthrough and reduced the maximum effluent concentrations of 1,2-dichlorobenzene, 1,3-dichlorobenzene, chlorobenzene, and naphthalene with respect to the baseline (i.e., sand only) column with sediment from both locations. Breakthrough of 1,2-dichlorobenzene, benzene, toluene, and ethylbenzene also were delayed, though the maximum effluent concentration was not reduced in amended columns compared with baseline columns for both locations. Observed retardation factors were smaller than those predicted from sorption isotherms for reasons that are not yet fully understood. Results indicate that organoclays can be effective sediment cap amendments for select single- and double-ring aromatics with low solubility (i.e., 1,2-dichlorobenzene, 1,3-dichlorobenzene, monochlorobenzene, and naphthalene); however, organoclay-amended caps might require supplementation, perhaps with activated carbon, to sorb highly soluble aromatics such as BTEX.

7.2 RECOMMENDATIONS FOR FUTURE WORK

7.2.1 Bacteria and Archaea Clone Libraries

An advantage of 16S ribosomal RNA gene clone library construction is the acquisition of DNA sequences that can be used to identify individual bacteria and query databases for known contaminant-degraders. This information would supplement the

diversity and similarity data generated by T-RFLP and provide added detail regarding the structure of the bacterial and archaeal communities in sediments and a sand cap. Additionally, the presence of iron-reducing bacteria could be confirmed by PCR of DNA extracted from sand cap columns 70049A and 70050 with primers for *Geobacter*, providing further evidence that apparent iron-reduction might have been biological. Confirmation of the presence of bacteria known to have a desired degradation capability in a sand cap would further the prospect of a cap becoming a zone of contaminant biotransformation.

7.2.2 Estimate the Biologically-Reducible Fraction of Ferric Iron in Sand

Quantification of the biologically-reducible fraction of ferric iron in sand should be repeated to increase the number of samples and provide a statistically meaningful estimate. Given the apparent significance of iron-reduction in laboratory flow-through sand cap columns and the growing list of iron-reducing bacteria known to be capable of hydrocarbon contaminant biodegradation, the sand's capacity to support and sustain iron reduction is an important consideration for contaminant biotransformation.

7.2.3 Identification of Contaminant-Degrading Bacteria by Molecular Methods

To better assess the potential for biotransformation in a sand cap, the active bacteria in the sediment and sand cap should be identified. This can be accomplished with methods such as stable isotope probing (SIP) and fluorescent in-situ hybridization (FISH). Batch sediment slurries, like those described in Chapter 3, should be spiked with ¹³C-labeled substrate and sampled over time to detect substrate removal and identification of the dominant terminal electron accepting process (TEAP). If available, detection of biomarkers of anaerobic biotransformation, such as benzylsuccinate for toluene or

naphthoic acid for naphthalene, should be attempted. Bacteria that have incorporated ^{13}C into their DNA can be identified by SIP, and FISH probes could be designed to probe for these bacteria in column experiments with sand and sediment.

Sand-capped sediment columns should be operated as described in Chapter 5 with sampling to provide information as to contaminant biotransformation and dominant TEAP recognition. Following column operation, sand from the cap column should be split into two fractions. The first sand fraction would be subject to SIP in batch slurries to identify the bacteria assimilating ^{14}C , as described in the previous paragraph. The second fraction would be sonicated to dislodge bacteria from sand grains. Sand cap bacteria will then be probed for contaminant-degraders from the sediment batch slurries.

Through the proposed procedure, the presence of contaminant-degraders from sediments can be confirmed in a sand cap. Additionally, the identities of degraders in the sand cap and sediment can be compared. Finally, TEAPs in both media will be identified. This method identifies active rather than just potential biodegraders and will provide additional insight into the potential for biodegradation in a sand cap.

7.2.4 Biodegradation of Contaminants Sorbed to Cap Amendments

Recent research suggests that hydrocarbon pollutants sorbed to organoclays can be biodegraded. Specifically, chlorobenzene and 2,4-dinitrophenol sorbed to a dodecyltrimethylammonium-modified montmorillonite were reportedly biodegraded by *Rhodococcus B528* (Witthuhn et al., 2006) and by *Ralstonia eutropha* (Witthuhn et al., 2005), respectively. Biodegradation of organoclay surfactants is a topic of interest as it could lead to a reduction in sorptive capacity. Similarly, the long-term stability of biopolymer-coated sands for enhanced sorption is a topic requiring further study, as is the

infusion of capping material with a carbon- and nutrient-rich material such as peat. A cap amendment that improves sorption relative to sand and encourages biodegradation by providing energy sources, electron acceptors, and nutrients could greatly reduce pollutant flux through a sediment cap.

7.2.5 Examine Inhibition of Biotransformation by Sediment Contaminants

Toxicity to bacteria by sediment contaminants can inhibit pollutant biotransformation (Cookson, 1995). Measuring biotransformation rates in sediment slurries over a range of sediment densities would show whether contaminant biotransformation rates are negatively affected by increasing sediment densities, provided that dissolved contaminant concentrations are similar and that substrate bioavailability does not become a rate-limiting factor. Slurries over a range of sediment densities could be used to screen for the presence of contaminant-degrading bacteria and to learn whether biotransformation is inhibited by sediment pollutants.

Appendix A. Supplemental Material for Chapter 3

A1. HEADSPACE GAS CHROMATOGRAPHY WITH FLAME IONIZATION DETECTION

Table A1: Settings and operating conditions for gas chromatography analysis of aqueous samples by headspace sample injection with flame ionization detection.

Gas Chromatograph	HP-5890
injector temperature	250°C
detector temperature	275°C
Column	Restek RTX-624
length	30 m
ID	0.53 mm
DF	3.0 µm
Temperature Method	Hold at 40°C x 3 minutes Ramp at 10°C/min to 140°C Ramp at 50°C/min to 220°C Hold at 220°C x 3 minutes
Carrier Gas	Helium (10 mL/min)
Detector Gases	Air (55 psi), N2 (20 psi), H2
Headspace Sampler	Tekmar 7000
equilibration temperature	80°C
equilibration time	15 minutes
mix power	7
mixing time	10 minutes
stabilize time	0.1 minutes
pressurization time	1.0 minutes
pressure equilibration time	0.25 minutes
loop volume	1.0 mL
loop equilibrium time	0.25 minutes
injection volume	1.0 mL
loop temperature	170°C
line temperature	170°C
vial pressurization	2.0 psi

Table A2: Representative GC-FID calibration for a 2-mL aqueous sample in a 9-mL headspace vial. Data satisfy the quality assurance standards of EPA SW-826 Method 8015 (Analysis of Nonhalogenated Volatiles by Gas Chromatography) by generating a relative standard deviation (RSD) for the calibration factor (computed by peak area divided by standard concentration) of less than or equal to 0.25. The response to the chlorinated benzenes and naphthalene also satisfied this criterion although Method 8015 with headspace sample injection is not explicitly approved for their analysis.

Standard (µg/L)	Peak Area								
	1,2-DCB	1,3-DCB	1,4-DCB	B	MCB	EB	N	T	m-X
0	0	0	0	0	0	0	0	0	0
17.4	8139	8606	8980	19073	13188	22455	5351	20294	21728
48.3	18273	18361	18809	35655	26501	40268	16168	38397	39882
96.4	31936	32740	33833	49475	41679	62757	32039	57085	62878
194.6	64051	66142	68107	112356	87170	136118	61915	124563	134989
395.6	192420	200332	207977	338735	263534	395009	181083	367998	397255
801.9	276321	295275	302271	547987	393101	643318	250743	587063	634807
1180.5	451004	471750	486869	782962	612140	920257	409692	845107	927927
Mean									
Calibration									
Factor	388.3	403.9	417.2	732.1	551.4	864.5	344.2	795.5	857.0
RSD	0.16	0.17	0.18	0.25	0.22	0.25	0.15	0.25	0.24

A2. LIQUID SCINTILLATION COUNTING

Table A3: Settings for Beckman Liquid Scintillation Counter

Preset Time	30 minutes
H#	3
Sample Channels Ratio	N
sample Repeat	1
Automatic Quench Compensation	N
Low Sample Reject	0.1 minutes
Low Sample Reject Interval	999.95 minutes
RS-232 Output	N
Random Coincidence Monitor (RCM)	Y
RCM Time	0.1 minutes
RCM INT	999.95 minutes
Count Channel	1
Channel Lower Limit	0
Channel Upper Limit	670
Channel 2 Sigma	0.5
Channel Background Subtract	0
Channel Background 2 Sigma	0
Channel LSR	0
Date Calculation Program	5
Print Format	1

A3. CALCULATIONS FOR ESTIMATING VOLUMES OF BIOGENIC GAS PRODUCTION

In the gas generation tests, the pressure of a closed system is measured to determine rates of gas generation. The “system” is comprised of the “tubing” (the plastic tubing from the needle to the fluid level in the manometer) and the “vial” (the headspace of the anaerobic tube). To determine the pressure contribution by the vial, each component of the system is considered individually. In terms of a mole balance,

$$n_{vial} + n_{tubing} = n_{system} \quad \text{Equation A1}$$

By the ideal gas law, each n in Equation A1 can be substituted by PV/RT . The temperature of the system can be determined by mole-weighted averaging:

$$\frac{n_{vial}T_{vial} + n_{tubing}T_{tubing}}{n_{vial} + n_{tubing}} = T_{system} \quad \text{Equation A2}$$

Substitution of Equation A1 (in terms of P , V , R , and T) into Equation A2 and solution for P_{vial} gives

$$P_{vial} = \frac{P_{system}V_{system} - P_{tubing}V_{tubing}}{V_{vial}} \quad \text{Equation A3}$$

The system volume is taken to be the sum of the tubing and vial headspace volumes and one-half the observed manometer fluid displacement (h), P_{tubing} is assumed to be atmospheric, and P_{system} is measured by manometry ($P_{system} = P_{atmospheric} + \rho gh$, where ρ is the density of the manometer fluid relative to the negligible air density). The observed vial pressure is attributable to new gas generation and residual pressure, since the vial pressure is not relieved between observations. Thus,

$$P_{gas} = P_{vial} - P_{residual} \quad \text{Equation A4}$$

where $P_{residual}$ is P_{vial} from the previous observation. The ideal gas law is employed again to determine the volume that would be occupied by the vial headspace were the pressure atmospheric:

$$V_{gas} = \frac{P_{vial} V_{vial}}{P_{atm}}$$

Equation A5

The volume of gas generated is divided by the length of time between observations and the mass of sediment in the vial to yield a sediment mass normalized rate of gas generation.

A4. ¹⁴C-TOLUENE BIODEGRADATION SLURRIES

Table A4: Data from ¹⁴C-toluene biodegradation slurries. The difference in activity between the sparged samples at pH 14 and pH 1, which represents the quantity of purgeable acidified metabolic products such as CO₂, is reported (CPM/mL) after 74 days. The difference between samples and controls (i.e., “w/ HgCl₂” and “no solids”) is not statistically significant.

Treatment	Solids	Replicate	CPM/mL	Mean	SD	P ($\alpha = 0.05$)
Unamended	Sand	1	1188	758	372.5	0.30
		2	535			
		3	552			
		w/ HgCl ₂	1159	--		--
	Sediment	1	907	720	163.3	0.13
		2	605			
		3	647			
		w/ HgCl ₂	12681	--		--
	No solids		1085	--		--
Amended w/ NH ₃ , PO ₄ , trace metals	Sand	1	1191	1161	265.1	0.30
		2	1409			
		3	882			
		w/ HgCl ₂	1332	--		--
	Sediment	1	777	798	32.8	0.17
		2	836			
		3	782			
		w/ HgCl ₂	758	--		--
	No solids		880	--		--
			Controls ^a	1043	227.3	--

^a The Hg-spiked control with sediment and unamended porewater was identified as an outlier and excluded from computation of the mean and standard deviation.

A5. BIOGENIC GAS PRODUCTION

Table A5: Cumulative gas production volumes in anaerobic sediment slurries normalized to sediment mass ($\mu\text{L/g}$)

Location	22°C	12°C	7°C
60098	0.41	6.05	0.19
	0.55	5.35	<0.08
60099	<0.08	<0.08	<0.08
	0.09	<0.01	<0.08
60100	27.22	0.55	0.48
	18.90	0.39	0.30
70048	6.92	2.43	1.64
	57.24	0.56	0.76
70049	66.29	8.64	13.12
	2.55	36.26	13.42
70050	1.02	<0.08	0.50
	1.02	<0.08	0.26
10114	0.55	1.03	1.14
	<0.08	<0.08	0.09
10115	0.86	0.64	0.42
	<0.08	0.14	1.09
10116	0.19	<0.08	0.50
	0.19	<0.08	0.50
10117	0.40	1.15	1.30
	0.09	<0.08	0.09
10118	0.18	0.14	1.30
	0.09	0.15	0.09
10119	0.35	0.44	0.89
	<0.08	0.13	<0.08

A6. GAS-PHASE CONTAMINANT TRANSPORT

Raoult's Law states that for an ideal solution, the partial pressure of species i is given by the product of its pure phase vapor pressure ($P_{v,i}$) and mole fraction in solution (x_i):

$$P_i = x_i P_{v,i} \quad \text{Equation A1}$$

Hexane has a molecular weight of 86 g/mol, a pure phase vapor pressure of 17.3 kPa and a liquid density of 0.69 g/cm³ at 20°C.

The vapor pressure of toluene is four-times smaller than that of benzene, and those of all other analytes are at least one order-of-magnitude smaller than that of benzene, suggesting that volatile loss from the hexane trap was minimal.

Table A6: Contaminant fluxes observed in gas-phase transport column tests ($\mu\text{g m}^{-2} \text{ d}^{-1}$).

Analyte	Sediment Sample Location			
	10116	10118	70048	70049
1,2-Dichlorobenzene	47.6	35.0	<15.8	22.0
1,3-Dichlorobenzene	<15.8	<15.8	<15.8	<15.8
1,4-Dichlorobenzene	97.7	41	<15.8	<15.8
Chlorobenzene	87.6	520	<15.8	<15.8
Ethylbenzene	<15.8	16.0	<15.8	18.0
Naphthalene	<15.8	<15.8	<15.8	19.0
Toluene	<15.8	86.0	<15.8	<15.8
Total Xylenes	45.7	138	<15.8	<15.8

A7. SAND GRAIN SIZE DISTRIBUTION

Table A7: Size distribution of sand provided by the N.Y. State Department of Transportation (NYSDOT). Results indicate that the material generally conforms to size distributions required for designation as NYSDOT 703-07 Concrete Sand.

Sieve Size		NYSDOT 703-07 Concrete Sand	% Passing by mass n = 4 Mean +/- St Dev
Coarse	3/8"	100	100.0 +/- 0
	#4	90-100	95.9 +/- 0.9
	#8	75-100	86.0 +/- 5.2
Medium	#10	--	--
	#16	50-85	76.1 +/- 9.6
	#30	25-60	62.6 +/- 14.3
Fine	#40	--	--
	#50	10-30	31.5 +/- 8.6
	#100	1-10	7.5 +/- 2.2
#200		0-3	1.5 +/- 0.4

Appendix B. Supplemental Material for Chapter 4

B1. DISSOLVED METHANE ANALYSIS BY GAS CHROMATOGRAPHY WITH FLAME IONIZATION DETECTOR (GC-FID)

Sample volume was 1.0 mL in a 9-mL headspace vial. Gas-chromatograph settings and operation as in Table A1.

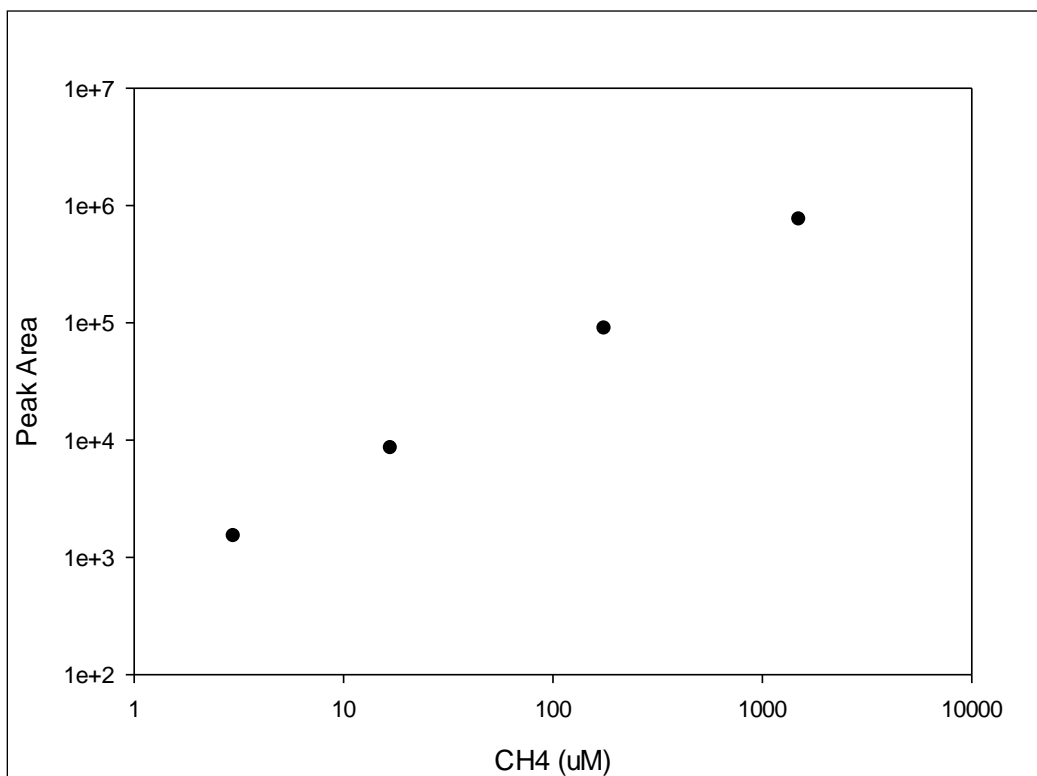


Figure B1: A representative calibration curve for dissolved methane by GC-FID.

B2. SULFIDE ANALYSIS BY THE METHYLENE BLUE METHOD

Reference: Cline, 1969

Column samples were collected in 1.0-mL lengths of Teflon tubing, then transferred to 0.7-mL polypropylene microcentrifuge tubes and closed without headspace. A solution of N,N-dimethyl-p-phenylenediamine sulfate (4.0 g/L) and ferric chloride hexahydrate (6.0 g/L) in 50% HCl was added to the sample (5.6 μ L). Samples were closed, shaken, and incubated at room temperature for 20 minutes to allow for color development. Three-hundred μ L were transferred to a 96-well plate and the absorbance at 670 nm was measured on a Biotek plate reader. Standard curves were prepared in Onondaga Lake surface water (OLSW).

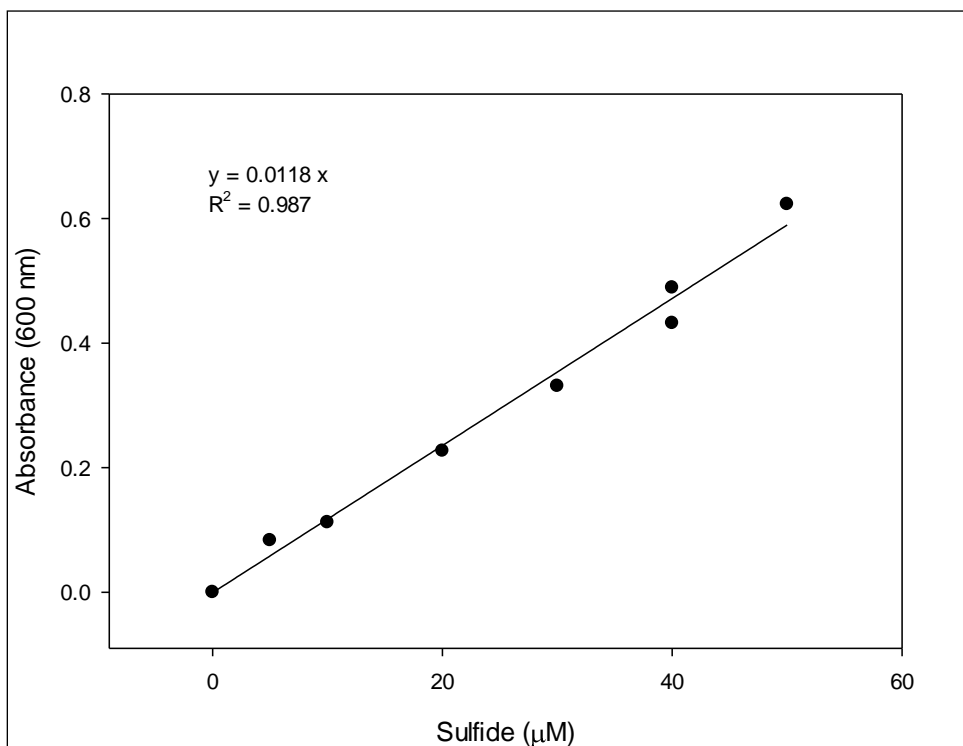


Figure B2: A representative calibration curve for sulfide analysis.

B3. FERROUS IRON BY THE PHENANTHROLINE METHOD

Reference: Method 3500-Fe B., Standard Methods, 2005

Reagent volumes were reduced proportionally and color development was performed in a 96-well microtiter plate in an anaerobic chamber. Sample absorbance at 510 nm was measured on a Biotek plate reader. (Note: absorbances were not corrected to a 1-cm pathlength).

Table B1: Reagents for the analysis of ferrous iron by the phenanthroline method.

Reagent	Volume (μL)
Sample	200
Concentrated HCl	4
Phenanthroline (1 mg/mL)	80
Ammonium Acetate Buffer Solution ^a	40

^a 250 g NH₄C₂H₃O₂ in 150 mL water and 700 mL glacial acetic acid

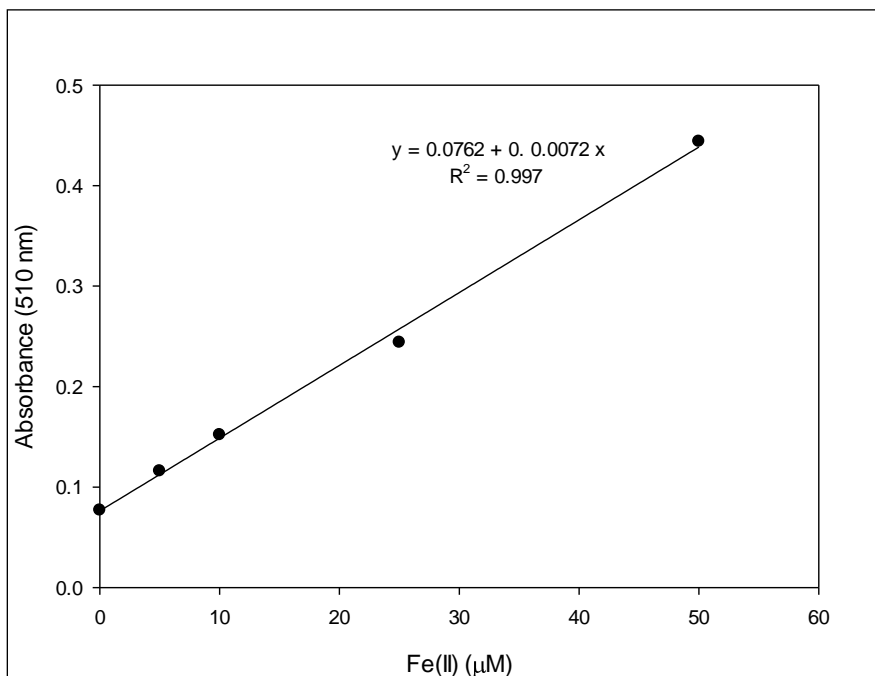


Figure B3: A representative calibration curve for ferrous iron.

B4. MICROBIALY-REDUCIBLE FERRIC IRON

Reference: Lovley and Phillips, 1987

B4.1 Quantitation of Fe(II)

Sand was dried and 0.1 g was added to 5 mL of 0.5 M HCl in a 20-mL glass vial. The vial was mixed gently by swirling for 30 seconds. After one hour at room temperature, 0.2 mL of extract was transferred to a microtiter plate and 80 μ L of 1 mg/mL phenanthroline solution and 40 μ L of ammonium acetate buffer solution (Appendix B5) were added.

B4.2 Quantitation of Fe(III) and Fe(II)

As above, except the extraction was performed with 5 mL of 0.25 M hydroxylamine hydrochloride in 0.25 M HCl.

Absorbance at all samples was measured at 510 nm on a Biotek plate reader. The difference between the hydroxylamine-extracted iron concentration and the hydrochloric acid-extracted iron concentration represents the microbially-reducible ferric iron content of the material.

B5. CHLORIDE, PHOSPHATE, AND SULFATE ANALYSIS BY ION CHROMATOGRAPHY

Anions were measured on a 700 Series ion chromatograph with a 15-cm MetroSep A Supp 5 column (Metrohm USA, Inc. Riverview, FL) (Method 4110, Eaton et al., 2005).

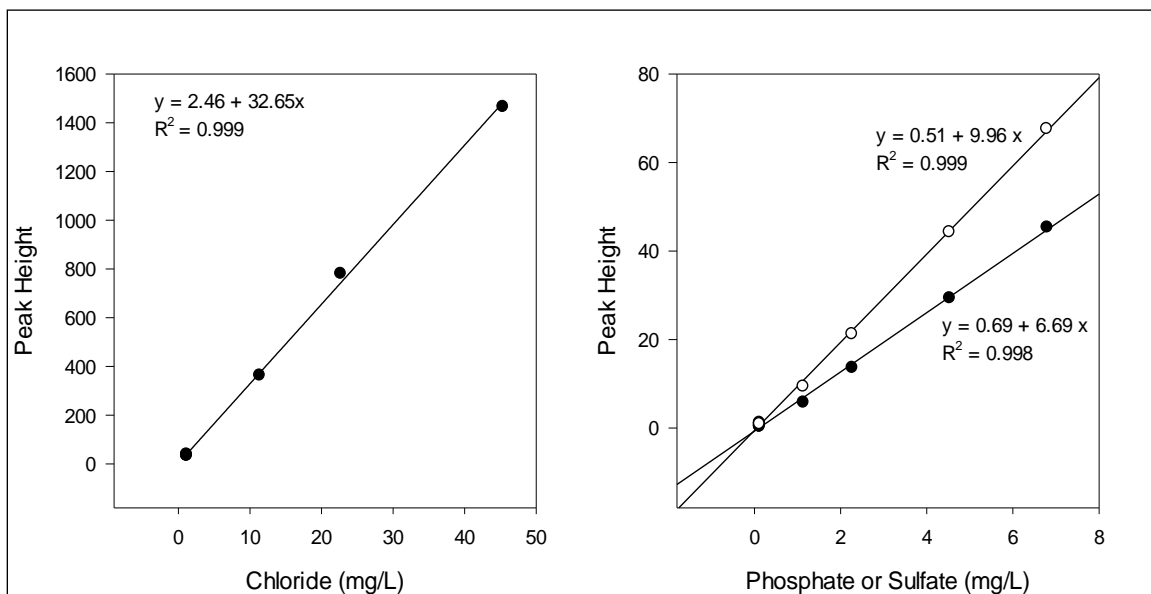


Figure B4: Calibration curves for chloride (left), phosphate (right, solid markers) and sulfate (right, hollow markers).

B6. MICROBIAL BIOMASS BY PHOSPHOLIPID QUANTIFICATION

Reference: Findlay et al., 1989

Note: All glassware was washed with phosphate-free detergent.

Phospholipids were extracted from ~4 g of sediment or sand in a 50-mL glass centrifuge tube with chloroform (CHCl_3), methanol (CH_3OH), and 50 mM dibasic potassium phosphate (K_2HPO_4) in volumes of 7.4 mL, 14.3 mL, and 5.9 mL, respectively. Tubes were shaken then incubated stationary at room temperature for three hours. Chloroform and phosphate were added (7.4 mL each) then tubes were shaken, centrifuged at 3000 rpm for five minutes, and incubated at room temperature overnight. The aqueous phase was aspirated, and the chloroform phase was transferred to a funnel with qualitative glass-fiber filter paper to remove suspended particles. Approximately 10 – 12 mL of the chloroform layer was collected, and this was reduced to 1 – 2 mL under a nitrogen stream. One-hundred μL were transferred to a 2-mL glass vial and removed completely under a nitrogen stream. Potassium persulfate ($\text{K}_2\text{S}_2\text{O}_8$) dissolved in 0.36 N H_2SO_4 (5 g in 100 mL) was added to the vial (0.45 mL) and the vial was incubated in a heat block at 95°C overnight. A solution of 0.1 mL of 2.5% ammonium molybdate ($(\text{NH}_4)_6\text{Mo}_7\text{O}_{24} \cdot 4\text{H}_2\text{O}$) in 5.72 N H_2SO_4 was added to the vial. After 10 minutes, 0.45 mL of a malachite green solution (0.111% polyvinyl alcohol dissolved in water at 80°C, then cooled for addition of malachite green to 0.011%) was added and vials were incubated for 30 minutes. Three-hundred μL samples were transferred to 96-well microtiter plates and the absorbance at 610 nm was measured on a Biotek platereader with absorbance correction to a 1 cm pathlength.

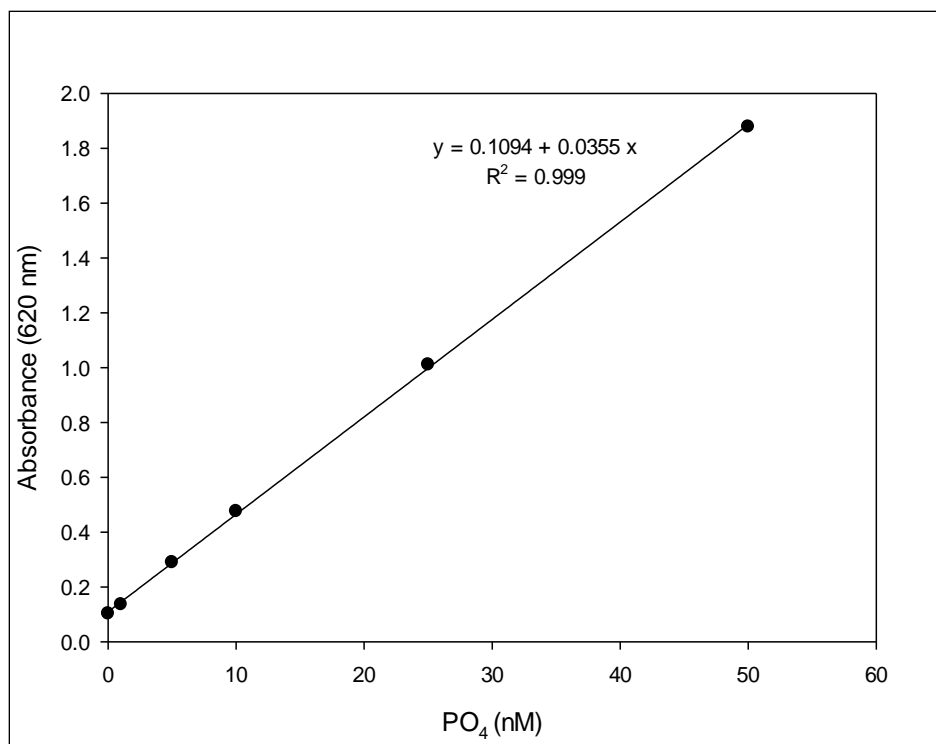


Figure B5: A representative calibration curve for molybdophosphate.

B7. SEQUENCES OF PCR PRIMERS

Table B2: Sequences of PCR primers for 16S rRNA and *bssA* gene amplification.

Primer Name	Target	Sequence
Fam-8f ^{1,3}	16S, Eubacteria	5'-AGA GTT TGA TCC TGG CTC AG-3'
11f ^{1,4}	16S, Universal	5'-GTT TGA TCC TGG CTC AG-3'
1492r ^{1,3}	16S, Universal	5'-GGT TAC CTT GTT ACG ACT T-3'
7772f ^{2,5}	<i>bssA</i>	5'-GAC ATG ACC GAC GCS ATY CT-3'
8546r ^{2,5}	<i>bssA</i>	5'-TCG TCG TCR TTG CCC CAY TT-3'

¹ References position on *E. coli* rRNA

² References position on *Thauera aromatica* K172 bss operon nucleotide numbering (Leuthner et al., 1998)

³ Sequence as reported by Reardon et al. (2004)

⁴ Sequence as reported by Kane et al. (1993)

⁵ Sequence as reported by Winderl, et al. (2007)

B8. SURFACE AREA ANALYSIS

Description of Surface Area Analysis Provided by Phil Bennett and Will Wolfe at the Jackson School of Geoscience

“Surface area analysis by gas adsorption involves determining the quantity of gas required to adsorb a thin layer (several molecules thick) onto all surfaces of a solid sample. To do this, the Quantachrome Autosorb-1 detects slight changes in pressure as small amounts of adsorbate gas (Nitrogen, Argon or Krypton) are injected into an evacuated chamber containing a sample held at constant temperature by a liquid nitrogen bath.

Sample preparation requires heating to 225°C under vacuum for 72 hours in order to clean the sample of contaminants such as water and oil that may affect the adsorption process. Therefore, substances with structural properties that are greatly altered by heat may not return accurate results (soils high in organic matter, etc.). Substances that react chemically with the adsorbate gas may also return negative results (substances containing high amounts of clay). In addition, the Quantachrome Autosorb-1 requires at least 0.5 m² of total surface area within each sample to perform an accurate analysis.

The outgasser heats to 275°C and vacuums to about 0.2 torr simultaneously. The sand sample outgassed for 48 hours, the sediment sample needed 96 hours and gave off a yellow oil when heated.”

Appendix C. Supplemental Material for Chapter 5

C1. FIT OF TRANSPORT EQUATION WITHOUT REACTION

Table C1: Summary of fit (i.e., R^2) of transport equation without reaction to column effluent data as of April, 2010.

Chemical	60103	60216	70024A	70024B	70049A	70049B	70050	70087	70123
1,2-Dichlorobenzene	--	--	0.78	0.91	0.84	0.91	0.89	0.85	0.85
1,3-Dichlorobenzene	--	--	0.89	--	--	--	--	--	--
1,4-Dichlorobenzene	--	--	0.88	0.93	0.74	0.94	0.91	0.79	0.87
Benzene	0.82	0.83	0.93	0.14	0.66	0.94	0.86	0.52	0.91
Chlorobenzene	0.95	0.93	0.75	0.89	0.77	0.88	0.89	0.77	0.99
Ethylbenzene	--	--	0.48	0.92	0.58	0.94	0.82	0.76	--
Naphthalene	0.17	--	0.81	0.82	0.87	0.96	0.93	0.92	--
Toluene	0.89	--	0.86	0.61	-0.28	0.73	0.17	0.50	0.43
Xylenes	0.82	0.94	0.50	0.87	0.51	0.91	0.87	0.80	0.96

C2. DISSOLVED HYDROGEN

Core samples collected with a 10-cm³ syringe with the tip removed were transferred to headspace vials that were capped with butyl rubber stoppers and crimp caps. The effective volume of the stoppered vial was 7.5 cm³ (nominal volume of 9.0 cm³ with a cap instead of a stopper).

Empty vials were weighed, then approximately 2 cm³ of sand or sediment was added and vials were weighed again. The mass of solids was used to estimate the volume occupied by solids using estimated wet densities of 2.6 g/cm³ and 1.6 g/cm³ for sand and sediment, respectively. The difference between the total volume and the volume occupied by solids was taken to be the headspace volume and was used for material balance calculations.

Ten cm³ of ultra-high purity nitrogen was withdrawn into a gas-tight syringe and 2 cm³ was transferred to the sample vial. The vial was briefly mixed by shaking, then 2 cm³ of headspace was withdrawn into the syringe containing 8 cm³ of nitrogen. Five cm³ of sample were injected into the reducing gas analyzer (Trace Analytical, Menlo Park, CA).

The peak area was converted to concentration by the calibration curve (Figure C1), which was then multiplied by the dilution factor. This value represented the equilibrium concentration in the gas phase (C_e^g). The equilibrium concentration in the aqueous phase (C_e^{aq}) was computed with Henry's Law constant (1240 atm L mol⁻¹ at 25°C). The total mass of hydrogen in the vial was then computed by summing the masses in each phase:

$$H_2^{\text{total}} = V^g C_e^g + V^{\text{aq}} C_e^{\text{aq}} \quad \text{Equation C1}$$

Samples of glovebox atmosphere were collected between every third core sample preparation, and glovebox atmospheric hydrogen was comparable in concentration to some of the samples collected. Background concentrations were subtracted from sample concentrations by assuming that the gas-phase hydrogen concentration was the same in background vials and sample vials. The mass of hydrogen in a sample vial attributable to background was thus

$$H_{2,s}^b = V^g C_b \quad \text{Equation C2}$$

where $H_{2,s}^b$ refers to hydrogen in the sample attributable to background and C_b is the hydrogen concentration measured in the background vial. Subtracting the mass of hydrogen attributable to background and dividing the mass of hydrogen by the estimated volume of water present provides the initial dissolved hydrogen concentration in the core:

$$C^{\text{aq}} = \frac{H_2^{\text{total}} - H_2^{\text{bgd}}}{V^{\text{aq}}} \quad \text{Equation C3}$$

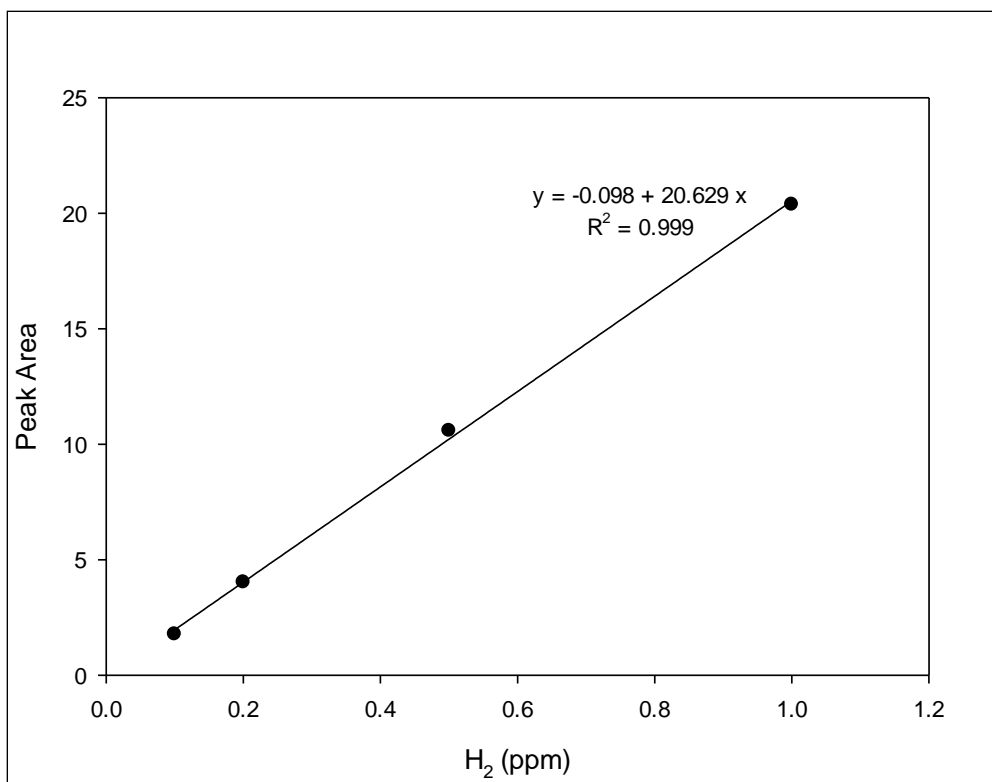


Figure C1: Calibration curve for hydrogen on the reducing gas analyzer.

Appendix D. Supplemental Material for Chapter 6

D1. CALIBRATION CURVES FOR HYDRAULIC TRACERS FLUORESC EIN AND BROMIDE

Fluorescein: the fluorescence intensity of a 100 μL sample in a black 96-well plate was measured on a Biomek plate reader at an excitation wavelength of 485 nm and an emission wavelength of 528 nm.

Bromide: standards prepared in site water, measured by electrode (Cole Parmer)

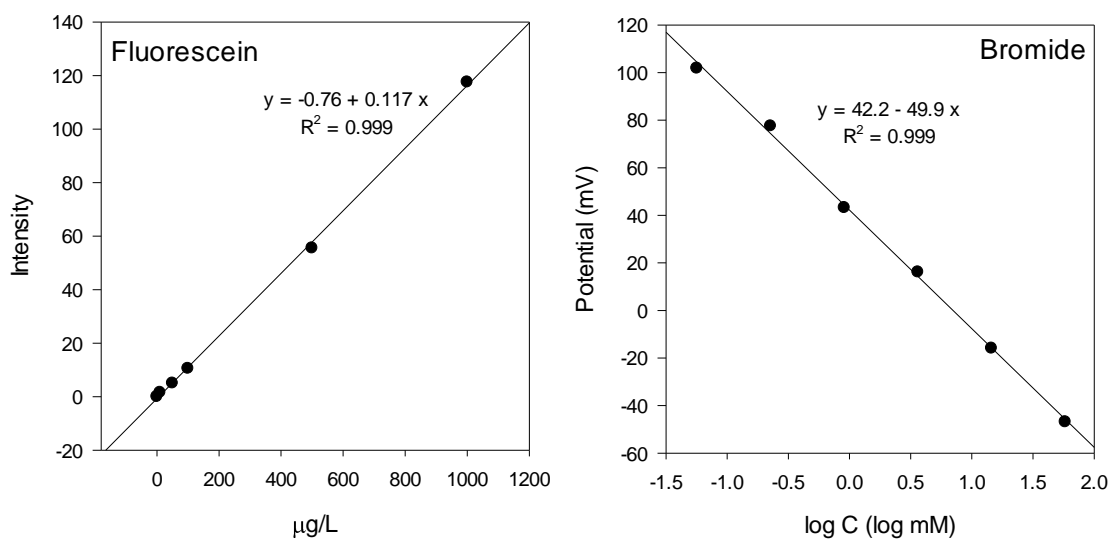


Figure D1: Standard curves for the hydraulic tracers fluorescein and bromide.

References

- Adams, D.D., N.J. Fendinger, and D.E. Glotfelty. 1990. "Biogenic gas production and mobilization of in-place sediment contaminants by gas ebullition." In *Sediments: Chemistry and Toxicity of In-Place Pollutants*, 215-236. Chelsea, MI: Lewis Publishers, Inc.
- Aislabie, J., M. McLeod, and R. Fraser. 1998. "Potential for biodegradation of hydrocarbons in soil from the Ross Dependency, Antarctica." *Applied Microbiology and Biotechnology* 49(2):210-214.
- Alexander, M. 1999. *Biodegradation and Bioremediation*. Second Ed. San Diego, CA: Academic Press.
- Alshawabkeh, A.N., N. Rahbar, and T. Sheahan. 2005. "A model for contaminant mass flux in capped sediment under consolidation." *Journal of Contaminant Hydrology* 78(3):147-165.
- Alumbaugh, R.E., L.M. Gieg, and J. A. Field. 2004. "Determination of alkylbenzene metabolites in groundwater by solid-phase extraction and liquid chromatography-tandem mass spectrometry." *Journal of Chromatography A* 1042(1-2):89-97.
- Alvarez, P.J.J. and W. Illman. 2006. *Bioremediation and Natural Attenuation*. Hoboken, NJ: John Wiley & Sons, Inc.
- Amos, R.T. and K.U. Mayer. 2006. "Investigating ebullition in a sand column using dissolved gas analysis and reactive transport modeling." *Environmental Science and Technology* 40(17):5361-5367.
- Anderson, R.T., J.N. Rooney-Varga, C.V. Gaw, and D.R. Lovley. 1998. "Anaerobic benzene oxidation in the Fe(III) reduction zone of petroleum-contaminated aquifers." *Environmental Science and Technology* 32(9):1222-1229.
- Apitz, S.E., B.P. Ayers, and V.J. Kirtay. 2004. *Use of Data on Contaminant/Sediment Interactions to Streamline Sediment Assessment and Management*. Technical Report. San Diego, CA: US Navy. (<http://www.spawar.navy.mil/sti/publications/pubs/tr/1918/tr1918cond.pdf>)
- Aronson, D. and P.H. Howard. 1997. *Anaerobic Biodegradation of Organic Chemicals in Groundwater: A Summary of Field and Laboratory Studies*. Syracuse, New York: Environmental Science Center, November 12. <http://esc.syrres.com/demos/ratecon.pdf>.

- Atlas, R.M. 1981. "Microbial degradation of petroleum hydrocarbons: an environmental perspective." *Microbiology and Molecular Biology Reviews* 45(1):180-209.
- Barker, J.J. 2004. "The effects of nutrient-bearing minerals on hydrocarbon biodegradation." MS Thesis, The University of Texas at Austin.
- Barry, D.A. and J.C. Parker. 1987. "Approximations for solute transport through porous media with flow transverse to layering." *Transport in Porous Media* 2(1):65-82.
- Beller, H.R., S.R. Kane, T.C. Legler, and P.J.J. Alvarez. 2002. "A real-time polymerase chain reaction method for monitoring anaerobic, hydrocarbon-degrading bacteria based on a catabolic gene." *Environmental Science and Technology* 36(18):3977-3984.
- Beller, H.R. 2002. "Analysis of benzylsuccinates in groundwater by liquid chromatography/tandem mass spectrometry and its use for monitoring in situ BTEX biodegradation." *Environmental Science and Technology* 36(12):2724-2728.
- Beurskens, J.E.M. "Microbial transformation of chlorinated aromatics in sediments." Doctoral Thesis, Wageningen Agricultural University, 1995.
- Blackwood, C.B., T. Marsh, S.-H. Kim, and E.A. Paul. 2003. "Terminal restriction fragment length polymorphism data analysis for quantitative comparison of microbial communities." *Applied and Environmental Microbiology* 69(2):926-932.
- Bloom, S.A. 1981. "Similarity indices in community studies: potential pitfalls." *Marine Ecology Progress Series* 5:125-128.
- Boyd, S.A., J.-F. Lee, and M.M. Mortland. 1988. "Attenuating organic contaminant mobility by soil modification." *Nature* 333(6171):345-347.
- Boyd, E., D. Cummings, and G. Geesey. 2007. "Mineralogy influences structure and diversity of bacterial communities associated with geological substrata in a pristine aquifer." *Microbial Ecology* 54(1):170-182.
- Bradley, P.M., and F.H. Chapelle. 1995. "Rapid toluene mineralization by aquifer microorganisms at Adak, Alaska: implications for intrinsic bioremediation in cold environments." *Environmental Science and Technology* 29(11):2778-2781.
- Braeckvelt, M., H. Rokadia, G. Imfeld, N. Stelzer, H. Paschke, P. Kuschke, M. Kastner, H. Richnow, and S. Weber. 2007. "Assessment of in situ biodegradation of monochlorobenzene in contaminated groundwater treated in a constructed wetland." *Environmental Pollution* 148(2):428-437.

- Bray, J.R. and J.T. Curtis. 1957. "An ordination of the upland forest communities of southern Wisconsin." *Ecological Monographs* 27(4):325-349.
- Bruce, L., A. Kolhatkar, and J. Cuthbertson. 2009. "Comparison of BTEX attenuation rates under anaerobic conditions." *Proceedings of the Annual International Conference on Soils, Sediments, Water and Energy* 14, Article 14.
- Burr, M., S. Clark, C. Spear, and A. Camper. 2006. "Denaturing gradient gel electrophoresis can rapidly display the bacterial diversity contained in 16S rDNA clone libraries." *Microbial Ecology* 51(4):479-486.
- Caldwell, M.E. and J.M. Suflita. 2000. "Detection of phenol and benzoate as intermediates of anaerobic benzene biodegradation under different terminal electron-accepting conditions." *Environmental Science and Technology* 34:1216-1220.
- Capone, D.G. and R.P. Kiene. 1988. "Comparison of microbial dynamics in marine and freshwater sediments: contrasts in anaerobic carbon catabolism." *Limnology and Oceanography* 33(4):725-749.
- Chang, W., Y. Um, B. Hoffman and T.R.P. Holoman. 2005. "Molecular characterization of polycyclic aromatic hydrocarbon (PAH)-degrading methanogenic communities." *Biotechnology Progress* 21:682-688.
- Chang, W., Y. Um and T. Holoman. 2006. "Polycyclic aromatic hydrocarbon (PAH) degradation coupled to methanogenesis." *Biotechnology Letters* 28(6):425-430.
- Chung, W.K., and G.M. King. 1999. "Biogeochemical transformations and potential polyaromatic hydrocarbon degradation in macrofaunal burrow sediments." *Aquatic Microbial Ecology* 19: 285-295.
- Cline, J.D. 1969. "Spectrophotometric determination of hydrogen sulfide in natural waters." *Limnology and Oceanography* 14(3):454-458.
- Coates, J.D., E.J. Phillips, D.J. Lonergan, H. Jenter, and D.R. Lovley. 1996. "Isolation of *Geobacter* species from diverse sedimentary environments." *Applied and Environmental Microbiology* 62(5):1531-1536.
- Coates, J.D., D.J. Ellis, C.V. Gaw, and D.R. Lovley. 1999. "*Geothrix fermentans* gen. nov., sp. nov., a novel Fe(III)-reducing bacterium from a hydrocarbon-contaminated aquifer." *International Journal of Systematic Bacteriology* 49(4):1615-1622.
- Coates, J.D., R. Chakraborty, and M.J. McInerney. 2002. "Anaerobic benzene biodegradation—a new era." *Research in Microbiology* 153(10):621-628.

- Conrad, R., F. Bak, H.J. Seitz, B. Thebrath, H.P. Mayer, and H. Schütz. 1989. "Hydrogen turnover by psychrotrophic homoacetogenic and mesophilic methanogenic bacteria in anoxic paddy soil and lake sediment." *FEMS Microbiology Letters* 62(5):285-293.
- Cookson, J.T. 1995. *Bioremediation Engineering*. USA: McGraw-Hill, Inc.
- Cord-Ruwisch, R., T.I. Mercz, C.-Y. Hoh, and G.E. Strong. 1997. "Dissolved hydrogen concentration as an on-line control parameter for the automated operation and optimization of anaerobic digesters." *Biotechnology and Bioengineering* 56(6):626-634.
- Corseuil, H.X., and W.J. Weber Jr. 1994. "Potential biomass limitations on rates of degradation of monoaromatic hydrocarbons by indigenous microbes in subsurface soils." *Water Research* 28 (6): 1415-1423.
- Dale, N.G. 1974. "Bacteria in intertidal sediments: factors related to their distribution." *Limnology and Oceanography* 19(3):509-518.
- Da Silva, M.L.B. and P.J.J. Alvarez. 2007. "Assessment of anaerobic benzene degradation potential using 16S rRNA gene-targeted real-time PCR." *Environmental Microbiology* 9(1):72-80.
- Dise, N., and E. Verry. 2001. "Suppression of peatland methane emission by cumulative sulfate deposition in simulated acid rain." *Biogeochemistry* 53(2):143-160.
- Dolfing, J., B.K. Harrison. 1992. "Gibbs free energy of formation of halogenated aromatic compounds and their potential role as electron acceptors in anaerobic environments." *Environmental Science and Technology* 26:2213-2218.
- Dolfing, J., A. Xu, N.D. Gray, S.R. Larter and I.M. Head. 2009. "The thermodynamic landscape of methanogenic PAH degradation." *Microbial Biotechnology* 2(5):566-574.
- Eaton, E.W., L.S. Clesceri, A.D. Rice, A.E. Greenberg, and M.A.H. Franson, Editors. 2005. *Standard Methods for the Examination of Water and Wastewater*. 21st ed. American Public Health Association American Water Works Association/Water Environment Federation, Washington, DC.
- Edwards, E.A. and D. Grbic-Galic. 1994. "Anaerobic degradation of toluene and o-xylene by a methanogenic consortium." *Applied and Environmental Microbiology* 60(1):313-322.

- Eek, E., G. Cornelissen, A. Kibsgaard, and G. Breedveld. 2008. "Diffusion of PAH and PCB from contaminated sediments with and without mineral capping: measurement and modeling." *Chemosphere* 71(9):1629-1638.
- Effler, S.W. 1987. "The impact of a chlor-alkali plant on Onondaga Lake and adjoining systems." *Water, Air, and Soil Pollution*. 33:85-115.
- Effler, S.W. and G. Harnett. 1996. "Background" in *Limnological and Engineering Analysis of a Polluted Urban Lake*, 1-31. Springer Series on Environmental Management. New York, NY: Springer-Verlag.
- Fava, F. and S.N. Agathos. 2006. "Uncertainty and research needs in the area of the biological restoration of contaminated sediments." In *Assessment and Remediation of Contaminated Sediments*, 73:239-246. NATO Science Series IV. Earth and Environmental Sciences. Dordrecht, The Netherlands: Springer.
- Fahy, A., A.S. Ball, G. Lethbridge, K.N. Timmis, and T.J. McGenity. 2008. "Isolation of alkali-tolerant benzene-degrading bacteria from a contaminated aquifer." *Letters in Applied Microbiology* 47(1):60-66.
- Fendinger, N.J., D.D. Adams, and D.E. Glotfelty. "The role of gas ebullition in the transport of organic contaminants from sediments," *Science of The Total Environment* 112(2-3):189-201.
- Findlay, R.H., G.M. King, and L. Watling. 1989. "Efficacy of phospholipid analysis in determining microbial biomass in sediments." *Applied and Environmental Microbiology* 55 (11): 2888-2893.
- Forstner, U., and S.E. Apitz. 2007. "Sediment remediation: U.S. focus on capping and monitored natural recovery." *Journal of Soils and Sediments* 7(6):351-358.
- Fung, J.M., B.P. Weisenstein, E.E. Mack, J.E. Vidumsky, T.A. Ei, and S.H. Zinder. 2009. "Reductive dehalogenation of dichlorobenzenes and monochlorobenzene to benzene in microcosms." *Environmental Science and Technology* 43(7):2302-2307.
- Grbic-Galic, D. and T.M. Vogel. 1987. "Transformation of toluene and benzene by mixed methanogenic cultures." *Applied and Environmental Microbiology* 53(2):254-260.
- Harwood, C.S., G. Burchhardt, H. Herrmann, and G. Fuchs. 1998. "Anaerobic metabolism of aromatic compounds via the benzoyl-CoA pathway." *FEMS Microbiology Reviews* 22(5): 439-458.

- Hayduk, W. and H. Laudie. 1974. "Prediction of diffusion coefficients for nonelectrolytes in dilute aqueous solutions." *AIChE Journal* 20(3):611-615.
- Heider, J., A.M. Spormann, H.R. Beller, and F. Widdel. 1998. "Anaerobic bacterial metabolism of hydrocarbons." *FEMS Microbiology Reviews* 22 (5): 459-473.
- Himmelheber, D.W. and J.B. Hughes. 2005. "Complete tetrachloroethene dechlorination in Anacostia River sediment." Presented at the SETAC 26th Annual Meeting in North America, Baltimore, MD.
- Himmelheber, D.W., K.D. Pennell, and J.B. Hughes. 2007. "Natural attenuation processes during in situ capping." *Environmental Science and Technology* 41(15):5306-5313.
- Himmelheber, D.W. 2008. "In situ capping of contaminated sediments: spatial and temporal characterization of biogeochemical and contaminant biotransformation processes." Doctoral Dissertation, Georgia Institute of Technology.
- Himmelheber, D.W., M. Taillefert, K.D. Pennell, and J.B. Hughes. 2008. "Spatial and temporal evolution of biogeochemical processes following in situ capping of contaminated sediments." *Environmental Science and Technology* 42(11):4113-4120.
- Himmelheber, D.W., S.H. Thomas, F.E. Loeffler, M. Taillefert, and J.B. Hughes. 2009. Microbial colonization of an in situ sediment cap and correlation to stratified redox zones. *Environmental Science and Technology* 43(1):66-74.
- Hoehler, T.M., M.J. Alperin, D.B. Albert, and C.S. Martens. 1998. "Thermodynamic control on hydrogen concentrations in anoxic sediments." *Geochimica et Cosmochimica Acta* 62(10): 1745-1756.
- Holliger, C. and A. Zehnder. 1996. "Anaerobic biodegradation of hydrocarbons." *Current Opinion in Biotechnology* 7:326-330.
- Hunkeler, D., D. Jorger, K. Haberli, P. Hohener, and J. Zeyer. 1998. "Petroleum hydrocarbon mineralization in anaerobic laboratory aquifer columns." *Journal of Contaminant Hydrology* 32(1-2):41-61.
- Hyun, S., C.T. Jafvert, L.S. Lee, and P.S.C. Rao. 2006. "Laboratory studies to characterize the efficacy of sand capping a coal tar-contaminated sediment." *Chemosphere* 63(10):1621-1631.
- Jaccard, P. 1912. "The distribution of the flora in the alpine zone." *New Phytologist* 11(2):37-50.

- Jackel, U. and S. Schnell. 2000. "Suppression of methane emission from rice paddies by ferric iron fertilization." *Soil Biology and Biochemistry* 32(11-12):1811-1814.
- Jackson, G.A. and S.E. Lochmann. 1992. "Effect of coagulation on nutrient and light limitation of an algal bloom." *Limnology and Oceanography* 37(1):77-89.
- Jackson, C.R., and A.Q. Weeks. 2008. "Influence of particle size on bacterial community structure in aquatic sediments as revealed by 16S rRNA gene sequence analysis." *Applied and Environmental Microbiology* 74(16):5237-5240.
- Jiang, H., H. Dong, G. Zhang, B. Yu, L.R. Chapman, and M.W. Fields. 2006. "Microbial diversity in water and sediment of Lake Chaka, an athalassohaline lake in northwestern China," *Applied and Environmental Microbiology* 72(6):3832-3845.
- Johnson, B.D., B.P. Boudreau, B.S. Gardiner, and R. Maass. 2002. "Mechanical response of sediments to bubble growth." *Marine Geology*. 187:347-363.
- Johnson, N.W., D.D. Reible, and L.E. Katz. 2010. "Biogeochemical changes and mercury methylation beneath an in-situ sediment cap." *Environmental Science and Technology* 44(19): 7280-7286.
- Kane, M.D., L.K. Poulsen, and D.A. Stahl. 1993. "Monitoring the enrichment and isolation of sulfate-reducing bacteria by using oligonucleotide hybridization probes designed from environmentally derived 16S rRNA sequences.," *Applied and Environmental Microbiology* 59(3):682-686.
- Kaplan, C.W., J.C. Astaire, M.E. Sanders, B.S. Reddy, and C.L. Kitts. 2001. "16S Ribosomal DNA terminal restriction fragment pattern analysis of bacterial communities in feces of rats fed *Lactobacillus acidophilus* NCFM." *Applied and Environmental Microbiology* 67(4):1935-1939.
- Kazumi, J., M.E. Caldwell, J.M. Suflita, D.R. Lovley, and L.Y. Young. 1997. "Anaerobic degradation of benzene in diverse anoxic environments." *Environmental Science and Technology* 31:813-818.
- Kim, Y.S., C.T. Jafvert, S. Yoon, S. Hyun, B. Johnson. 2009. "Potential consolidation-induced NAPL migration from coal tar impacted river sediment under a remedial sand cap." *Journal of Hazardous Materials* 162(2-3):1364-1370.
- Kotsyurbenko, O.R., M.V. Glagolev, A.N. Nozhevnikova, and R. Conrad. 2001. "Competition between homoacetogenic bacteria and methanogenic archaea for hydrogen at low temperature," *FEMS Microbiology Ecology* 38(2-3):153-159.

- Kotsyurbenko, O.R. 2005. "Trophic interactions in the methanogenic microbial community of low-temperature terrestrial ecosystems," *FEMS Microbiology Ecology* 53(1):3-13.
- Kunapuli, U., C. Griebler, H.R. Beller, and R.U. Meckenstock. 2008. "Identification of intermediates formed during anaerobic benzene degradation by an iron-reducing enrichment culture." *Environmental Microbiology* 10(7):1703-1712.
- Kunapuli, U., M.K. Jahn, T. Lueders, R. Geyer, H.J. Heipieper, and R.U. Meckenstock. 2010. "*Desulfitobacterium aromaticivorans* sp. nov. and *Geobacter toluenoxydans* sp. nov., iron-reducing bacteria capable of anaerobic degradation of monoaromatic hydrocarbons." *International Journal of Systematic and Evolutionary Microbiology* 60(3):686-695.
- Lampert, D.J. 2010. "An assessment of the design of in situ management approaches for contaminated sediments." Doctoral Thesis, The University of Texas at Austin.
- Langenhoff, A.A.M., A.J.B. Zehnder, and G. Schraa. 1989. "Behavior of toluene, benzene and naphthalene under anaerobic conditions in sediment columns." *Biodegradation* 7(3):267-274.
- Langworthy, D.E., R.D. Stapleton, G.S. Sayler, and R.H. Findlay. 2002. "Lipid analysis of the response of a sedimentary microbial community to polycyclic aromatic hydrocarbons," *Microbial Ecology* 43(2):189-198.
- Lapidus, L. and N.R. Amundson. 1952. "Mathematics of adsorption in beds. vi. the effect of longitudinal diffusion in ion exchange and chromatographic columns." *Journal of Physical Chemistry* 56(8):984-988.
- Lee, S., J.H. Pardue, and W.M.M. Kim. 2009. "Effect of sorption and desorption-resistance on biodegradation of chlorobenzene in two wetland soils." *Journal of Hazardous Materials* 161:492-498.
- Lerman, A. 1979. *Geochemical Processes: Water and Sediment Environments*. USA: John Wiley & Sons, Inc.
- Leuthner, B., C. Leutwein, H. Schulz, P. Horth, W. Haehnel, and E. Schiltz. 1998. "Biochemical and genetic characterization of benzysuccinate synthase from *Thauera aromatic*: a new glycyl radical enzyme catalyzing the first step in anaerobic toluene metabolism." *Molecular Microbiology* 28:615-628.
- Li, Y.H. and S. Gregory. 1974. "Diffusion of ions in sea water and in deep-sea sediments." *Geochimica et Cosmochimica Acta* 38:703-714.

- Liu, W.T., T.L. Marsh, H. Cheng, and L.J. Forney. 1997. "Characterization of microbial diversity by determining terminal restriction fragment length polymorphisms of genes encoding 16S rRNA." *Applied and Environmental Microbiology* 63(11):4516-4522.
- Lizlovs, S. 2005. "Industrial waste contamination: past, present, and future." *Clearwaters* 35 (Summer):25-29.
- Lovley, D.R. and S. Goodwin. 1988. "Hydrogen concentrations as an indicator of the predominant terminal electron-accepting reactions in aquatic sediments." *Geochimica et Cosmochimica Acta* 52:2993-3003.
- Lovley, D.R. and M.J. Klug. 1982. "Intermediary metabolism of organic matter in the sediments of a eutrophic lake." *Applied and Environmental Microbiology* 43(3):552-560.
- Lovley, D.R. and M.J. Klug. 1986. Model for the distribution of sulfate reduction and methanogenesis in freshwater sediments. *Geochimica et Cosmochimica Acta* 50(1):11-18.
- Lovley, D.R., and D.J. Lonergan. 1990. "Anaerobic oxidation of toluene, phenol, and p-cresol by the dissimilatory iron-reducing organism, GS-15." *Applied and Environmental Microbiology* 56 (6): 1858-1864.
- Lovley, D.R. and E.J.P. Phillips. 1986. "Organic matter mineralization with reduction of ferric iron in anaerobic sediments." *Applied and Environmental Microbiology* 51(4):683-689.
- Lovley, D.R., and E.J.P. Phillips. 1987a. "Rapid assay for microbially reducible ferric iron in aquatic sediments." *Applied and Environmental Microbiology* 53(7):1536-1540.
- Lovley, D.R. and E.J.P. Phillips. 1987b. "Competitive mechanisms for inhibition of sulfate reduction and methane production in the zone of ferric iron reduction in sediments." *Applied and Environmental Microbiology* 53(11):2636-2641.
- Lovley, D.R., J.D. Coates, J.C. Woodward, and E.J.P. Phillips. 1995. "Benzene oxidation coupled to sulfate reduction." *Applied and Environmental Microbiology* 61(3):953-958.
- Madsen, T. and J. Aamand. 1991. "Effects of sulfuroxy anions on degradation of pentachlorophenol by a methanogenic enrichment culture." *Applied and Environmental Microbiology* 57(9):2453-2458.

- Masunaga, S., S. Susarla, and Y. Yonezawa. 1996. "Dechlorination of chlorobenzenes in anaerobic estuarine sediment." *Water Science and Technology* 33(6):173-180.
- Matisoff, G., J.B. Fisher, and S. Matis. 1985. "Effects of benthic macroinvertebrates on the exchange of solutes between sediments and freshwater." *Hydrobiologia* 122(1):19-33.
- Matthews, D.A., S.W. Effler, and C.M. Matthews. 2005. "Long-term trends in methane flux from the sediments of Onondaga Lake, NY: Sediment diagenesis and impacts on dissolved oxygen resources." *Archiv fur Hydrobiologie* 163(4):435-462.
- Maurer, M. and B.E. Rittmann. 2004. "Modeling intrinsic bioremediation for interpret observable biogeochemical footprints of BTEX biodegradation: The Need for Fermentation and Abiotic Chemical Processes." *Biodegradation* 15(6):405-417.
- McDonough, K.M. and D.A. Dzombak. 2005. "Microcosm experiments to assess the effects of temperature and microbial activity on polychlorinated biphenyl transport in anaerobic sediment." *Environmental Science and Technology* 39(24):9517-9522.
- McDonough, K.M., P. Murphy, J. Olsta, Y. Zhu, D. Reible, and G.V. Lowry. 2007. "Development and placement of a sorbent-amended thin layer sediment cap in the Anacostia River." *Soil & Sediment Contamination* 16(3):313-322.
- McLinn, E.L. and T.R. Stolzenburg. 2009a. "Ebullition-facilitated transport of manufactured gas plant tar from contaminated sediment." *Environmental Toxicology and Chemistry* 28(11):2298-2306.
- Meckenstock, R.U. 1999. "Fermentative toluene degradation in anaerobic defined syntrophic cocultures." *FEMS Microbiology Letters* 177(1):67-73.
- Meek, M.E., M. Giddings, R. Gomes. 1994. "1,2-Dichlorobenzene: Evaluation of risks to health from environmental exposure in Canada." *Journal of Environmental Science and Health, Part C, Environmental Carcinogenesis and Ecotoxicology Reviews*, 12(2):269-275.
- Monod, J. 1949. "The growth of bacterial cultures." *Annual Reviews in Microbiology* 3:371-394.
- Mosher, J.J., R.H. Findlay, and C.G. Johnston. 2006. "Physical and chemical factors affecting microbial biomass and activity in contaminated subsurface riverine sediments." *Canadian Journal of Microbiology* 52(5):397-403.

- Muñoz, R., L.F. Díaz, S. Bordel, and S. Villaverde. 2007. "Inhibitory effects of catechol accumulation on benzene biodegradation in *Pseudomonas putida* F1 cultures." *Chemosphere* 68 (2):244-252.
- Murphy, P., A. Marquette, D.D. Reible, and G.V. Lowry. 2006. "Predicting the performance of activated carbon-, coke-, and soil-amended thin layer sediment caps." *Journal of Environmental Engineering* 132 (7): 787-794.
- Nealson, K.H. 1997. "Sediment bacteria: Who's there, what are they doing, and what's new?" *Annual Reviews in Earth and Planetary Science* 25:403-434.
- Neilson, A.H. and A.S. Allard. 2008. *Environmental Degradation and Transformation of Organic Chemicals*. Boca Raton, FL: CRC Press.
- Nowak, J., N.H. Kirsch, W. Hegemann, and H.J. Stan. 1996. "Total reductive dechlorination of chlorobenzenes to benzene by a methanogenic mixed culture enriched from Saale river sediment." *Applied Microbiology and Biotechnology* 45(5):700-709.
- N.Y. DEC and U.S. EPA. 2005. Record of Decision: Onondaga Lake Bottom Subsite of the Onondaga Lake Superfund Site. July. (http://www.dec.ny.gov/docs/remediation_hudson_pdf/onondagalakerod.pdf.)
- N.Y. DEC. 2009. "Draft Onondaga Lake dredging, sediment management & water treatment initial design submittal". Last updated February, 2009, accessed 6/3/09. (<http://www.dec.ny.gov/chemical/54571.html>)
- Nzengung, V.A., P. Nkedi-Kizza, R.E. Jessup, and E.A. Voudrias. 1997. "Organic cosolvent effects on sorption kinetics of hydrophobic organic chemicals by organoclays." *Environmental Science and Technology* 31(5):1470-1475.
- Ogata, A., and R.B. Banks. 1961. *A Solution of the differential equation of longitudinal dispersion in porous media*. U.S. Geological Survey, Technical Bulletin #411-A.
- Oka, A.R., C.D. Phelps, X. Zhu, D.L. Saber, and L.Y. Young. 2011. "Dual biomarkers of anaerobic hydrocarbon degradation in historically contaminated groundwater." *Environmental Science and Technology* 45(8):3407-3414.
- Osborn, A.M., E.R.B. Moore, and K.N. Timmis. 2000. "An evaluation of terminal-restriction fragment length polymorphism (T-RFLP) analysis for the study of microbial community structure and dynamics." *Environmental Microbiology* 2(1):39-50.

- Paller, M.H. and A.S. Knox. 2010. "Amendments for the in situ remediation of contaminated sediments: Evaluation of potential environmental impacts." *Science of the Total Environment* 408(20):4894-4900.
- Perelo, L.W. 2010. "Review: In situ and Bioremediation of Organic Pollutants in Aquatic Sediments." *Journal of Hazardous Materials* 177: 81-89.
- Pernyeszi, T., R. Kasteel, B. Witthuhn, P. Klahre, H. Vereecken, and E. Klumpp. 2006. "Organoclays for soil remediation: Adsorption of 2,4-dichlorophenol on organoclay/aquifer material mixtures studied under static and flow conditions." *Applied Clay Science* 32(3-4):179-189.
- Phelps, C. and L. Young. 1999. "Anaerobic Biodegradation of BTEX and gasoline in various aquatic sediments." *Biodegradation* 10(1):15-25.
- Phelps, C.D., J. Battistelli, and L.Y. Young. 2002. "Metabolic biomarkers for monitoring anaerobic naphthalene biodegradation *in situ*." *Environmental Microbiology* 4 (9): 532-537.
- Polymenakou, P.N., S. Bertilsson, A. Tselepides, and E.G. Stephanou. 2005. "Links between Geographic Location, Environmental Factors, and Microbial Community Composition in Sediments of the Eastern Mediterranean Sea." *Microbial Ecology* 49(3):367-378.
- Putz, A.R. 2004. "Biological activated carbon: the relative role of metabolism and cometabolism in extending service life and improving process performance." Doctoral Thesis, The University of Texas at Austin.
- Qu, X., P. Liu, and D. Zhu. 2008. "Enhanced sorption of polycyclic aromatic hydrocarbons to tetra-alkyl ammonium modified smectites via cation- π interactions." *Environmental Science and Technology* 42(4):1109-1116.
- Quayle, J. R. and N. Pfennig. 1975. "Utilization of methanol by *Rhodospirillaceae*." *Archives of Microbiology* 102(1):193-198.
- Ramanand, K., M.T. Balba, and J. Duffy. 1993. "Reductive dehalogenation of chlorinated benzenes and toluenes under methanogenic conditions." *Applied and Environmental Microbiology* 59(10):3266-3272.
- Reardon, C.L., D.E. Cummings, L.M. Petzke, B.L. Kinsall, D.B. Watson, B.M. Peyton, G.G. Geesey. 2004. "Composition and diversity of microbial communities recovered from surrogate minerals incubated in an acidic uranium-contaminated aquifer," *Applied and Environmental Microbiology* 70(10):6037-6046.

- Reible, D.D. 2004. "In-situ sediment remediation through capping: status and research needs." Report for the Hazardous Substance Research Center/South and Southwest. Pp. 1-20.
- Reible, D.D., D. Lampert, D. Constant, R.D. Mutch Jr., Y. Zhu. 2006. "Active capping demonstration in the Anacostia River, Washington, D.C." *Remediation Journal* 17(1):39-53.
- Reible, D.D., C. Kiehl-Simpson, and A. Marquette. 2009. "Steady-state model of chemical migration in a sediment cap." *Contaminated Sediments* 5:161-178.
- Ridgway, R.M. 2001. "Anaerobic reduction dehalogenation of trichloroethylene in unacclimated freshwater sediments." Doctoral Dissertation, Purdue University.
- Rittmann, B.E., and P. L. McCarty. 2001. *Environmental Biotechnology: Principles and Applications*. New York, NY: McGraw-Hill, Inc. Pp. 165-168.
- Robertson, B.R., and D.K. Button. 1987. "Toluene induction and uptake kinetics and their inclusion in the specific-affinity relationship for describing rates of hydrocarbon metabolism." *Applied and Environmental Microbiology* 53(9):2193-2205.
- Röling, W.F.M., B.M. van Breukelen, M. Braster, B. Lin, and H.W. van Verseveld. 2001. "Relationships between microbial community structure and hydrochemistry in a landfill leachate-polluted aquifer." *Applied and Environmental Microbiology* 67(10):4619-4629.
- Rooney-Varga, J.N., R.T. Anderson, J.L. Fraga, D. Ringelberg, and D.R. Lovley. 1999. "Microbial communities associated with anaerobic benzene degradation in a petroleum-contaminated aquifer." *Applied and Environmental Microbiology* 65(7):3056-3063.
- Rowell, H.C. 1996. "Paleolimnology of Onondaga Lake: The history of anthropogenic impacts on water quality." *Lake and Reservoir Management*. 12(1):35-45.
- Sander, R. 1999. "Compilation of Henry's Law constants for inorganic and organic species of potential importance in environmental chemistry (Version 3)." Last updated Nov. 25, 2010. Accessed May 12, 2011. <http://www.henrys-law.org>.
- Schaaning, M., B. Breyholtz, and J. Skei. 2006. "Experimental results on effects of capping on fluxes of persistent organic pollutants (POPs) from historically contaminated sediments." *Marine Chemistry* 102(1-2):46-59.

- Schink, B. 1988. "Principles and limits of anaerobic degradation: environmental and technological aspects." In *Biology of Anaerobic Microorganisms*, pp. 771-846. USA: John Wiley & Sons, Inc.
- Schwarzenbach, R.P., P.M. Gschwend, and D.M. Imboden. 2003. *Environmental Organic Chemistry*. Second Ed. Hoboken, NJ: John Wiley & Sons, Inc.
- Sharma, B., K.H. Gardner, J. Melton, A. Hawkins, and G. Tracey. 2009. "Effect of humic acid on adsorption of polychlorinated biphenyls onto organoclay." *Environmental Engineering Science* 26(8):1279-1287.
- Sharmasarkar, S., W.F. Jaynes, and G.F. Vance. 2000. "BTX sorption by montmorillonite organo-clays: TMPA, ADAM, HDTMA." *Water, Air, & Soil Pollution* 119(1):257-273.
- Sheng, G. and S.A. Boyd. 2000. "Polarity effect on dichlorobenzene sorption by hexadecyltrimethylammonium-exchanged clays." *Clay and Clay Minerals* 48(1):43-50.
- Sheng, G., S. Xu, and S.A. Boyd. 1996. "Mechanism(s) controlling sorption of neutral organic contaminants by surfactant-derived and natural organic matter." *Environmental Science and Technology* 30(5):1553-1557.
- Singleton, D.R., S.N. Powell, R. Sangaiah, A. Gold, L.M. Ball and M.D. Aitken. 2005. "Stable-isotope probing of bacteria capable of degrading salicylate, naphthalene, or phenanthrene in a bioreactor treating contaminated soil." *Applied and Environmental Microbiology* 71(3):1202-1209.
- Smatlak, C.R., J.M. Gossett, and S.H. Zinder. 1996. "Comparative kinetics of hydrogen utilization for reductive dechlorination of tetrachloroethene and methanogenesis in an anaerobic enrichment culture." *Environmental Science and Technology* 30(9):2850-2858.
- Smith, B. and J.B. Wilson. 1996. "A consumer's guide to evenness indices." *Oikos* 76:70-82.
- Smith, A.M. 2006. "Effects of bioturbation on the bacterial community in contaminated sediment." M.S. Thesis, The University of Texas at Austin.
- Stumm, W. and J.J. Morgan. *Aquatic Chemistry: Chemical Equilibria and Rates in Natural Waters*. Third Ed. New York, NY: John Wiley & Sons, Inc., 1996.
- Suarez, M.P. and H.S. Rifai. 1999. "Biodegradation rates for fuel hydrocarbons and chlorinated solvents in groundwater." *Bioremediation Journal* 3(4):337-362.

- Thoma, G.J., D.D. Reible, K.T. Valsaraj, and L.J. Thibodeaux. 1993. "Efficiency of capping contaminated sediments in situ. 2. Mathematics of diffusion-adsorption in the capping layer." *Environmental Science and Technology* 27(12):2412-2419.
- Toride, N., F.J. Leij, and M.T. van Genuchten. 1999. "The CXTFIT code for estimating transport parameters from laboratory or field tracer experiments, Version 2.1." U.S. Salinity Laboratory, Riverside, CA. 132 pp.
- U.S. EPA. 1998. "EPA's Contaminated Sediment Management Strategy". EPA-823-R-98-001. U.S. Environmental Protection Agency, Office of Water, Washington, DC.
- U.S. EPA. 2001. "Methods for collection, storage and manipulation of sediments for chemical and toxicological analyses: Technical Manual." EPA 823-B-01-002. U.S. Environmental Protection Agency, Office of Water, Washington, DC.
- U.S. EPA. 2005. "Contaminated sediment remediation guidance for hazardous waste sites". EPA-540-R05-012. U.S. Environmental Protection Agency, Office of Solid Waste and Emergency Response, Washington, DC.
- U.S. EPA. 2011. "Onondaga Lake Superfund Site." U.S. Environmental Protection Agency, Region 2 Superfund, Washington, DC. Updated January 31, 2011, accessed May 3, 2011. (<http://www.epa.gov/region02/superfund/npl/onondagalake/index.html>).
- Van Cappellen, P., and Y. Wang. 1996. "Cycling of iron and manganese in surface sediments: a general theory for the coupled transport and reaction of carbon, oxygen, nitrogen, sulfur, iron, and manganese." *American Journal of Science* 296:197-243.
- Van Genuchten, M.T. and W.J. Alves. 1982. *Analytical solutions of the one-dimensional convective-dispersive solute transport equation*. Technical Bulletin No. 1661. US Department of Agriculture.
- Viana, P., K. Yin, X. Zhao, and K. Rockne. 2007. "Active sediment capping for pollutant mixtures: control of biogenic gas production under highly intermittent flows." *Land Contamination & Reclamation* 15(4):413-425.
- Vinas, M., J. Sabate, M.J. Espuny, and A.M. Solanas. 2005. "Bacterial community dynamics and polycyclic aromatic hydrocarbon degradation during bioremediation of heavily creosote-contaminated soil." *Applied and Environmental Microbiology* 71(11):7008-7018.

- Vlassopoulos, D., J. Goin, B. Bessinger, C. Kiehl-Simpson, and E. Glaza. 2011. "Evaluation of pH-buffering amendments for in situ capping of hyperalkaline contaminated sediments." Poster presented at the Battelle: Sixth International Conference on Remediation of Contaminated Sediments, New Orleans, LA.
- Vogel, T.M. and D. Grbic-Galic. 1986. "Incorporation of oxygen from water into toluene and benzene during anaerobic fermentative transformation." *Applied and Environmental Microbiology* 52(1):200-202.
- Wang X.Q., L.J. Thibodeaux, K.T. Valsaraj, and D.D. Reible. 1991. "Efficiency of capping contaminated bed sediments in situ. 1. Laboratory-scale experiments on diffusion-adsorption in the capping layer." *Environmental Science and Technology* 25(9):1578-1584.
- Wang, Q., I.I. Kassem, V. Sigler, and C. Gruden. 2009. "Short-term effect of capping on microbial communities in freshwater sediments." *Water Environment Research* 81:441-449.
- Weber, K.A., L.A. Achenbach, and J.D. Coates. 2006. "Microorganisms pumping iron: anaerobic microbial iron oxidation and reduction." *Nature Reviews Microbiology* 4(10):752-764.
- Weissberg, H.L. 1963. "Effective diffusion coefficient in porous media." *Journal of Applied Physics* 34(9):2636-2639.
- Whyte, L.G., J. Hawari, E. Zhou, L. Bourbonniere, W.E. Inniss, and C.W. Greer. 1998. Biodegradation of variable-chain-length alkanes at low temperatures by a psychrotrophic *Rhodococcus* sp. *Applied and Environmental Microbiology* 64:2578-2584.
- Williams, W.A., and R.J. May. 1997. Low-temperature microbial aerobic degradation of polychlorinated biphenyls in sediment. *Environmental Science and Technology* 31:3491-3496.
- Winderl, C., S. Schaefer, and T. Lueders. 2007. "Detection of anaerobic toluene and hydrocarbon degraders in contaminated aquifers using benzylsuccinate synthase (bssA) genes as a functional marker." *Environmental Microbiology* 9(4):1035-1046.
- Wilson, B.H., G.B. Smith, and J.F. Rees. 1986. "Biotransformations of selected alkylbenzenes and halogenated aliphatic hydrocarbons in methanogenic aquifer material: a microcosm study." *Environmental Science and Technology* 20(10):997-1002.

- Witthuhn, B., T. Pernyeszi, P. Klauth, H. Vereecken, and E. Klumpp. 2005. "Sorption study of 2,4-dichlorophenol on organoclays constructed for soil bioremediation." *Colloids and Surfaces A: Physicochemical and Engineering Aspects* 265(1-3):81-87.
- Witthuhn, B., P. Klauth, T. Pernyeszi, H. Vereecken, and E. Klumpp. 2006. "Organoclays for aquifer bioremediation: adsorption of chlorobenzene on organoclays and its degradation by *Rhodococcus* B528." *Water, Air, & Soil Pollution: Focus* 6(3):317-329.
- Yang, Y. and P.L. McCarty. 1998. "Competition for hydrogen within a chlorinated solvent dehalogenating anaerobic mixed culture." *Environmental Science and Technology* 32(22):3591-3597.
- Yaws, C. 1999. *Chemical Properties Handbook: Physical, Thermodynamic, Environmental, Transport, Safety, and Health*. New York: McGraw-Hill.
- Yin, K., P. Viana, X. Zhao, and K. Rockne. 2010. "Characterization, performance modeling, and design of an active capping remediation project in a heavily polluted urban channel." *Science of the Total Environment* 408:3454-3463.
- Young, L.Y. and C.D. Phelps. 2005. "Metabolic biomarkers for monitoring in situ anaerobic hydrocarbon degradation." *Environmental Health Perspectives* 113(1):62-67.
- Yuan, Q., K.T. Valsaraj, D.D. Reible, C.S. Willson. 2007. "A laboratory study of sediment and contaminant release during gas ebullition." *Journal of the Air & Waste Management Association* 57(9):1103-1111.
- Yuan, Q., K. Valsaraj, and D. Reible. 2009. "A model for contaminant and sediment transport via gas ebullition through a sediment cap." *Environmental Engineering Science* 26(9):1381-1394.
- Zhang, X. and L.Y. Young. 1997. "Carboxylation as an initial reaction in the anaerobic metabolism of naphthalene and phenanthrene by sulfidogenic consortia." *Applied and Environmental Microbiology* 63(12):4759-4764.

Vita

Anthony Smith was born in Wisconsin in 1977 and lived with his parents and three brothers in Colorado and California. In 2000, he graduated with a B.S. in Biochemistry from Cal Poly, San Luis Obispo. After working for a biotech start-up in South San Francisco, Anthony enrolled in the Environmental and Water Resources Engineering program at the University of Texas-Austin and completed the M.S.E. degree in 2006.

Permanent address: 324 Green Moor Place, Thousand Oaks, CA, 91361

This dissertation was typed by the author.